CHAPTER IV

RESULTS AND DISCUSSION

4.1. INTRODUCTION

To understand the evolution of Malani igneous province (MIP), temporal status of various associations must be established. Keeping this in view, systematic dating of each association was undertaken using K-Ar, ^{40}Ar-^{39}Ar and Rb-Sr methods. The K-Ar method was employed only in the initial phase of the work for preliminary screening of the samples while ^{40}Ar-^{39}Ar and/or Rb- Sr methods were used in subsequent studies, depending upon suitability of the technique for eliciting chronological informations. The samples dated by ^{40}Ar-^{39}Ar method were also studied for Sr isotopic composition, in order to know their petrogenesis.

About half of the samples under investigation were provided by Prof. R. K. Srivastava of Deptartment of Geology, M. L. Sukhadia University, Udaipur, Rajasthan. Most of these samples were collected by his students working for their doctoral thesis from different parts of the Malani province (Maheswari, 1983; Agrawal, 1984; Gaur, 1984; Yadav, 1988; Yadav, 1991). The remaining samples were collected during a field trip to Rajasthan in 1986.

4.2. ASSOCIATION I (*MALANI VOLCANICS*)

The felsic volcanics of Gurapratap Singh and Diri of Pali district (Fig. 1.3), commonly referred to as Malani volcanics, have been grouped in this association. The analytical results of ^{40}Ar-^{39}Ar and Rb-Sr studies are discussed below.

4.2.1. ^{40}Ar-^{39}Ar STUDIES

Three samples were analyzed from basalt-andesite-dacite-rhyolite association of Diri and Gurapratap Singh, Pali district, for ^{40}Ar-^{39}Ar studies. The dated samples include a basalt (D/88), a dacite (D/25) and a rhyolite (D/174).

The samples were irradiated in two batches. The minimum and maximum value of J was 0.00224 ± 0.00002 and 0.00275 ± 0.00004 for D/88 and D/25, respectively.

Analytical results of the $^{40}Ar/^{39}Ar$ analysis of these samples are presented in Tables 4.1 to 4.3. The values are corrected for K-and Ca-derived Ar isotopes. After correction for Ca-derived ^{36}Ar, the ^{36}Ar is used to correct for trapped ^{40}Ar on the assumption that the $^{40}Ar/^{36}Ar$ ratios of the trapped argon has the modern atmospheric value of 295.5. Minnesota hornblende (MMhb-1), with an age of 520.4 ± 1.7 Ma (Samson and Alexander, 1987), has been used as monitor for all the samples. The total or integrated ages are calculated by adding the isotopic abundances of all the temperature steps. The errors have been computed by quadratically propagating the errors in the measured ratios, blanks and interfering isotopes. The error quoted on the apparent and integrated ages include the error in J but the error boxes in age spectra plots do not include the error in J. All the errors quoted here after are at 2σ level.

The age spectra are plotted in Fig. 4.1 to 4.3, which exhibit a step-wise age increase in all the samples with increasing temperature. Similar patterns, normally interpreted as resulting from argon loss by diffusion, have been obtained for slowly cooled rocks and for rocks that have been reheated subsequent to the time of their formation (Hanson et al., 1975; Berger and York, 1981; Harrison and McDougall, 1981 and Zeitler, 1987).

The apparent ages for the initially released gas in each sample provide an estimate of the time of reheating or the time since the rock began to retain argon quantitatively owing to cooling below the blocking temperature of different rock-forming minerals (Frank and Stettler, 1979). Also shape of the release spectra will vary depending upon the grain size, the amount of argon loss and the conditions of episodic heating (Turner, 1968, 1969; Gillespie et al., 1982)

In the sample D/88 (basalt) four temperature steps (550 to 700°C; 28.4% ^{39}Ar

Notes for tables:

1. Radiogenic ^{40}Ar as percentage of total ^{40}Ar.
2. All data are corrected for blank, mass discrimination and interference.
3. ^{37}Ar and ^{39}Ar are corrected for decay and error quoted for age includes error in J.
4. Errors quoted are at 2σ level.
5. Errors on $^{87}Rb/^{86}Sr$ ratios are 2% at 2σ level.

Table 4.1. Step heating argon isotopic compositions and apparent ages of sample D/88 (DIRI BASALT)
J=0.00224 ± 0.00002

Temp. (°C)	$^{36}Ar/^{39}Ar$	$^{37}Ar/^{39}Ar$	$^{40}Ar/^{39}Ar$	Age (Ma)	^{39}Ar (%)	$^{40}Ar^*$ (%)
400	0.1347 ±0.0041	3.3566 ±0.0679	183.80 ±1.50	503 ±11	1.1	78.3
450	0.0405 0.0010	3.1229 0.0063	130.44 0.88	424 6	4.2	90.8
500	0.0154 0.0013	2.6167 0.0052	135.24 0.87	462 7	4.9	96.6
550	0.0158 0.0007	3.9964 0.0079	142.72 0.87	485 6	6.4	96.7
600	0.0143 0.0007	3.7099 0.0074	144.64 0.89	493 6	6.1	97.1
650	0.0122 0.0005	2.6369 0.0075	145.02 0.86	496 6	8.5	97.5
700	0.0069 0.0006	1.9187 0.0066	143.06 0.86	494 6	7.4	98.6
750	0.0079 0.0005	2.1446 0.0042	149.53 0.89	513 6	8.9	98.4
800	0.0057 0.0002	3.0859 0.0061	160.84 0.93	549 6	18.6	98.9
850	0.0066 0.0003	3.1620 0.0063	152.98 0.89	525 6	16.6	98.7
900	0.0178 0.0005	4.7422 0.0094	168.17 0.99	560 7	8.3	96.9
1000	0.0523 0.0009	20.6720 0.0413	221.50 1.30	684 8	4.5	93.6
1100	0.0702 0.0012	42.7900 0.0855	236.10 1.50	709 9	3.5	91.2
1250	0.1211 0.0073	21.9300 0.0438	240.30 2.20	679 17	1.1	85.1
TOTAL	0.0178 0.0002	5.5509 0.0042	158.30 0.30	531 4	100.0	96.7

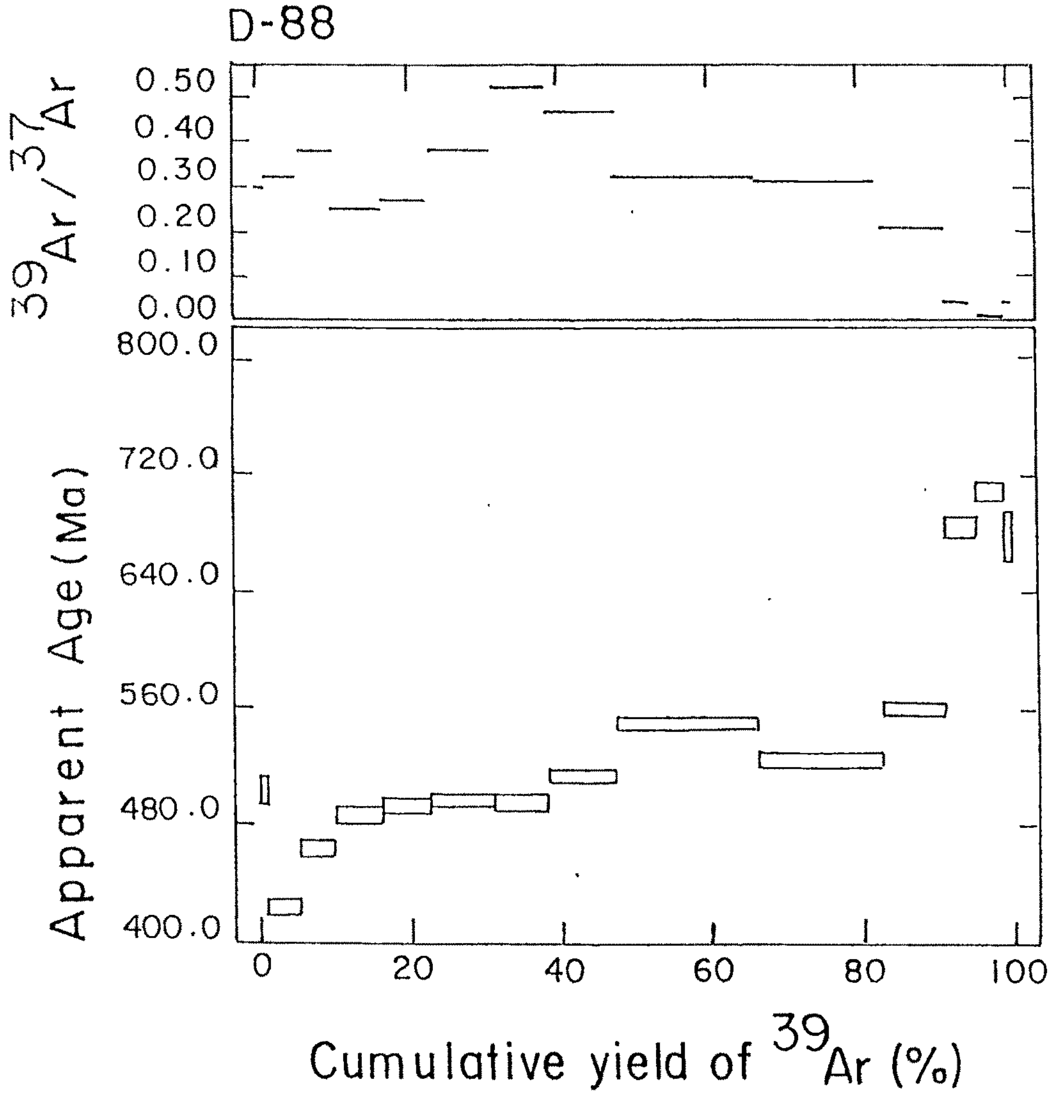

Fig. 4.1. ^{40}Ar-^{39}Ar Age Spectrum for Diri Basalt (D/88).

Table 4.2. Step heating argon isotopic compositions and apparent ages of sample D/25 (DIRI DACITE) J=0.00275 ± 0.00004

Temp. (°C)	$^{36}Ar/^{39}Ar$	$^{37}Ar/^{39}Ar$	$^{40}Ar/^{39}Ar$	Age (Ma)	^{39}Ar (%)	$^{40}Ar^{*}$ (%)
500	0.0799	1.1334	134.31	479	1.4	82.4
	±0.0028	±0.0147	±0.91	±11		
550	0.0408	0.6650	122.75	479	3.1	90.2
	0.0012	0.0320	0.74	8		
600	0.0389	0.3688	132.27	517	5.1	91.3
	0.0008	0.0165	0.77	8		
650	0.0166	0.2680	125.10	515	8.9	96.1
	0.0006	0.0027	1.30	8		
700	0.0059	0.2239	120.62	510	12.0	98.5
	0.0003	0.0037	0.70	8		
750	0.0044	0.4216	116.07	495	10.8	98.9
	0.0004	0.0034	0.67	8		
800	0.0042	0.6351	118.40	504	14.9	98.9
	0.0003	0.0041	0.76	8		
850	0.0073	1.7925	127.00	532	20.9	98.3
	0.0002	0.0099	1.80	9		
900	0.0065	1.8422	144.86	598	12.6	98.7
	0.0004	0.0229	0.95	9		
950	0.0231	4.7171	234.20	876	5.0	97.0
	0.0012	0.0094	1.40	13		
1000	0.0336	7.7124	376.60	1258	1.6	97.4
	0.0042	0.0154	2.40	17		
1050	0.0493	10.6501	458.40	1439	1.0	97.0
	0.0073	0.0213	3.30	20		
1200	0.0809	10.1821	468.00	1440	1.0	95.0
	0.0189	0.1581	3.49	32		
1500	0.1440	9.4665	473.30	1410	2.0	91.0
	0.0351	0.0208	6.90	58		
TOTAL	0.0158	1.5885	148.30	600	100.0	96.9
	0.0012	0.0041	8.90	8		

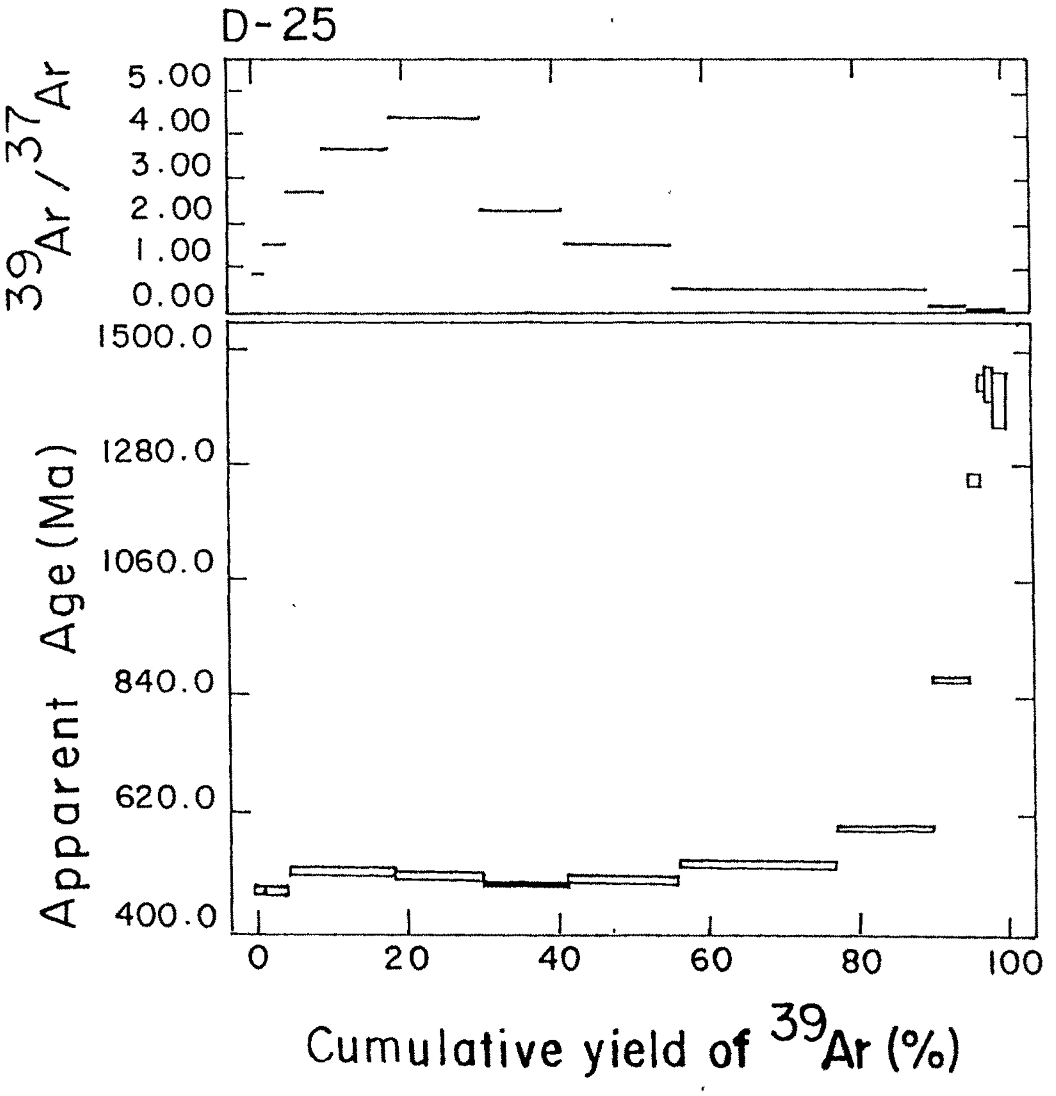

Fig. 4.2. ^{40}Ar-^{39}Ar Age Spectrum for Diri Dacite (D/25).

Table 4.3. Step heating argon isotopic compositions and apparent ages of sample D/174 (DIRI RHYOLITE)
J=0.00269 ± 0.00004

Temp. (°C)	$^{36}Ar/^{39}Ar$	$^{37}Ar/^{39}Ar$	$^{40}Ar/^{39}Ar$	Age (Ma)	^{39}Ar (%)	$^{40}Ar^{*}$ (%)
500	0.0246 ±0.0009	-	143.22 ±0.83	562 ±9	2.1	94.9
550	0.0047 0.0002	0.0758 0.0022	124.80 0.72	517 8	3.5	98.9
600	0.0024 0.0001	-	126.41 0.73	523 8	10.7	99.4
650	0.0011 0.0001	-	124.65 0.74	520 8	11.5	99.8
700	0.0006 0.0001	-	132.40 1.00	549 8	12.2	99.8
750	0.0019 0.0001	-	146.95 0.84	598 9	13.7	99.6
800	0.0035 0.0001	-	183.80 1.60	721 11	14.8	99.4
850	0.0029 0.0002	0.0843 0.0025	161.25 0.93	646 10	14.4	99.5
900	0.0031 0.0001	-	200.50 1.60	774 11	7.6	99.5
950	0.0050 0.0005	0.1458 0.0091	240.40 1.40	895 13	3.5	99.4
1200	0.0130 0.0008	-	319.30 4.00	1107 15	3.7	98.8
1500	0.0145 0.0086	-	362.80 2.50	1217 22	2.0	99.0
TOTAL	0.0036 0.0002	0.0198 0.0004	166.13 0.38	662 8	100.0	99.4

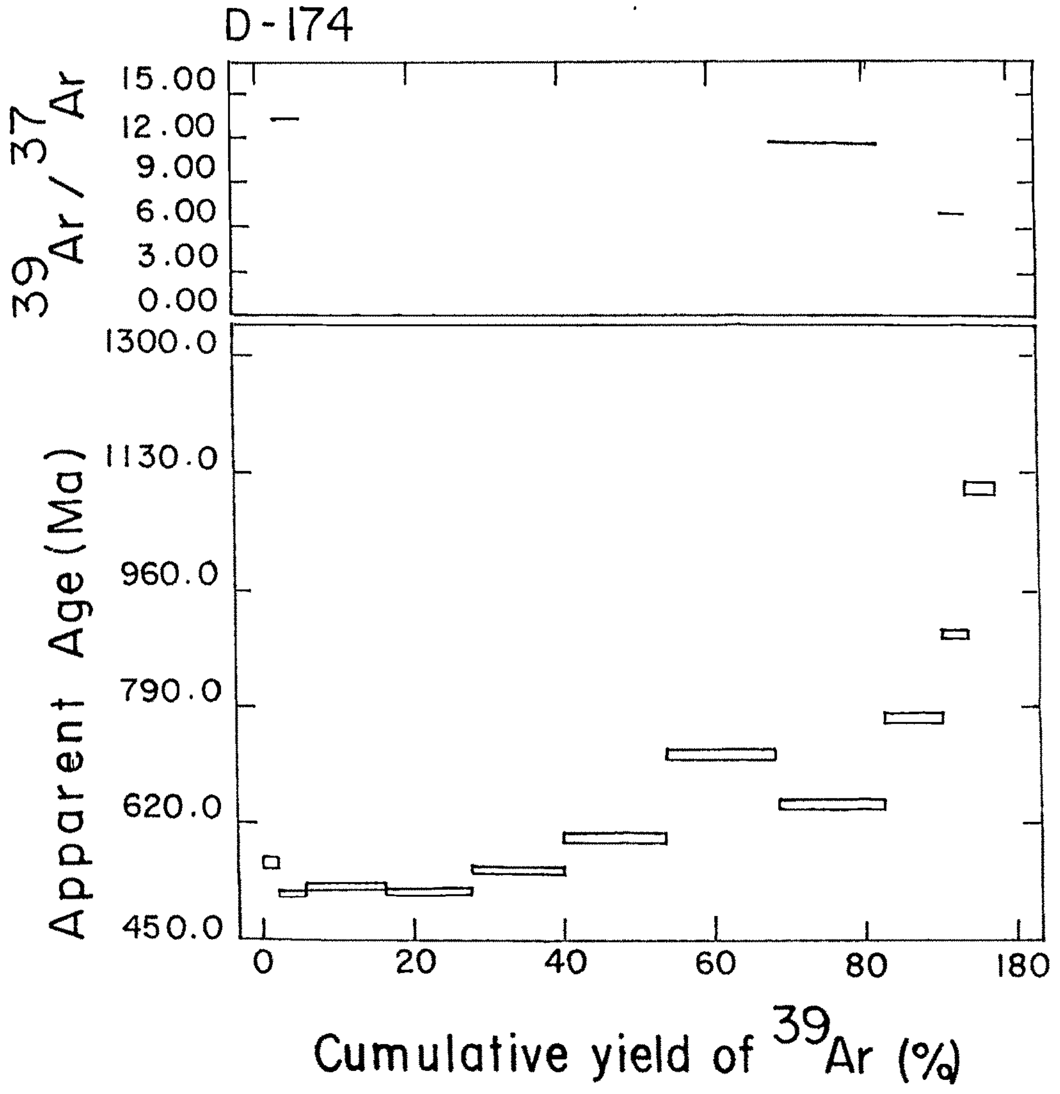

Fig. 4.3. ^{40}Ar-^{39}Ar Age Spectrum for Diri Rhyolite (D/174).

release) exhibit apparent ages which are mutually similar and give a pseudo plateau age of 492.0 ± 4.7 Ma (Fig. 4.1). The higher temperature steps give successively higher ages. The total age is 530.9 ± 4.4 Ma. Sample D/25 (dacite) defines plateau of five intermediate temperature steps (600 to 800°C) with 51.7% of total ^{39}Ar released forming the pseudo palteau at 507.8 ± 8.2 Ma (Fig. 4.2). While in the sample D/174 (rhyolite) only three temperature steps (550 to 650°C, 25.7%, ^{39}Ar release) constitute a pseudo plateau at 520.5 ± 9.6 Ma (Fig. 4.3). The latter two samples have higher temperature steps exhibiting apparent ages which are well above of their formation age of 779 ± 10 Ma as obtained by Rb-Sr studies (discussed in Rb-Sr study part of this section), suggesting presence of excess argon. The total ages for these samples are 600.7 ± 8.0 Ma and 662.2 ± 8.4 Ma, respectively.

Where excess ^{40}Ar is known to be present, two different age patterns have been distinguished. The first is a **'saddle-shaped'** spectrum where the apparent age of successive gas increments decreases systematically to a minimum and then increases for the remaining ^{39}Ar release (Lanphere and Dalrymple, 1971). The minimum apparent age is greater than the known age of the sample. This pattern occurs in whole rocks as well as mineral separates like biotite, pyroxene and plagioclase from a number of geological environments but in general tends to be associated with the crystallization of igneous rocks (Lanphere and Dalrymple, 1976; Kaneoka, 1974; Stettler and Bochsler, 1979)

The second pattern is associated with the metamorphism of pre-existing rocks. In this case the age spectra either rise steeply to a relatively flat plateau over most of the ^{39}Ar release or show step-wise age increase with increasing temperature, with apparent ages well in excess of the metamorphic and/or formation age and in some cases older than the age of the earth. This type of pattern has been demonstrated in biotites from Greenland by Pankhurst et al. (1973) and for Alpine biotites by Roddick et al. (1980).

A third pattern (Seidemann, 1976) which may show excess ^{40}Ar in the low-temperature steps but approximates the correct cooling age in the high-temperature release. However, as both Seidemann (1976) and Lanphere and Dalrymple (1977) indicate that this effect does not apply to the common rock forming minerals.

The release spectra of samples D/25 amd D/174 exhibit the second pattern mentioned above, and the anomalously high age is attributed to the presence of excess radiogenic argon, a portion of which was lost by diffusion during cooling after a thermal event around 500-550 Ma ago. Similar release curves have been obtained by Phillips and Onstotte (1986) also for the phlogopites from southern African Kimberlites.

It is clear from above that none of the three samples analyzed gave a perfect plateau but showed the spectra typical of rocks which have been reheated at about 500-550 Ma ago subsequent to their formation. Earlier Rb-Sr mineral ages determined on different granite bodies from Sendra, Sadri-Ranakpur and Sai have also indicated thermal event to reset mineral ages around 500-550 Ma ago, which otherwise have the whole rock pooled Rb-Sr age of 800 ± 50 Ma (Choudhary, 1984).

The $^{40}Ar/^{39}Ar$ studies of volcanics from Pali district have, thus, indicated the existence of this thermal event in the rocks exposed further west of Aravalli range in Rajasthan.

4.2.2. Rb-Sr STUDIES

4.2.2.A. BASALT-ANDESITE-DACITE-RHYOLITE SEQUENCE

As the ^{40}Ar-^{39}Ar studies could not reveal the time of formation, Rb-Sr whole rock dating was employed to elucidate the time of primary crystallization of felsic volcanics from Diri, Gura pratap Singh and Manihari, Pali district.

Five samples, ranging in composition from basalt to rhyolite, were selected for Rb-Sr isotopic studies. The selected samples showed good spread in Rb/Sr ratios (0.1 to 7). The analytical data are given in Table 4.4. All the errors quoted are at 2σ level and the errors on $^{87}Rb/^{86}Sr$ ratios are 2%. When these data points are plotted on a Rb-Sr evolution diagram (Fig. 4.4) they define a best fit line corresponding to an age of 786 ± 11 Ma with an initial Sr isotopic ratio of 0.70559 ± 0.00043. The MSWD is 2.26. However, when the sample D/88 (basalt) is omitted from the calculation, the remaining four samples define an isochron age of 779 ± 10 Ma with an initial Sr isotopic ratio of 0.70612 ± 0.00046. The MSWD reduces to 0.29 from 2.26 which indicates that the fit

Table 4.4. Rb-Sr isotopic data of Malani volcanics from Diri, Gurapratap Singh and Manihari, Pali district.

Sample No.	^{87}Rb (ppm)	^{86}Sr (ppm)	^{87}Rb/^{86}Sr (atomic)	^{87}Sr/^{86}Sr (atomic)
D/88	13.184	33.996	0.383	0.70804 ± 0.00084
D/10	41.320	26.329	1.551	0.72336 ± 0.00012
D/117	70.509	7.607	9.163	0.80929 ± 0.00011
D/5	84.519	7.068	11.820	0.83694 ± 0.00018
GM/219	70.691	3.463	20.1778	0.92887 ± 0.00035

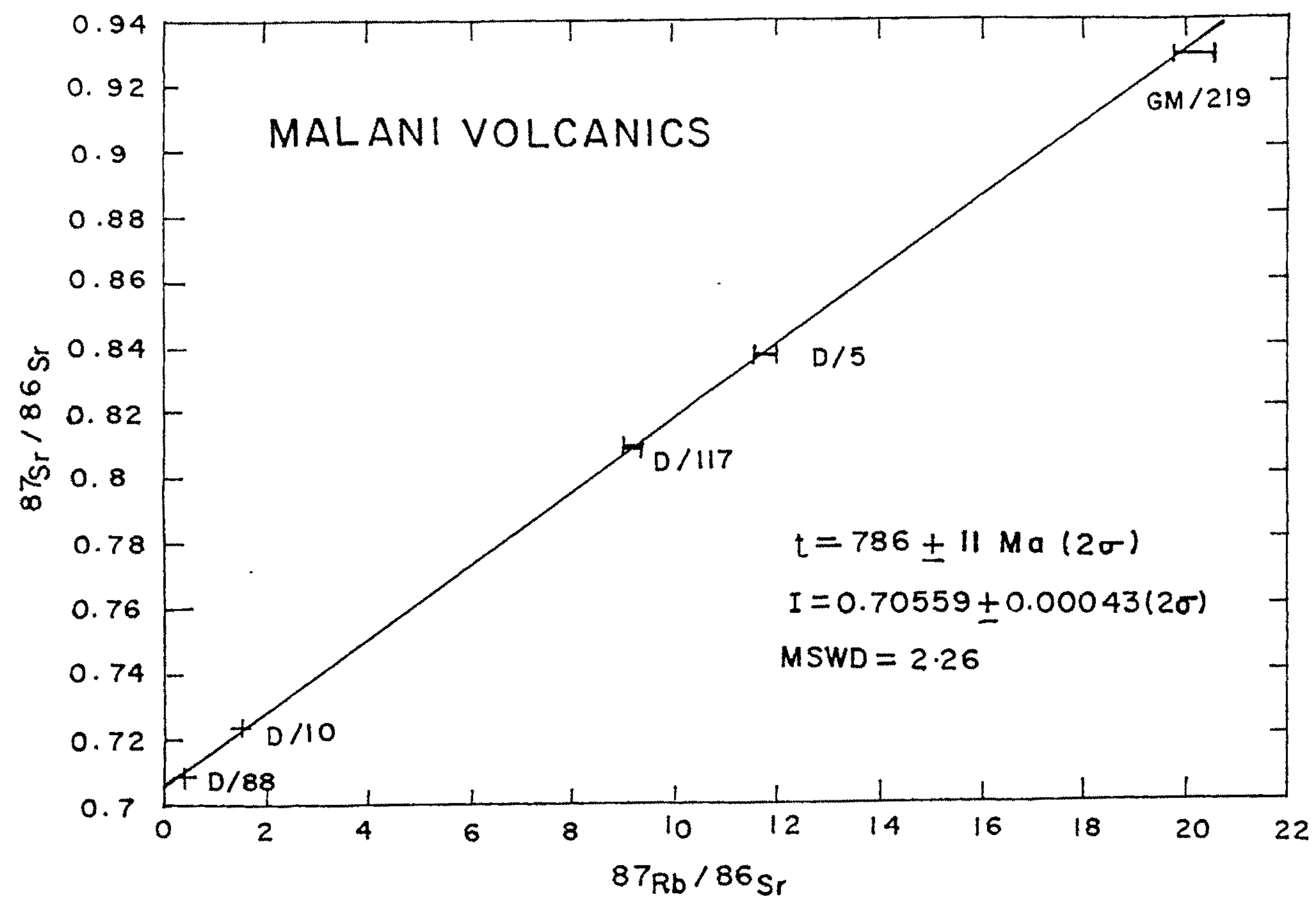

Fig. 4.4. Rb-Sr Conventional Isochron Diagram for Basalt-Andesite-Dacite-Rhyolite Association from Diri and Gurapratap Singh.

is very good and that the samples have evolved as closed systems after their crystallization. The initial Sr ratio is indicative of crustal origin of the magma.

Further, if D/88 (basalt) is substituted for D/10 (dacite) in the calculation then the data points define an isochron age of 792 ± 11 Ma with MSWD 0.66, which is not different from the age obtained when D/88 is excluded from the calculation, suggesting contemporaneity of D/88 with the other rocks. However, the initial Sr ratio comes down to 0.70385 ± 0.00062 from 0.70612 ± 0.00046 which is quite different. This exercise, thus, suggests that though D/88 (basalt) has also crystallized at the same time, but belongs to a different, upper mantle, source. This conviction becomes more pronounced when the data points are plotted on best isochron diagram (Fig. 4.5) as developed by Provost (1990).

Recently Provost (1990) has evolved a new graphical means of displaying the data points. He named this as a best isochron diagram (BID) which has certain advantages over the conventional isochron diagram (CID) like:

(1) *Unlike the CID, the initial ratios in BID is at a scale where its precision can be easily seen.*

(2) *Unlike the CID, the BID displays the radiometric age as an intercept (on the right-hand border), again on an appropriate scale.*

(3) *On the BID, highly radiogenic samples are not unduly emphasized and there is no need for inserts nor enlargements.*

(4) *The whole height of the BID is available for displaying the analytical errors and deviations from the (nearly horizontal) isochron and there is no need for a Papanastassiou-Wasserburg insert (Papanastassiou and Wasserburg, 1971).*

Due to these optimal properties, the BID allows one to simultaneously visualize the experimental data and their analytical precision, to judge the quality of the linear fit, to appraise the accuracy of the age and initial ratio results, and to quantitatively appreciate the influence of any existing or expected datum. From the Fig. 4.5 it can be seen that the sample D/88 (basalt) is falling distinctly away (below) on the best isochron diagram indicating a different source though it is contemporaneous with the other volcanics i.e. andesite, dacite and rhyolite from Diri, Gurapratap Singh and Manihari of

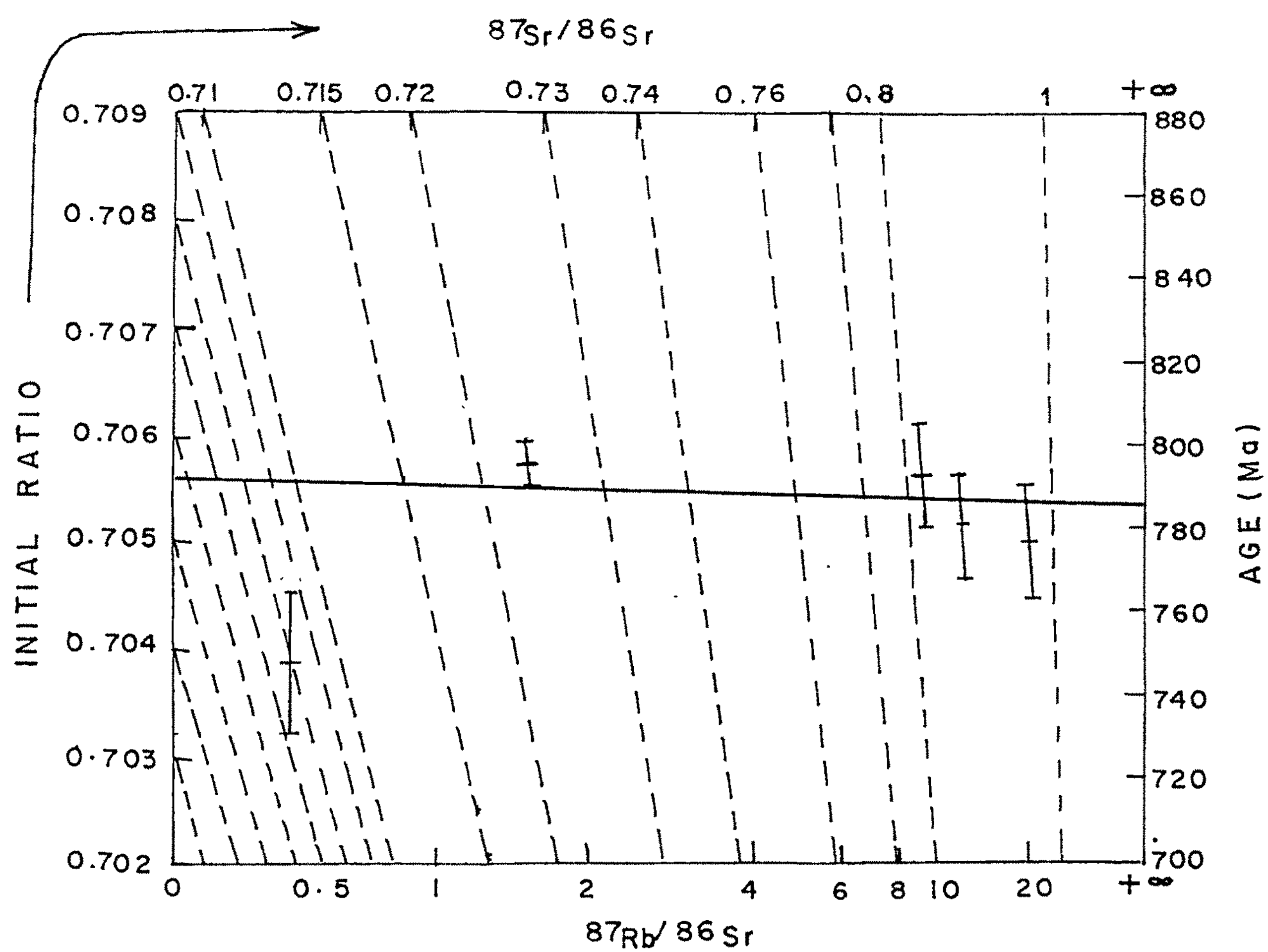

Fig. 4.5. Rb-Sr Best Isochron Diagram for Basalt - Andesite - Dacite - Rhyolite Association from Diri and Gurapratap Singh.

Pali district. It is interesting to note here that Srivastava et al. (1989a) also reported that the field disposition of the basalt whether in the form of dyke or a flow could not be ascertained which further props up the present conviction.

4.2.2.B. ULTRAPOTASSIC RHYOLITES

A few flows of ultrapotassic rhyolites are also found at Diri, Gurapratap Singh and Manihari along with the other felsic volcanics (andesite, dacite and rhyolite etc.). These ultrapotassic rhyolites are different in their chemical behavior from the associated felsic volcanics (Fig. 2.3) and presumably mark a different phase of magmatic activity.

Five samples of ultrapotassic rhyolites from Manihari were selected for Rb-Sr studies in order to know their exact relationship with the associated felsic volcanics. The Rb/Sr ratios of the selected samples range from 3.3 to 14.6. The analytical data are given in Table 4.5. Excluding one sample (GM/31), others conform to a linear array corresponding to an age of 681 ± 15 Ma (Fig. 4.6) with an initial Sr ratio of 0.7135 ± 0.0025. The MSWD of the fit is 1.75. The discrepancy of GM/31 may be due to either small size of the sample or slight alteration.

The primary crystallization age of 681 ± 15 Ma obtained for ultrapotassic rhyolites is about 100 Ma (at least 73 Ma) less than the age of 779 ± 10 Ma obtained for other associated felsic volcanics from Diri, Gurapratap Singh and Manihiri, indicating a different magmatic episode. Further, the initial $^{87}Sr/^{86}Sr$ ratio of ultrapotassic rhyolites is much higher (0.7135 ± 0.0025) than that of the associated andesite-dacite-rhyolite association (0.70612 ± 0.00046). The high initial Sr ratio of ultrapotassic rhyolites is due to incorporation of radiogenic ^{87}Sr from the country rock, by assimilation or fusion, into the residual fraction of the magma in the crust which gave rise to other differentiated rocks of the association.

Table 4.5. Rb-Sr isotopic data of ultrapotassic rhyolites from Manihari, Pali district.

Sample No.	^{87}Rb (ppm)	^{86}Sr (ppm)	^{87}Rb/^{86}Sr (atomic)	^{87}Sr/^{86}Sr (atomic)
GM/62	60.522	7.178	8.335	0.79639 ± 0.00016
GM/32	63.407	6.455	9.710	0.80579 ± 0.00011
GM/31*	95.384	6.821	13.823	0.85709 ± 0.00026
GM/350	95.186	5.014	18.766	0.89310 ± 0.00009
GM/396	79.964	1.799	43.923	1.14558 ± 0.00038

*** Not included in calculation**

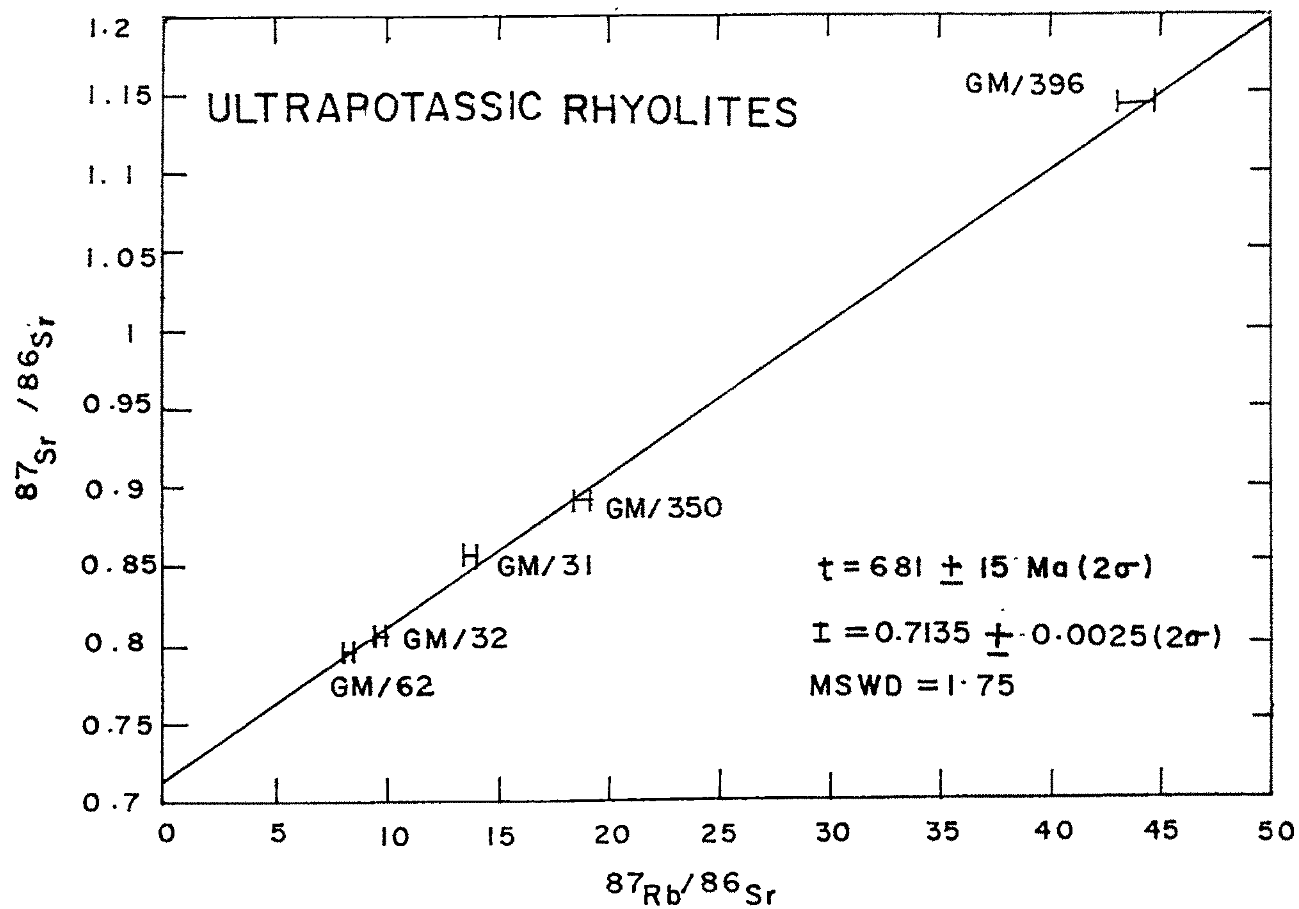

Fig. 4.6. Rb-Sr Conventional Isochron Diagram for Ultrapotassic Rhyolites from Diri and Gurapratap Singh.

4.3 ASSOCIATION II (*GRANITES AND ASSOCIATED VOLCANICS*)

As mentioned earlier the granites and associated volcanics constitute the most important rock types of the province. These rocks are mainly exposed in and around Jalore and Siwana area. The granites are divided into two groups i.e. peraluminous or normal granites (Jalore granite) and peralkaline granites (Siwana granite). The peralkaline granites occur in a ring structure along with the associated peralkaline volcanics as well as normal rhyolites (Fig. 2.7). These normal rhyolites have been named as outer rhyolites.

The petrology and geochemistry of these rocks have been studied by various workers (Murthy, 1962; Venkataraman et al., 1964; Bhusan and Yagi, 1981; Bhusan and Mohanty, 1988; Yadav 1988; Kochhar, 1989; Bhusan, 1991 and Yadav, 1991). However, the geochronological studies are very limited and the work is confined to only one isochron of Crawford and Compston (1970), which has yielded an age of 745 ± 10 Ma. These authors got the isochron from the rocks which were not only differing in their chemical compositions but also their field relationship was not known. Therefore, it is very important to study individual rock groups which are supposed to be cogenetic. In the present study, an attempt is made to date Jalore and Siwana granites as well as associated peralkaline volcanics and normal (outer) rhyolites separately to know their mutual relationship and understand, ultimately, the evolution of these granites and volcanics.

4.3.1. ^{40}Ar-^{39}Ar STUDIES

Two granite samples viz. JR/15 and JR/17 were analyzed for ^{40}Ar-^{39}Ar studies. The analytical results are given in Tables 4.6 and 4.7 and the age spectra are shown in Fig. 4.7 and 4.8. Both the samples have experienced secondary thermal disturbance. The age spectrum of JR/15 (Fig. 4.7) is more complicated owing to the presence of excess argon as has been indicated by U-shaped release curve. The minima of the spectrum is at 515 ± 6 Ma. In the successive higher temperature steps the age increases up to 924 ± 13 Ma

Table 4.6. Step heating argon isotopic compositions and apparent ages of sample JR 86/15 (JALORE GRANITE) J=0.00237 ± 0.00002

Temp. (°C)	$^{36}Ar/^{39}Ar$	$^{37}Ar/^{39}Ar$	$^{40}Ar/^{39}Ar$	Age (Ma)	^{39}Ar (%)	$^{40}Ar^*$ (%)
400	0.0266 ±0.0002	0.0399 ±0.0011	226.00 ±1.30	751 ±8	3.4	96.5
450	0.0107 0.0000	0.0614 0.0005	155.59 0.89	556 6	3.1	97.9
500	0.0072 0.0001	0.0679 0.0013	161.34 0.93	577 7	1.5	98.7
550	0.0072 0.0001	0.0760 0.0016	157.42 0.91	565 6	2.1	98.6
600	0.0057 0.0002	0.1277 0.0016	156.75 0.91	564 6	1.0	98.9
650	0.0066 0.0002	0.1453 0.0017	158.71 0.92	570 6	1.1	98.8
700	0.0081 0.0001	0.1312 0.0041	167.87 0.97	597 7	1.8	98.6
750	0.0078 0.0001	0.1224 0.0011	172.12 0.99	610 7	3.0	98.6
800	0.0071 0.0003	0.0745 0.0001	148.77 0.86	538 6	5.7	98.6
850	0.0079 0.0001	0.0518 0.0001	141.82 0.82	515 6	13.1	98.3
900	0.0083 0.0001	0.0379 0.0001	160.34 0.92	573 6	39.1	98.5
1000	0.0096 0.0001	0.0381 0.0004	170.13 0.98	602 7	23.1	98.3
1050	0.0369 0.0017	0.3389 0.0051	212.10 1.20	703 8	0.7	94.9
1100	0.0512 0.0035	0.6645 0.0034	273.80 1.60	862 11	0.3	94.5

contd.

Table 4.6. (contd.)

Temp. (°C)	$^{36}Ar/^{39}Ar$	$^{37}Ar/^{39}Ar$	$^{40}Ar/^{39}Ar$	Age (Ma)	^{39}Ar (%)	$^{40}Ar^*$ (%)
1150	0.0794 ±0.0081	1.0291 ±0.0251	288.50 ±2.00	879 ±17	0.1	91.9
1200	0.1201 0.0141	1.5870 0.0951	309.00 3.30	901 26	0.1	88.0
1250	0.1021 0.0072	0.9600 0.0211	301.90 2.20	897 16	0.2	90.0
1500	0.1555 0.0045	0.8910 0.0111	328.30 2.50	924 13	0.4	86.0
TOTAL	0.0104 0.0001	0.0627 0.0001	164.03 0.45	583 5	100.0	98.1

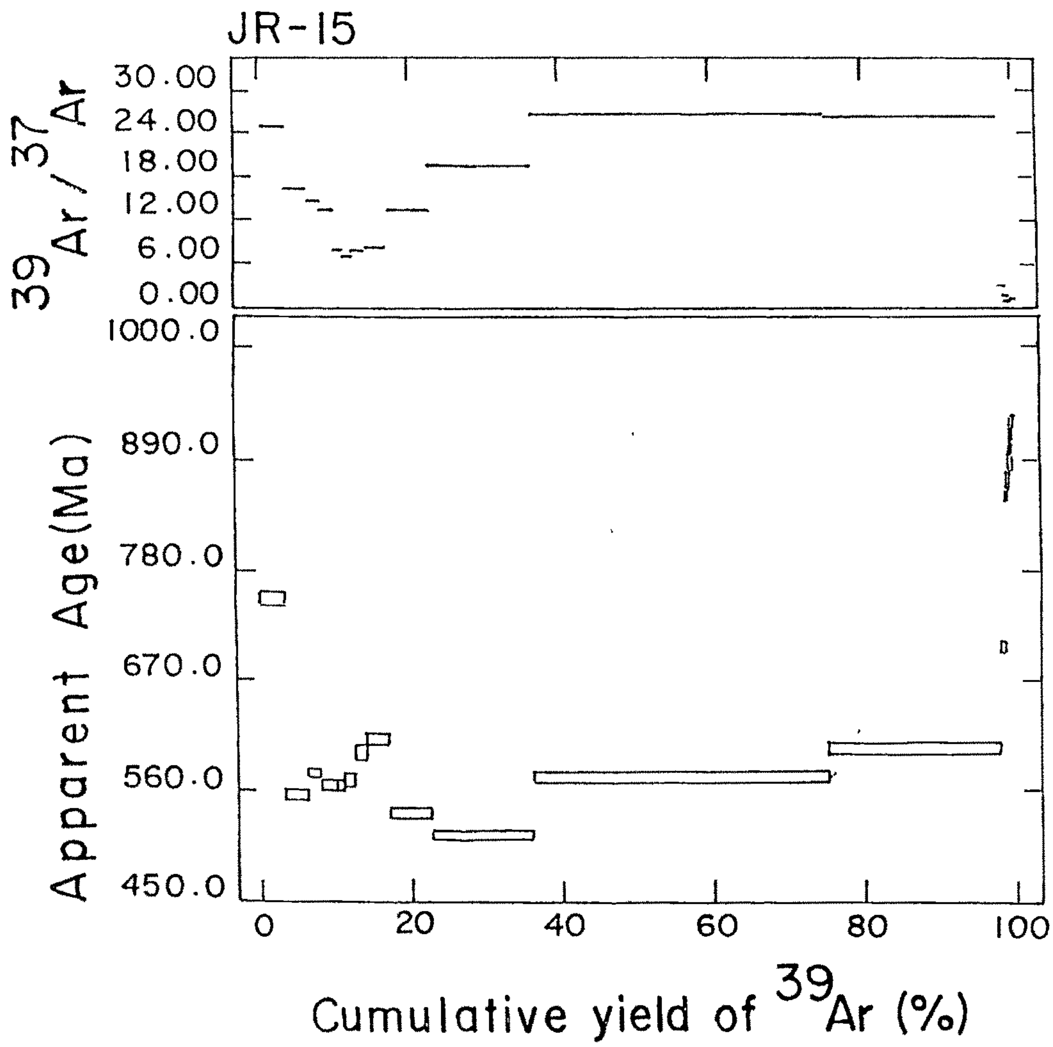

Fig. 4.7. ^{40}Ar-^{39}Ar Age Spectrum for Jalore Granite (JR 86/15).

Table 4.7. Step heating argon isotopic compositions and apparent ages of sample JR 86/17 (JALORE GRANITE) J=0.00238 ± 0.00005

Temp. (°C)	$^{36}Ar/^{39}Ar$	$^{37}Ar/^{39}Ar$	$^{40}Ar/^{39}Ar$	Age (Ma)	^{39}Ar (%)	$^{40}Ar^*$ (%)
500	0.0192 ±0.0007	0.0938 0.0053	134.52 ±0.68	482 12	3.2	95.8
550	0.0069 0.0004	-	128.53 0.65	475 11	4.3	98.4
600	0.0083 0.0008	0.1331 0.0077	146.06 0.74	530 13	2.3	98.3
650	0.0076 0.0047	-	161.02 0.83	578 16	1.6	98.6
700	0.0058 0.0013	0.1506 0.0038	170.94 0.88	611 14	1.7	99.0
750	0.0073 0.0013	0.1252 0.0010	181.68 0.93	642 15	1.6	98.8
800	0.0079 0.0009	0.1461 0.0003	184.72 0.94	650 15	2.4	98.7
850	0.0068 0.0005	0.1457 0.0036	152.39 0.77	552 13	5.1	98.7
900	0.0054 0.0002	0.0602 0.0017	147.60 1.30	538 14	9.3	98.9
950	0.0065 0.0001	-	148.76 0.74	541 13	15.1	98.7
1000	0.0062 0.0001	0.0525 0.0004	153.52 0.77	556 13	25.0	98.8
1050	0.0081 0.0001	-	152.51 0.76	551 13	22.9	98.4
1100	0.0308 0.0002	0.1585 0.0027	175.02 0.97	600 14	1.4	94.8
1500	0.0256 0.0073	0.1424 0.0046	170.72 1.50	592 21	4.1	95.6
TOTAL	0.0083 0.0003	0.0484 0.0004	152.75 0.32	552 12	100.0	98.4

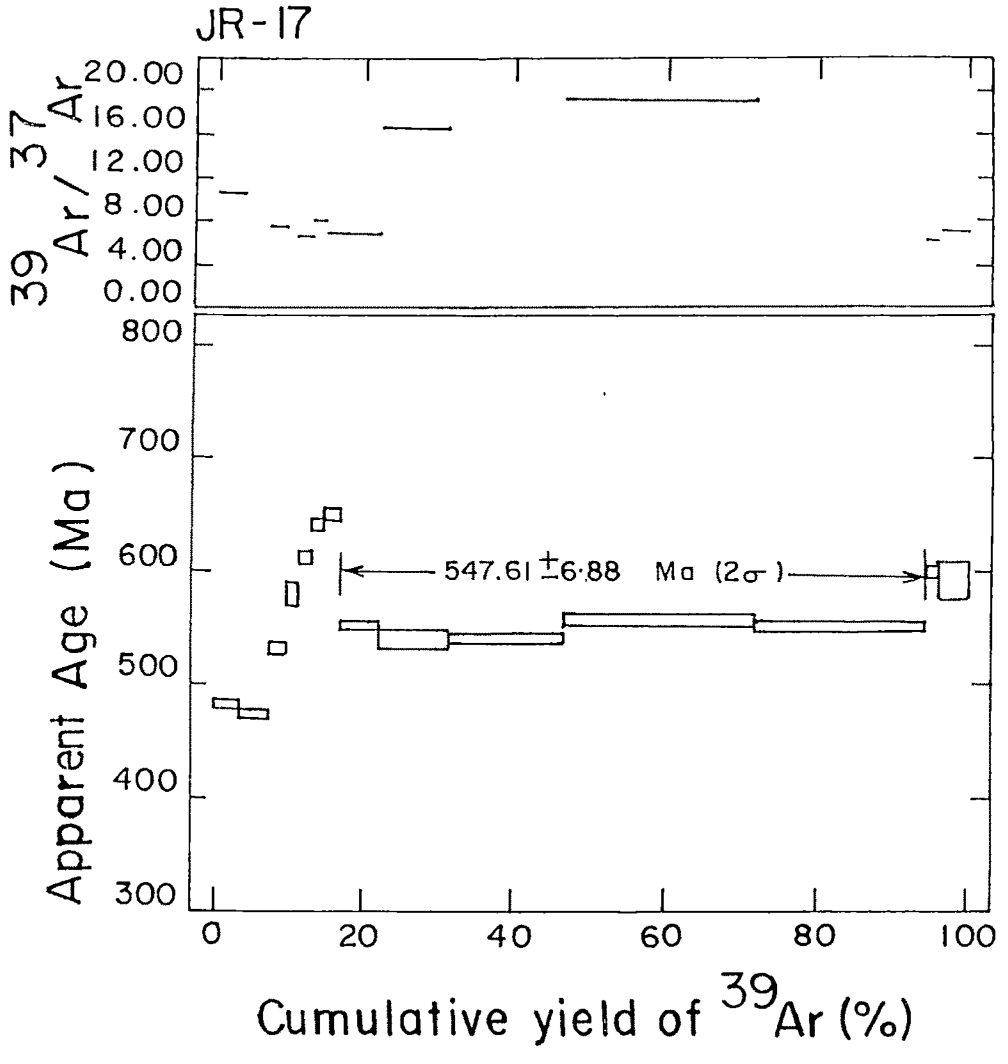

Fig. 4.8. ^{40}Ar-^{39}Ar Age Spectrum for Jalore Granite (JR 86/17).

though the last six temperature steps amount only 1.7% of total ^{39}Ar release. The total age is 583 ± 5 Ma.

As the emplacement time of the Jalore granites have been inferred at about 730 Ma ago by Rb-Sr studies (discussed in Rb-Sr studies part) the release spectrum of JR/15 can be interpreted as to indicate the time of secondary thermal disturbance at about 500 Ma ago.

The sample JR/17 shows more or less complete isotopic reequilibration as indicated by the straight/simple release spectrum (Fig. 4.8). However, the disturbance observed in both the samples, in initial seven temperature steps, have been from low temperature mineral phases which has been substantiated by $^{39}Ar/^{37}Ar$ plots also (Fig. 4.7 and 4.8). The intermediate five temperature steps (850 to 1050°C) of JR/17 apparently form a pseudo plateau at 548 ± 7 Ma amounting 77.4% of total ^{39}Ar release. The total age is 552 ± 12 Ma, which is not different from the plateau age, suggesting that the sample was completely reequilibrated at about 550 Ma ago. Thus, the ^{40}Ar-^{39}Ar studies of Jalore granites have also indicated the presence of secondary thermal disturbance between 500-550 Ma ago as has been witnessed by the felsic volcanics of Pali district.

4.3.2. Rb-Sr STUDIES

Here also, as the ^{40}Ar- ^{39}Ar studies could not reveal the time of formation due to secondary thermal event, Rb-Sr whole rock dating was employed to infer the emplacement time of Jalore and Siwana granites as well as associated volcanics. In the following sections individual isochrons are described in detail.

4.3.2.A. JALORE GRANITES (PERALUMINOUS GRANITES)

Seven whole rock samples of peraluminous granites were analyzed for Rb-Sr isotopic studies. The analytical data are given in Table 4.8 and plotted on a Sr evolution diagram shown in Fig. 4.9. The dispersion in Rb/Sr ratio among the samples is good ranging from 0.3 to 19.9. As can be seen all the samples except one (JR/15) conform

Table 4.8. Rb-Sr isotopic data of peraluminous granites from Jalore district.

Sample No.	^{87}Rb (ppm)	^{86}Sr (ppm)	$^{87}Rb/^{86}Sr$ (atomic)	$^{87}Sr/^{86}Sr$ (atomic)
SR/10	23.159	24.930	0.918	0.71520 ± 0.00030
JH/165	51.959	17.249	2.978	0.73608 ± 0.00035
TR/12	80.369	7.659	10.372	0.81620 ± 0.00152
JH/158	95.554	5.066	18.645	0.89636 ± 0.00014
JR/14	96.923	5.072	18.890	0.90022 ± 0.00013
JR/15*	129.702	2.729	46.973	1.25289 ± 0.00011
JR/17	127.699	2.060	61.278	1.34798 ± 0.00212

*** - Not included in calculation**

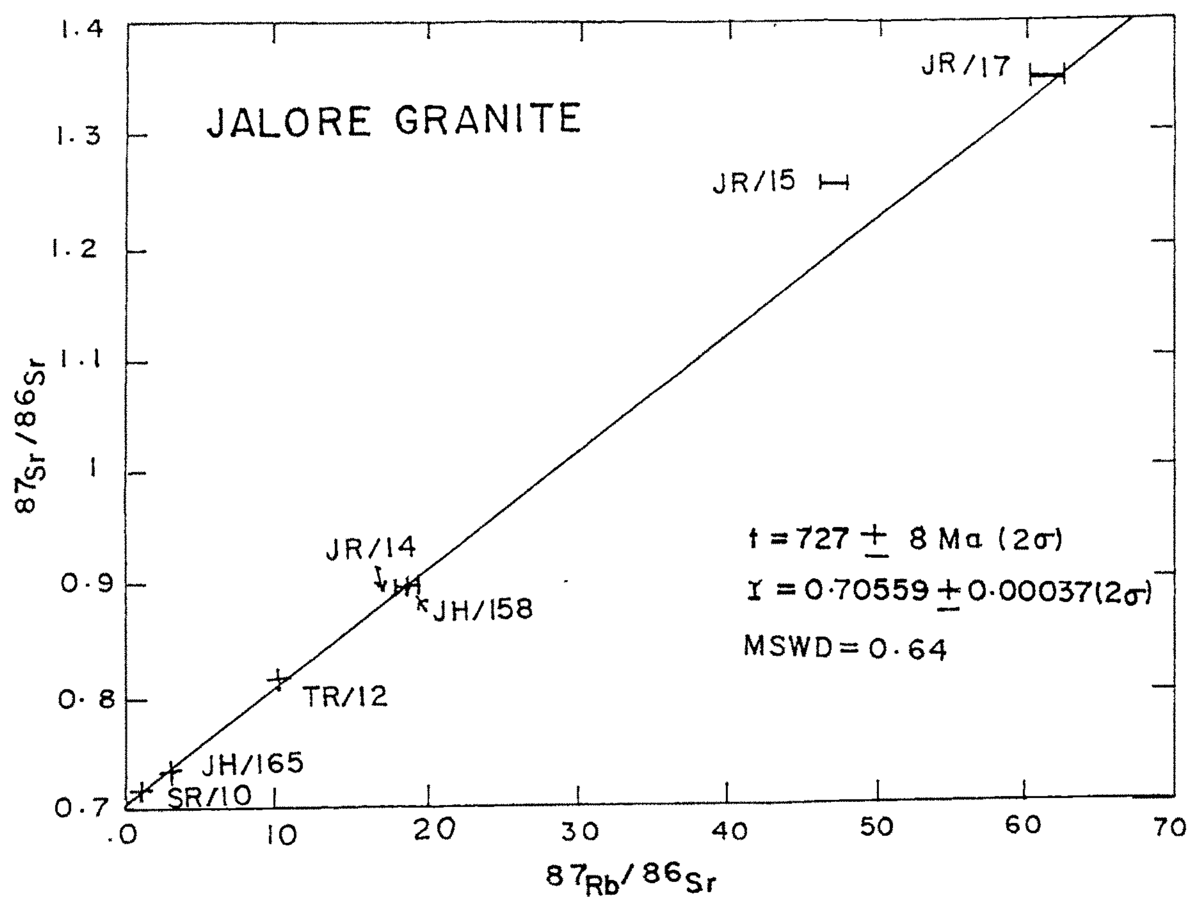

Fig. 4.9. Rb-Sr Conventional Isochron Diagram for Jalore Granite.

closely and evenly to a linear array. While the more radiogenic sample (JR/17) defines the slope within narrow limits, the least radiogenic samples (SR/10 and JH/165) constrains the intercept very closely. Two error regression of the six data points yields an isochron corresponding to an age of 727 ± 8 Ma and an intercept at 0.70559 ± 0.00037. The fit of the data points to a straight line is very good as indicated by very low MSWD of 0.69. This shows that all the analyzed samples have evolved as closed system from a common Sr composition about 730 Ma ago. The initial Sr isotopic ratio suggest lower crustal derivation of the magma. The age of 730 Ma represents the emplacement or primary crystallization time of the Jalore granites. Out of the seven samples analyzed three (i.e. JH/150, JH/165 and JR/14) were from main Jalore pluton while two samples i.e. SR/10 and TR/12 were from Sanphara and Tikhi, respectively. Sample JR/15 was from RSMDC mine (Kala Ghata) while JR/17 was from back of Jalore fort hill.

4.3.2.B. SIWANA GRANITES (PERALKALINE GRANITES)

Six whole rock samples of peralkaline granites were analyzed for Rb-Sr studies. Out of these four samples viz. A/D/32, A/F/41, A/K/91 and A/K/102 were collected from main Siwana granite pluton while the remaining two samples i.e. DR/25 and MO/19 were collected from Dewra and Mokalsar, respectively (Fig. 2.7). The analytical data are given in Table 4.9. The samples show good radiogenic enrichment and mutual spread in Rb/Sr ratios. A well defined isochron (Fig. 4.10) can be obtained from the data points which gives an age of 698 ± 10 Ma with an initial Sr ratio of 0.7067 ± 0.0041. The fit of the data to a straight line is excellent with the MSWD of 0.85.

From the foregoing discussion it is clear that Siwana granites are certainly younger, by atleast 11 Ma, than that of the Jalore (Peraluminous) granites. Therefore, these two type of granites i.e. peraluminous (Jalore type) and peralkaline (Siwana type) granites represent two different magmatic activities at short interval. The initial Sr ratios, however, could not be distinguished and suggest lower crustal origin of the magmas.

Table 4.9. Rb-Sr isotopic data of peralkaline granites and peralkaline volcanics from Siwana, Barmer district.

Sample No.	^{87}Rb (ppm)	^{86}Sr (ppm)	$^{87}Rb/^{86}Sr$ (atomic)	$^{87}Sr/^{86}Sr$ (atomic)
A/D/32	44.21	3.05	13.68	0.84110 ± 0.00021
DR/25	83.054	2.980	27.548	0.99030 ± 0.00140
MO/19	46.674	1.550	29.762	1.00100 ± 0.00200
A/E/101^{v}	102.19	1.599	63.187	1.33903 ± 0.00072
A/K/91	111.4	1.673	65.81	1.36050 ± 0.00004
A/K/102	71.57	0.803	88.10	1.57990 ± 0.00066
A/E/102^{v}	145.46	1.578	91.111	1.58591 ± 0.00059
A/F/51	129.11	1.38	92.48	1.61820 ± 0.00074

^{v} **peralkaline volcanics**

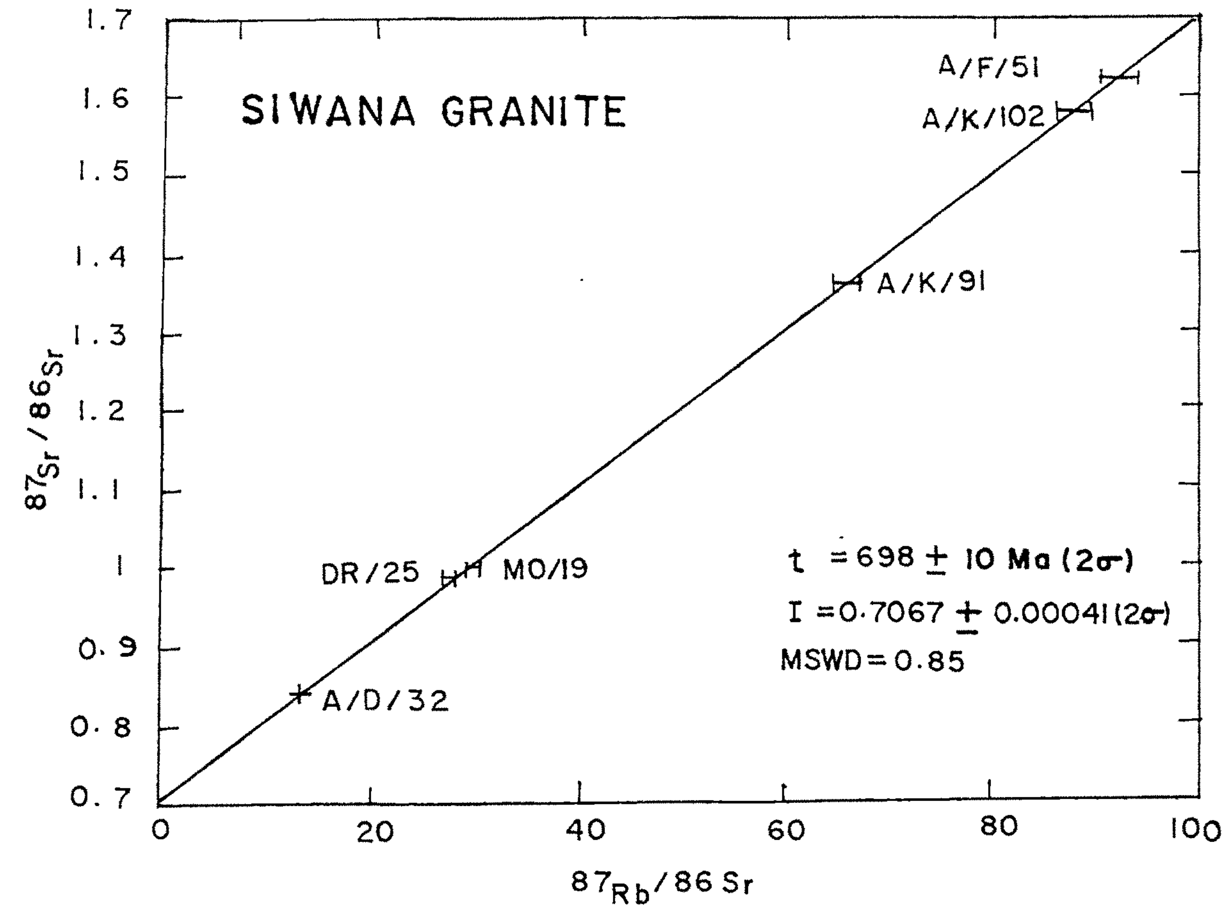

Fig. 4.10. Rb-Sr Conventional Isochron Diagram for Siwana Granite.

4.3.2.C. PERALKALINE VOLCANICS

The peralkaline volcanics i.e. soda-trachytes and pantellerites occur in association with the peralkaline granites (Fig. 2.7). To understand their temporal and genetic relationship with the peralkaline granites, two pantellerites (i.e. A/E/101 and A/E/102) were analyzed for Rb-Sr studies. The analytical data are given in Table 4.9. When these samples are regressed with the Siwana granites, the pooled isochron define an age of 693 ± 8 Ma with an initial Sr ratio of 0.7079 ± 0.0038 (Fig. 4.11). The MSWD of the fit is excellent at 0.92. This age and initial ratio is not different from the age and initial ratio of granites alone, thus, suggesting contemporaneity and cogenetic nature of these volcanics with that of the granites.

4.3.2.D. OUTER RHYOLITES

In addition to peralkaline granites and volcanics, normal rhyolites are also present at Siwana. These rhyolites occur at the southern extremity of the Siwana ring structure (Fig. 2.7) and have been named as outer rhyolites. In order to know their relationship with the peralkaline rocks, a set of five samples were selected which ranged in Rb/Sr ratio from 5.1 to 20.1. The analytical data are given in Table 4.10. One sample A/A/33 was excluded from the calculation as it was falling off from the best fit line. The line fitted to remaining four data points (Fig. 4.12) corresponds to an age of 674 ± 25 Ma with initial Sr ratio of 0.7110 ± 0.0066. The MSWD is 2.27 indicating that the fit of the straight line is reasonably good.

Though the age of the outer rhyolites cannot be distinguished from that of the associated peralkaline granites and volcanics, the Sr isotopic ratio is relatively high (0.7110) compared to the associated peralkaline rocks (0.7067 to 0.7079). Further, the age as well as initial Sr isotopic ratio of the outer rhyolites are remarkably similar to that of the ultrapotassic rhyolites of Manihari (681 ± 15 Ma, 0.7135 ± 0.0025), Pali district. This similarity got further bolstered from the fact that when the outer rhyolites and the ultrapotassic rhyolites are plotted together on the Sr evolution diagram. The eight data

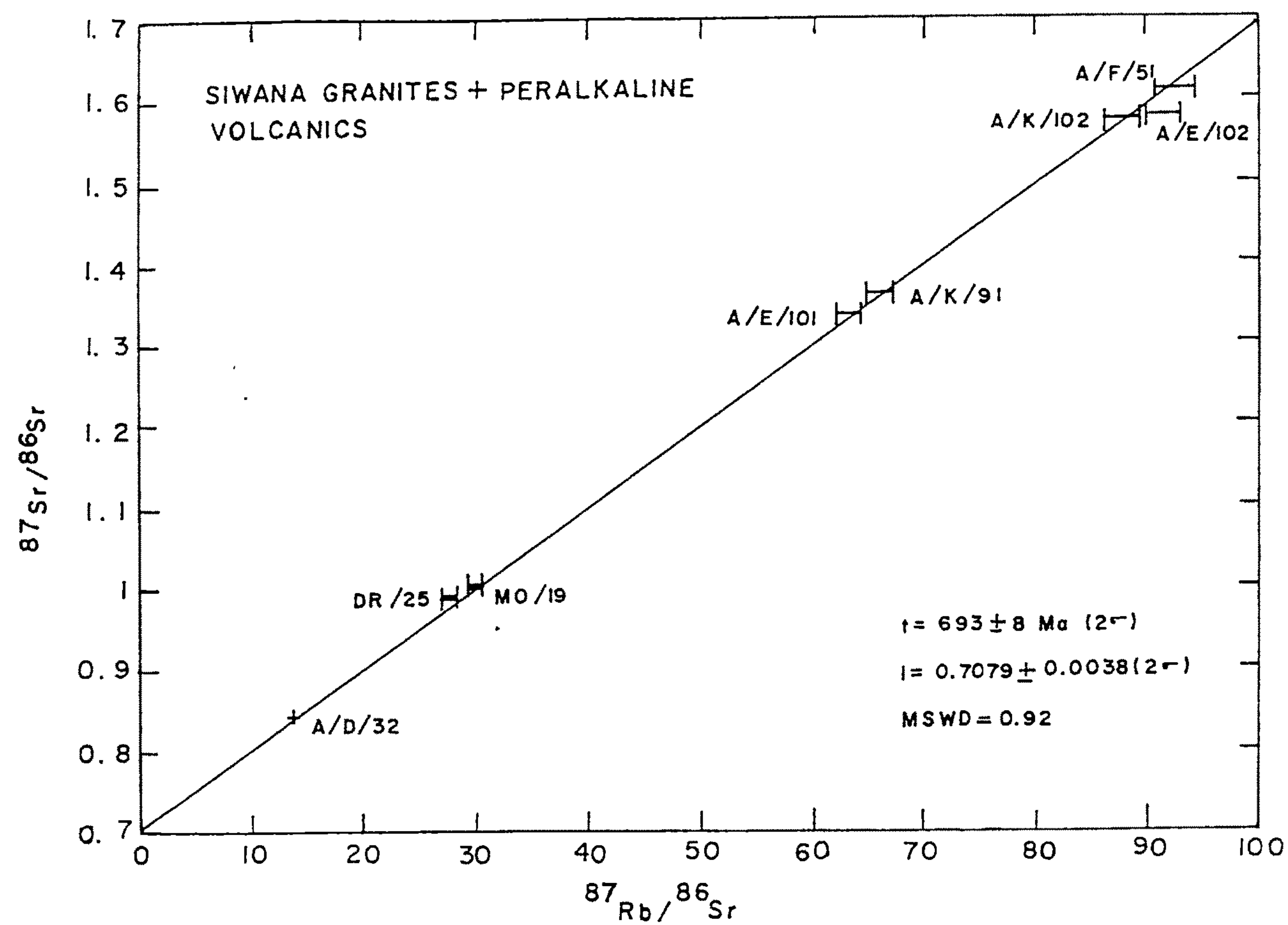

Fig. 4.11. Rb-Sr Conventional Pooled Isochron Diagram for Peralkaline Granites and Peralkaline Volcanics from Siwana.

Table 4.10. Rb-Sr isotopic data of outer rhyolites from South of Siwana, Barmer district.

Sample No.	^{87}Rb (ppm)	^{86}Sr (ppm)	$^{87}Rb/^{86}Sr$ (atomic)	$^{87}Sr/^{86}Sr$ (atomic)
A/D/12	44.316	2.940	14.899	0.85690 ± 0.00019
A/F/14	47.352	2.893	16.182	0.86641 ± 0.00016
A/I/21	58.121	2.459	23.369	0.92849 ± 0.00059
A/B/31*	52.582	1.663	31.259	1.01824 ± 0.00031
A/A/33	65.653	1.046	62.052	1.38111 ± 0.00053

*** - Not included in calculation**

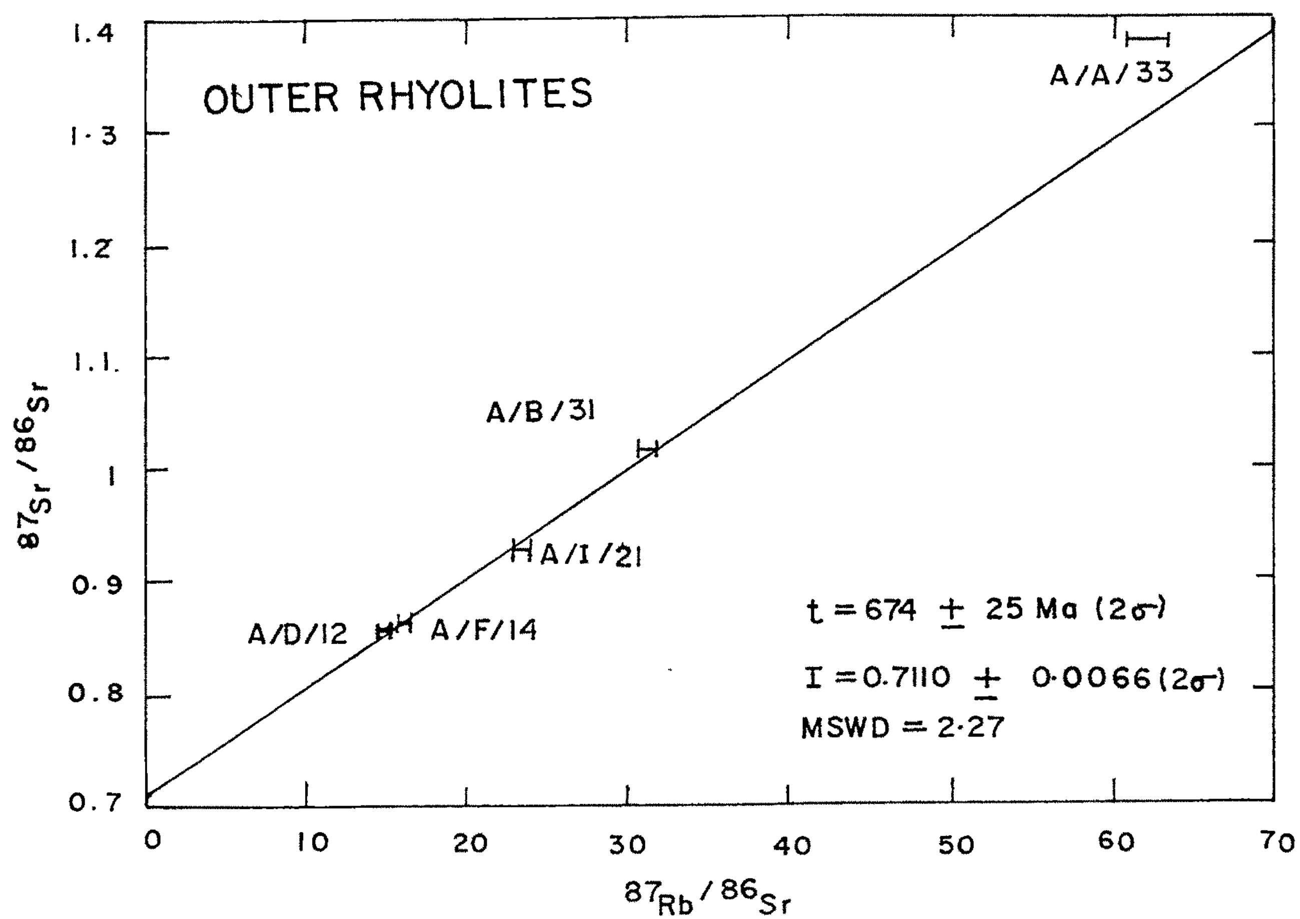

Fig. 4.12. Rb-Sr Conventional Isochron Diagram for Outer Rhyolites from Siwana.

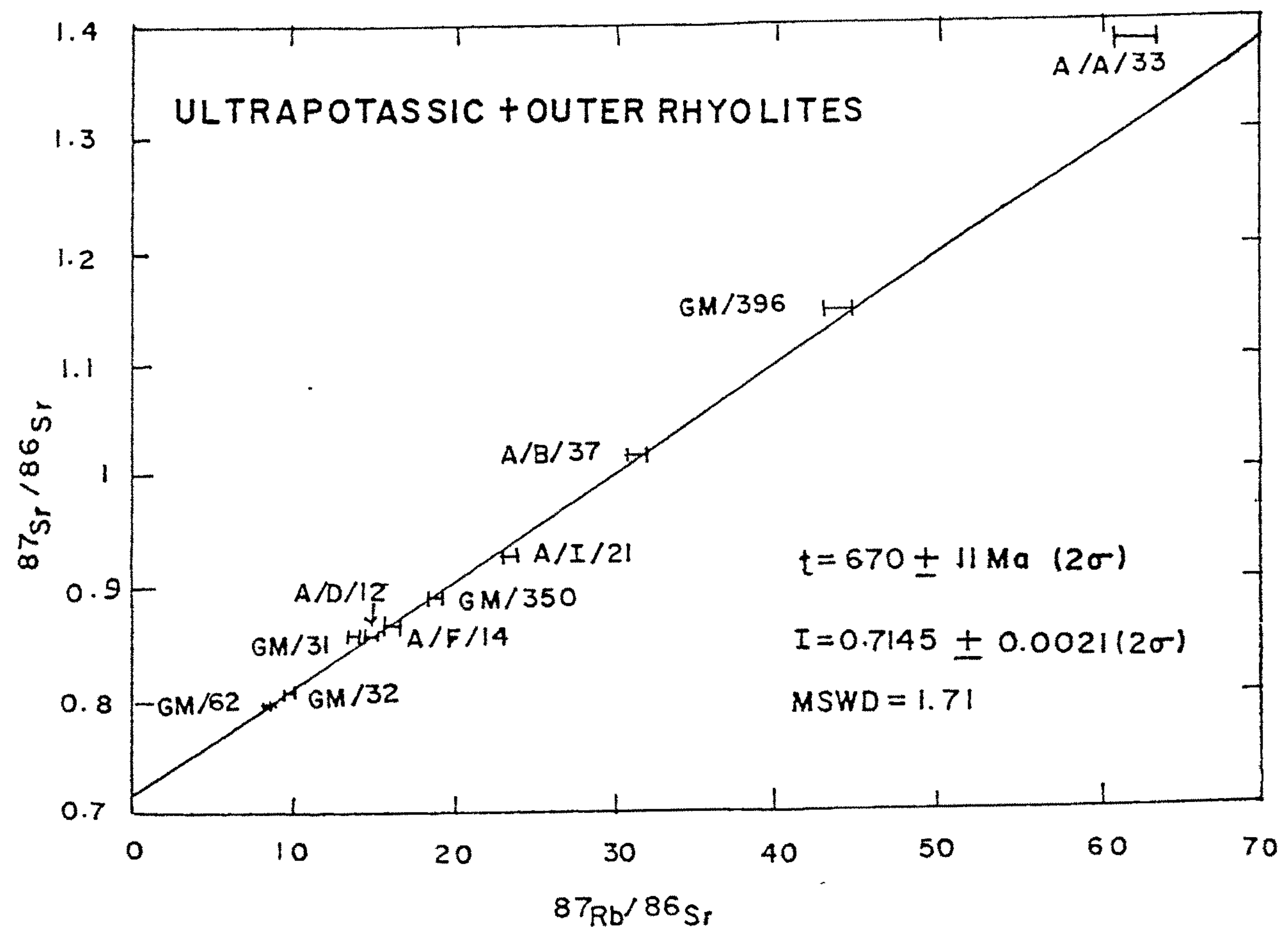

Fig. 4.13. Rb-Sr Conventional Pooled Isochron Diagram for Outer and Ultrapotassic Rhyolite.

points (excluding GM/31 and A/A/33) gave an isochron age of 670 ± 11 Ma (Fig. 4.13) with an initial Sr isotopic ratio of 0.7145 ± 0.0021. This age and initial Sr isotopic ratio is similar to the age and initial ratio obtained for ultrapotassic and outer rhyolites separately. Further, the MSWD comes down to 1.71 from 1.75 and 2.27, respectively.

This exercise, thus, indicates that the outer rhyolites and ultrapotassic rhyolites are probably derived from the same magma and crystallized at about 670 Ma ago. It may also be possible that the outer rhyolites are cogenetic with the peralkaline rocks and probably represent the end phase of the peralkaline activity, as suggested by Jacobson et al. (1958) and Bowden and Kinnaird (1978) for the Nigerian younger granitic province. According to these authors the peralkaline magma at the start of the magmatic cycle may turn to metaluminous to peraluminous at the end, giving rise to a close association of both metaluminous and peralkaline rocks within a single ring complex, the situation as observed at Siwana.

However, in either of the cases, the high initial ratio of the outer as well as ultrapotassic rhyolites is attributed to incorporation of radiogenic Sr in the residual crustal magma.

4.4. ASSOCIATION III (*TAVIDAR VOLCANICS*)

Agrawal (1984) has carried out detailed petrographic and geochemical studies of the mildly alkaline rocks of Tavidar volcanics. The various rocks from Tavidar belong to trachy basalt-trachy andesite-trachyte and rhyolite association (Fig. 1.3).

4.4.1. K-Ar STUDIES

In the initial phase of the work, seven samples were dated by K-Ar method and the results are given in Table 4.11. As the K-Ar ages showed wide scatter, ranging from 45 to 75 Ma, ^{40}Ar-^{39}Ar studies were carried out on the same samples. Out of the seven samples dated by K-Ar method, the ages of five samples were in agreement with ^{40}Ar-^{39}Ar ages within the experimental errors.

Table 4.11. Analytical data and calculated K-Ar ages of Tavidar volcanics, Jalore district.

Sample No. (Rock type)	K (wt%)	Total ^{40}Ar (10^{-6} cc $STPg^{-1}$)	Rad ^{40}Ar (10^{-6} cc $STPg^{-1}$)	Age (Ma)
VA/181 (K-Andesite)	2.83	10.90	8.58	76.4 ± 3.2
VA/181(**D**) (K-Andesite)	2.83	9.22	8.35	74.4 ± 3.8
VA/181(**T**) (K-Andesite)	2.83	9.67	8.48	75.5 ± 3.2
K/67 (K-Andesite)	3.08	22.45	5.42	44.7 ± 1.8
VA/58 (Trachyte)	3.69	13.83	10.01	68.3 ± 3.0
VA/A (Qtz-Trachyte)	4.72	19.07	12.05	64.5 ± 2.6
VA/168 (K-Rhyolite)	7.12	44.43	17.78	63.1 ± 2.6
VA/119 (Hawaiite)	1.68	5.61	4.51	67.9 ± 2.6
K/69A (Hawaiite)	0.85	3.24	2.12	63.0 ± 4.5

D - Duplicate and **T** - Triplicate analysis

However, two samples viz. K/67 and VA/181, both potassic andesites, gave very discordant K-Ar ages. The sample K/67 gave a K-Ar age of about 45 Ma which is quite low as compared to its ^{40}Ar-^{39}Ar age of 65 Ma. Sample VA/181 which was analyzed in triplicate, gave consistently higher K-Ar age of about 75 Ma, while its plateau age by ^{40}Ar-^{39}Ar method was 66 Ma. The anomalous but consistent higher K-Ar age of this sample as well as low age of other sample (K/67) could probably be due to K inhomogenity in the samples.

4.4.2. ^{40}Ar-^{39}Ar STUDIES

To assign precisely the formation time to the Tavidar volcanics, in all eight samples were analyzed by ^{40}Ar-^{39}Ar method. Out of the eight samples analyzed, two were potassic andesites (VA/181 and K/67), two trachytes (VA/58 and K/30), one rhyolite (VA/183), one potassic rhyolite (VA/168) and two hawaiites (VA/119 and K/69A). The samples were irradiated in two batches. The J factor varied from 0.00222 ± 0.00002 to 0.00234 ± 0.00005. The minimum and maximum values of J were those obtained for samples VA/181 and K/67, respectively.

The argon isotopic composition and abundances of these samples are given in Tables 4.12 to 4.19. Their age spectra and correlation diagrams are shown in Fig. 4.14 to 4.29. A summary of ^{40}Ar-^{39}Ar results is given in Table 4.20.

Interpretation of the results of ^{40}Ar-^{39}Ar incremental heating experiments is strongly influenced by graphical methods of presentation. Age spectrum diagrams are widely used and there is general agreement on the interpretation of the shape of age spectra. Isotope correlation plots of $^{40}Ar/^{39}Ar$ vs. $^{39}Ar/^{36}Ar$ (using data pertaining to the plateau steps), commonly referred to as isochron diagrams, have been used to present ^{40}Ar-^{39}Ar data, ever since the technique was first developed by Merrihue and Turner (1966). In this diagram the slope of the correlation line (isochron) is proportional to the age of the sample. The intercept on the $^{40}Ar/^{36}Ar$ axis is the isotopic composition of non-radiogenic argon in the sample, which is also called as ***'initial or trapped argon'***. It is generally assumed that the trapped argon in a sample and any background contribution from laboratory extraction apparatus is atmospheric in composition. This assumption is quite reasonable for the Tavidar volcanics, as all the samples have the intercept value of atmospheric composition i.e. $^{40}Ar/^{36}Ar = 295.5$ (Table 4.20) within the 2σ errors. Thus, the points that define an isochron are mixtures of radiogenic and atmospheric argon. The correlation lines for all the samples are well fitted with all values of MSWD less than 1 at 2σ level except for one sample VA/168, which has given MSWD of 1.2.

The age spectra for potassic andesites viz. VA/181 and K/67 (Fig. 4.14 and 4.15) define good plateaus, comprising 94% and 65.8% of ^{39}Ar released, with plateau ages of 65.9 ± 0.5 Ma and 64.6 ± 0.9 Ma, respectively. Their isochron ages (Fig. 4.16 and 4.17) are 65.5 ± 0.9 Ma and 63.5 ± 1.8 Ma, respectively. There is good agreement between the plateau and isochron ages of potassic andesites, within the experimental error, indicating that these samples have not lost any significant amount of radiogenic argon during their history. The undisturbed nature of these samples is reflected in the integrated or total ages also which are 66.6 ± 0.7 Ma and 65.7 ± 1.7 Ma for VA/181 and K/67, respectively.

The concordance of plateau, isochron and integrated ages for these two samples and considering somewhat disturbed nature of sample K/67, as inferred from its age spectrum diagram, the formation age of potassic andesites is taken as 65.9 Ma.

The release curve for two trachytes viz. VA/58 and K/30 define excellent plateaus (Fig. 4.18 and 4.19), comprising 80.4% and 100% of ^{39}Ar released and yielding plateau ages of 67.2 ± 0.4 Ma and 65.5 ± 0.6 Ma, respectively. The isochron ages (Fig. 4.20 and 4.21) for these samples are 67.6 ± 1.1 Ma and 65.5 ± 1.7 Ma, respectively. The plateau and isochron age of VA/58 is slightly higher than that of K/30.

However, the total ages of these samples are 65.6 ± 0.7 Ma and 65.6 ± 1.7 Ma, respectively, which are in excellent agreement with the plateau and isochron ages of K/30. Taking this fact into account, together with the straightforward interpretation of the perfect plateau of K/30 (100% ^{39}Ar release), it is believed that the trachytes were formed about 65.5 Ma ago. This age is indistinguishable from the age of andesites which were formed 65.9 Ma ago.

Sample VA/183 (rhyolite) has given an excellent plateau at 65.0 ± 0.4 Ma (Fig.

Table 4.12. Step heating argon isotopic compositions and apparent ages of sample VA/181 (TAVIDAR POTASSIC ANDESITE) J=0.00222 ± 0.00002

Temp. (°C)	$^{36}Ar/^{39}Ar$	$^{37}Ar/^{39}Ar$	$^{40}Ar/^{39}Ar$	Age (Ma)	^{39}Ar (%)	$^{40}Ar^{*}$ (%)
450	0.3164	1.7664	112.88	75.8	0.40	17.20
	±0.0078	±0.0137	0.96	19.0		
500	0.2154	1.6199	82.79	74.9	0.50	23.10
	0.0061	0.0062	0.74	14.8		
550	0.0115	0.5221	22.26	73.7	5.13	84.62
	0.0006	0.0038	0.14	1.8		
750	0.0033	0.3061	17.79	65.9	30.61	94.53
	0.0001	0.0026	0.10	0.9		
800	0.0020	0.1244	17.25	65.3	13.95	96.53
	0.0000	0.0006	0.10	0.9		
900	0.0044	0.0945	18.01	65.5	10.13	92.64
	0.0001	0.0019	0.11	0.9		
1000	0.0095	0.1117	20.03	67.4	16.82	85.86
	0.0004	0.0014	0.12	1.4		
1050	0.0108	0.2175	20.17	66.5	10.28	84.07
	0.0003	0.0007	0.12	1.3		
1150	0.0108	0.8969	20.24	66.8	5.24	84.16
	0.0006	0.0024	0.13	1.9		
1250	0.0123	3.0455	20.05	64.4	3.64	81.85
	0.0004	0.0065	0.14	1.6		
1350	0.0094	2.8513	19.78	66.7	2.30	86.00
	0.0014	0.0057	0.22	3.8		
1500	0.0089	2.2713	19.65	66.7	0.90	86.60
	0.0018	0.0141	0.34	4.8		
TOTAL	0.0088	0.4500	19.61	66.6	100.00	86.63
	0.0001	0.0009	0.05	0.7		

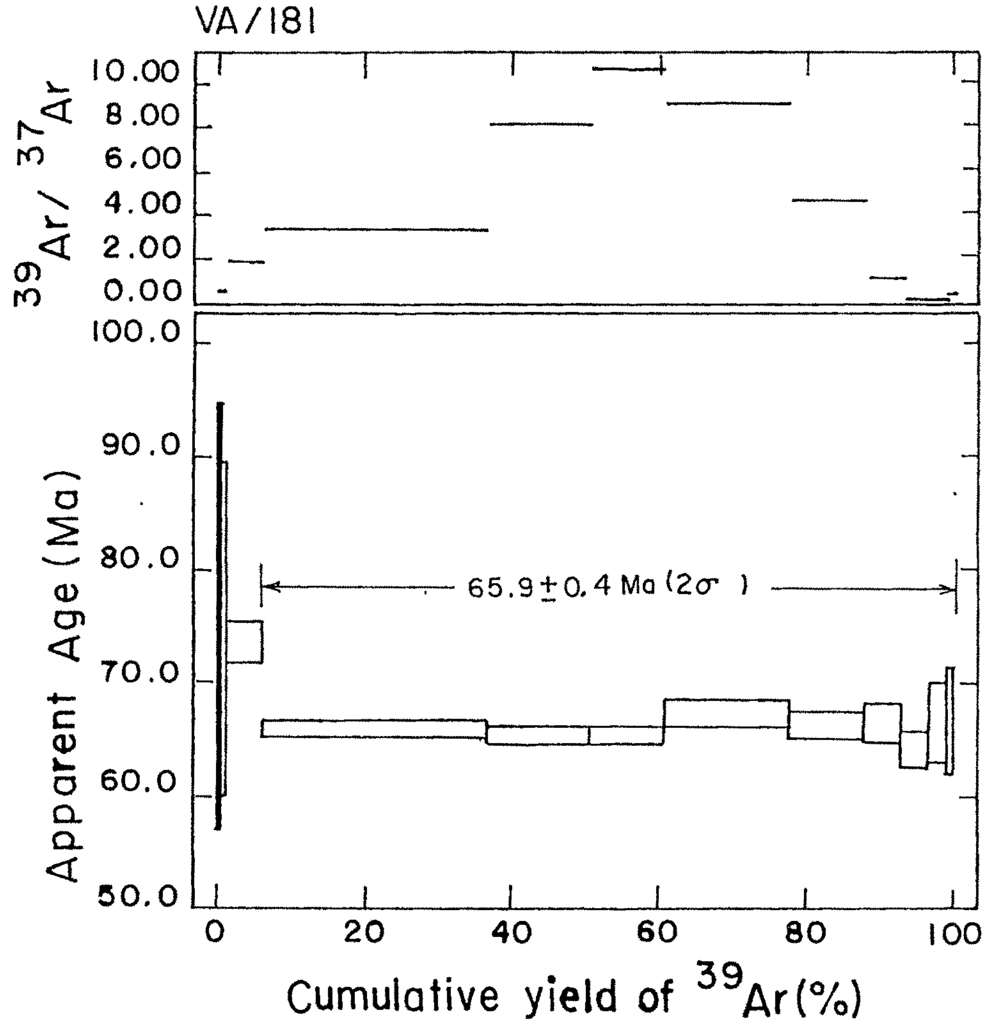

Fig. 4.14. ^{40}Ar-^{39}Ar Age Spectrum for Tavidar Andesite (VA/181).

Table 4.13. Step heating argon isotopic compositions and apparent ages of sample K/67 (TAVIDAR POTASSIC ANDESITE) J=0.00234 ± 0.00005

Temp. (°C)	$^{36}Ar/^{39}Ar$	$^{37}Ar/^{39}Ar$	$^{40}Ar/^{39}Ar$	Age (Ma)	^{39}Ar (%)	$^{40}Ar^*$ (%)
500	0.0961 ±0.0006	0.5864 ±0.0016	43.07 ±0.25	60.9 ±1.8	3.90	34.00
550	0.0124 0.0003	0.5168 0.0042	19.46 0.12	65.4 2.0	4.00	81.10
600	0.0141 0.0002	0.3891 0.0012	20.87 0.14	69.2 2.2	4.50	80.10
650	0.0222 0.0002	0.2991 0.0008	23.84 0.14	71.4 2.2	6.00	72.40
700	0.0173 0.0002	0.2921 0.0005	22.05 0.13	70.1 2.0	5.70	76.70
750	0.0151 0.0001	0.2728 0.0014	20.93 0.12	68.3 1.9	10.02	78.77
800	0.0083 0.0001	0.2666 0.0007	18.18 0.11	65.2 1.8	14.16	86.42
850	0.0101 0.0001	0.3057 0.0009	18.40 0.11	63.9 1.8	13.78	83.78
900	0.0152 0.0001	0.4167 0.0023	19.73 0.11	63.2 1.8	17.65	77.15
950	0.0145 0.0002	1.0283 0.0021	19.62 0.12	63.6 1.9	7.90	78.14
1000	0.0356 0.0006	1.4046 0.0028	26.20 0.18	64.9 2.6	2.70	59.80
1050	0.0350 0.0007	1.3061 0.0026	26.60 0.17	67.3 2.8	4.40	61.00
1100	0.0321 0.0018	1.2877 0.0046	26.70 0.37	71.3 5.4	1.00	64.50

contd.

Table 4.13. (contd.)

Temp. (°C)	$^{36}Ar/^{39}Ar$	$^{37}Ar/^{39}Ar$	$^{40}Ar/^{39}Ar$	Age (Ma)	^{39}Ar (%)	$^{40}Ar^{*}$ (%)
1200	0.0373 0.0006	1.3794 0.0028	26.88 0.24	65.7 3.0	3.30	59.00
1500	0.0011 ±0.0024	1.5901 ±0.0401	17.00 ±2.20	69.0 ±19.0	0.90	98.10
TOTAL	0.0192 0.0001	0.5262 0.0006	21.53 0.04	65.7 1.7	100.00	73.63

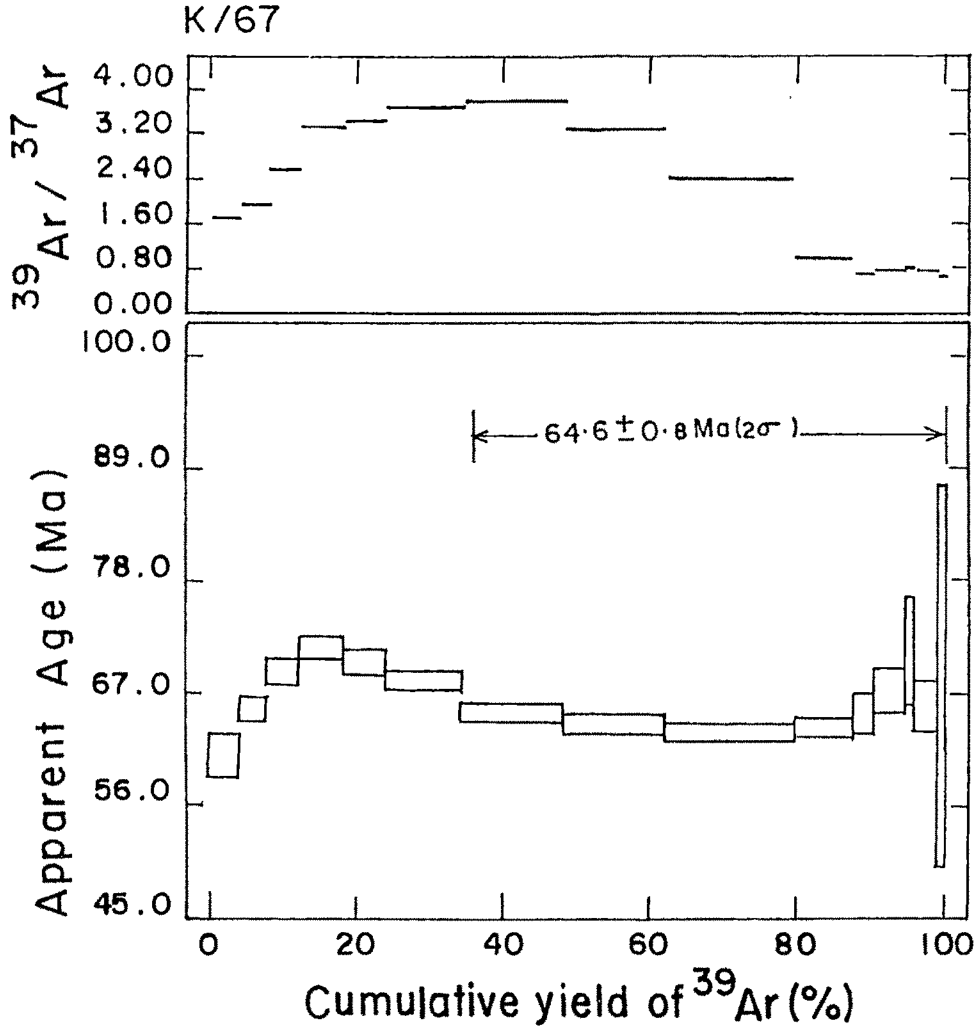

Fig. 4.15. ^{40}Ar-^{39}Ar Age Spectrum for Tavidar Andesite (K/67).

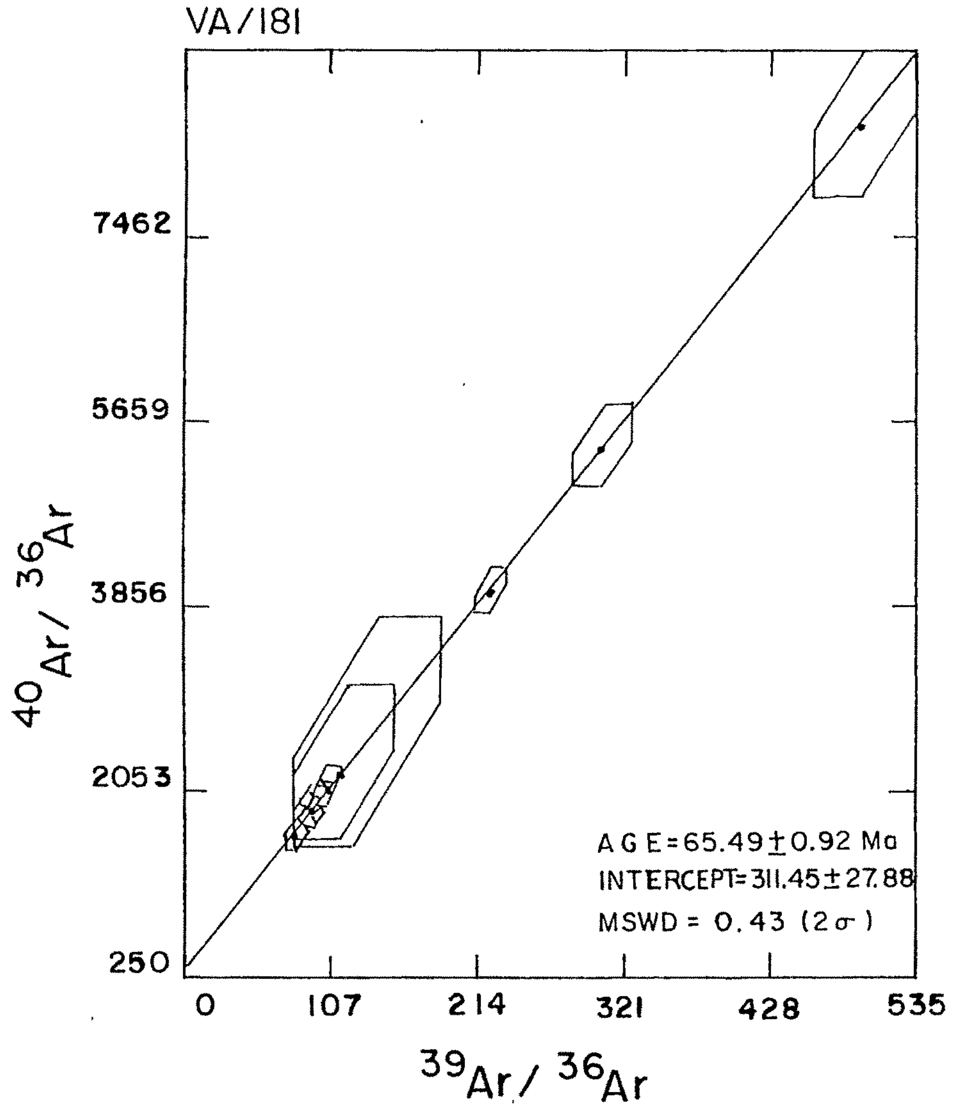

Fig. 4.16. **$^{40}Ar/^{36}Ar$ vs. $^{39}Ar/^{36}Ar$ Isochron Plot for Tavidar Andesite (VA/181).**

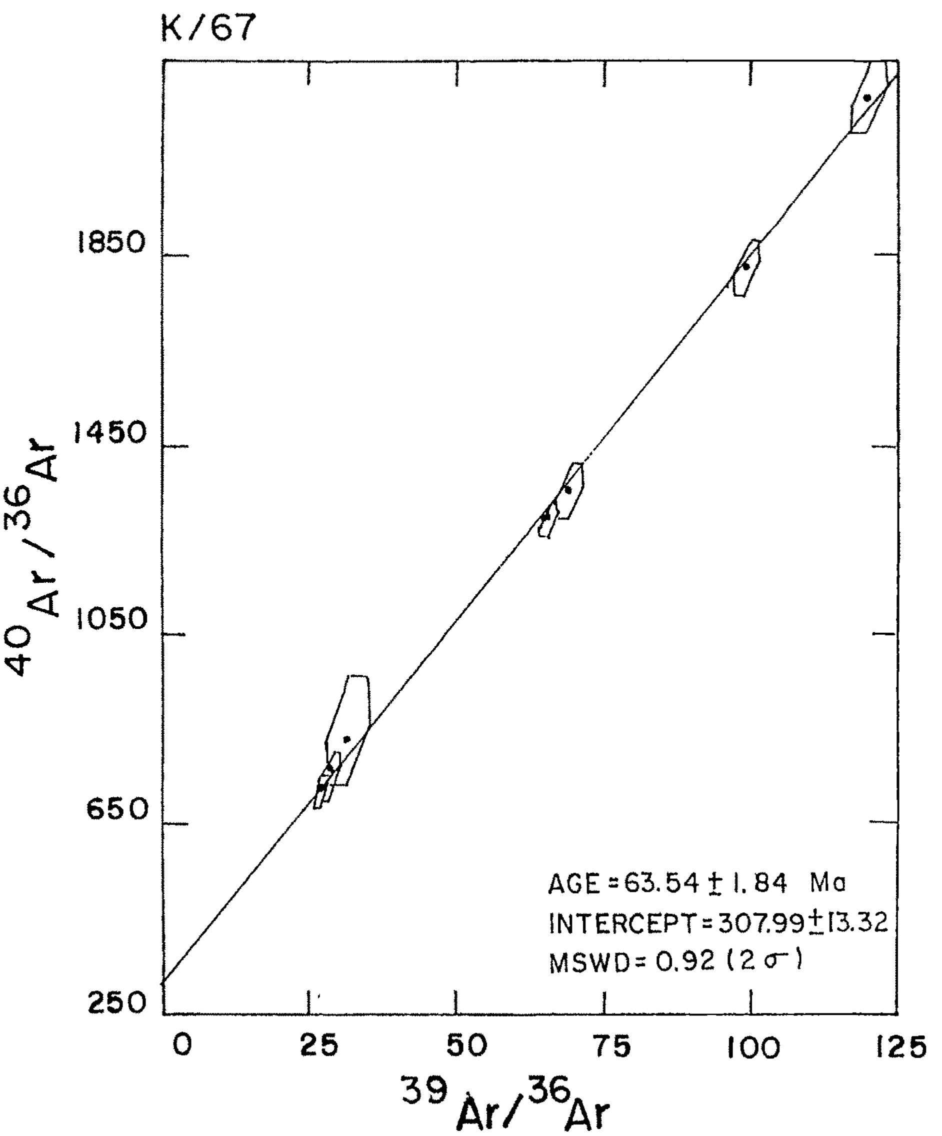

Fig. 4.17. $^{40}Ar/^{36}Ar$ vs. $^{39}Ar/^{36}Ar$ Isochron Plot for Tavidar Andesite (K/67).

Table 4.14. Step heating argon isotopic compositions and apparent ages of sample VA/58 (TAVIDAR TRACHYTE)
J=0.00224 ± 0.00002

Temp. (°C)	$^{36}Ar/^{39}Ar$	$^{37}Ar/^{39}Ar$	$^{40}Ar/^{39}Ar$	Age (Ma)	^{39}Ar (%)	$^{40}Ar^{*}$ (%)
350	0.0703 ±0.0003	0.3186 ±0.0009	33.74 0.20	51.7 1.7	6.23	38.41
500	0.0229 0.0003	0.3195 0.0014	22.42 0.13	62.2 1.4	9.28	69.75
550	0.0204 0.0004	0.6114 0.0074	21.65 0.15	62.1 1.6	4.12	72.14
700	0.0135 0.0004	0.9025 0.0021	20.55 0.15	65.7 1.6	4.09	80.54
750	0.0112 0.0001	0.2259 0.0036	20.49 0.14	68.1 1.2	5.10	83.76
800	0.0109 0.0004	0.1126 0.0006	20.08 0.14	66.8 1.5	4.70	83.82
900	0.0088 0.0001	0.0993 0.0003	19.83 0.12	68.3 1.0	19.01	86.75
1000	0.0109 0.0001	0.1265 0.0005	20.15 0.12	67.2 1.0	19.44	83.91
1100	0.0216 0.0001	0.2748 0.0007	22.92 0.13	65.6 1.1	20.50	72.04
1250	0.0414 0.0003	0.4363 0.0008	29.32 0.21	67.8 1.8	5.24	58.26
1350	0.0441 0.0024	0.4698 0.0015	31.07 0.69	71.5 7.8	1.50	58.00
1500	0.0874 0.0098	0.5459 0.0201	46.06 0.92	79.9 23.6	1.00	43.90
TOTAL	0.0207 0.0001	0.2624 0.0004	22.65 0.05	165.6 0.7	100.00	72.90

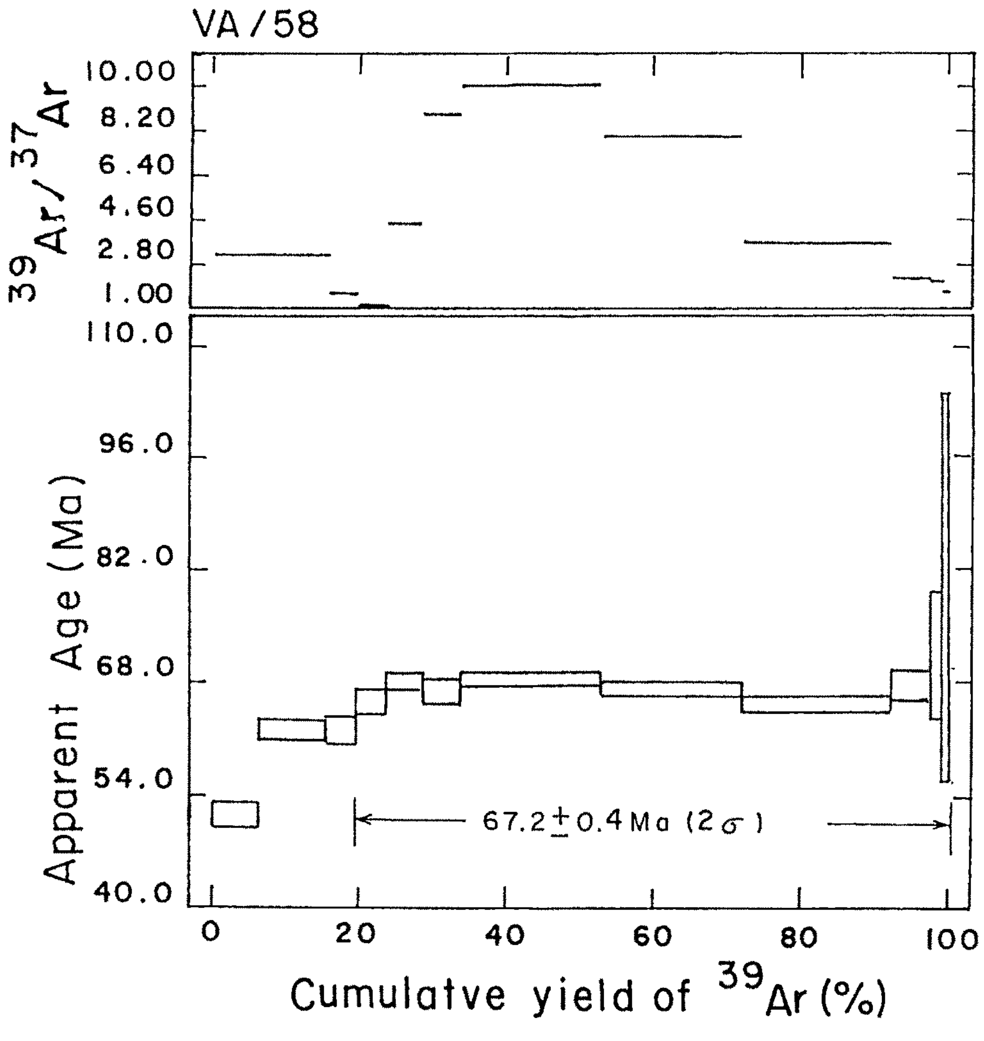

Fig. 4.18. ^{40}Ar-^{39}Ar Age Spectrum for Tavidar Trachyte (VA/58).

Table 4.15. Step heating argon isotopic compositions and apparent ages of sample K/30 (TAVIDAR TRACHYTE)
J=0.00233 ± 0.00005

Temp. (°C)	$^{36}Ar/^{39}Ar$	$^{37}Ar/^{39}Ar$	$^{40}Ar/^{39}Ar$	Age (Ma)	^{39}Ar (%)	$^{40}Ar^{*}$ (%)
500	0.2653	0.2505	94.57	66.6	1.70	17.10
	±0.0011	±0.0005	0.68	5.6		
550	0.0458	0.2568	29.75	66.7	2.40	54.50
	0.0003	0.0013	0.18	2.2		
600	0.0248	0.4799	23.60	67.0	5.26	68.95
	0.0001	0.0009	0.14	1.9		
650	0.0668	0.6632	35.61	65.4	6.30	44.60
	0.0002	0.0026	0.21	2.2		
700	0.0019	0.0708	16.62	66.1	20.70	96.53
	0.0001	0.0005	0.01	1.8		
750	0.0029	0.0486	16.84	65.8	8.99	94.85
	0.0001	0.0001	0.01	1.8		
800	0.0063	0.0647	17.70	65.2	6.15	89.35
	0.0001	0.0006	0.10	1.8		
850	0.0093	0.0608	18.52	64.9	7.60	85.03
	0.0001	0.0016	0.11	1.8		
900	0.0106	0.0648	18.89	64.9	9.13	83.35
	0.0001	0.0014	0.11	1.8		
950	0.0144	0.0832	20.26	65.9	11.85	78.90
	0.0001	0.0001	0.12	1.9		
1000	0.0199	0.1011	21.58	64.6	7.56	72.67
	0.0001	0.0007	0.13	1.9		
1050	0.0217	0.1788	22.33	65.6	4.70	71.30
	0.0002	0.0004	0.13	2.0		
1100	0.0206	0.2253	22.12	65.9	4.79	72.42
	0.0002	0.0004	0.13	1.9		
1200	0.0216	0.2632	21.93	64.1	2.80	70.90
	0.0004	0.0005	0.17	2.2		
TOTAL	0.0197	0.1551	21.76	65.6	100.00	73.20
	0.0001	0.0002	0.04	1.7		

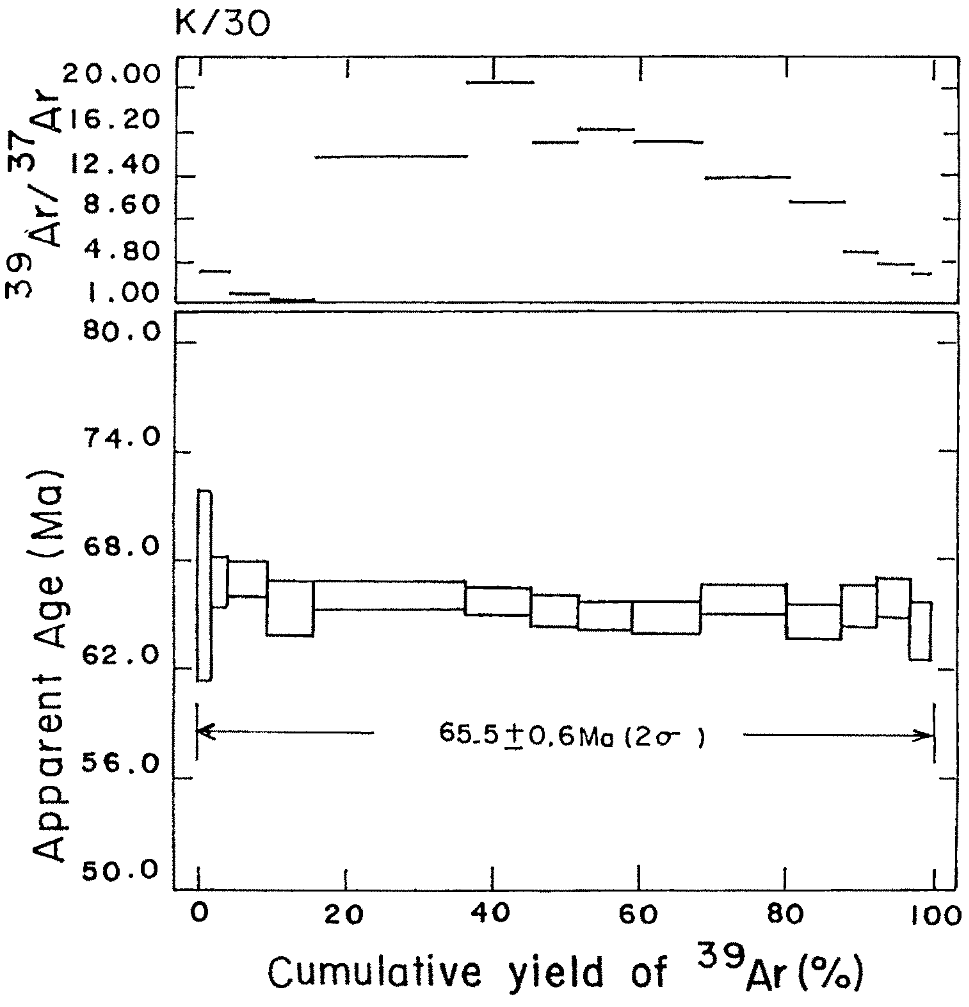

Fig. 4.19. ^{40}Ar-^{39}Ar Age Spectrum for Tavidar Trachyte (K/30).

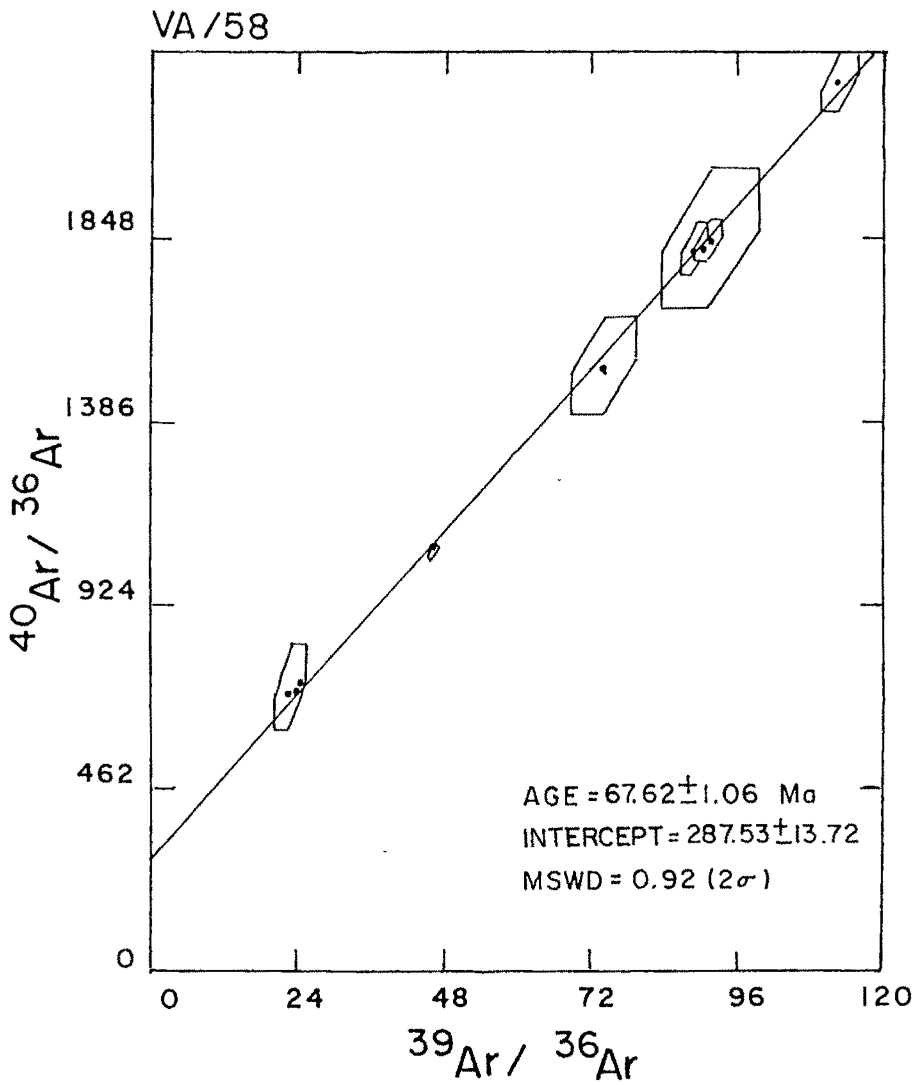

Fig. 4.20. $^{40}Ar/^{36}Ar$ vs. $^{39}Ar/^{36}Ar$ **Isochron Plot for Tavidar Trachyte (VA/58).**

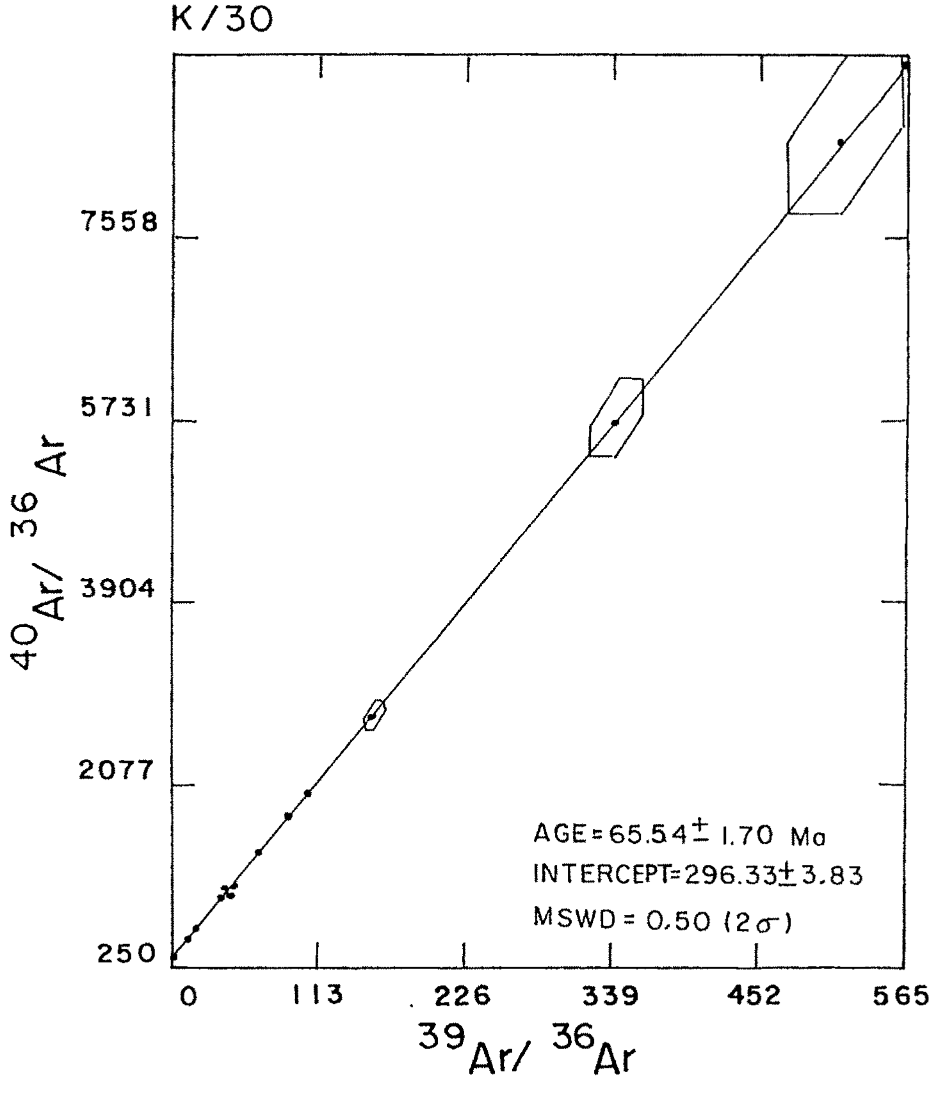

Fig. 4.21. $^{40}Ar/^{36}Ar$ vs. $^{39}Ar/^{36}Ar$ Isochron Plot for Tavidar Trachyte (K/30).

4.22) consisting of 100% ^{39}Ar released. The isochron (Fig. 4.23) and total ages for this sample are 64.5 ± 0.8 Ma and 65.1 ± 0.6 Ma, respectively. The concordance of plateau, isochron and total ages of VA/183 suggest that the rhyolite was formed 65 Ma ago.

One potassic rhyolite (VA/168) has been analyzed. In this sample comparatively less amount of ^{39}Ar release exhibit the plateau. The sample apparently shows a bi-modal ^{39}Ar release pattern (Fig. 4.24). The initial four temperature steps (excluding first step), comprising about 24% of total ^{39}Ar released, display a stair case pattern with progressively decreasing apparant ages, while the higher eight temperature steps (900° to fusion), comprising 59.5% of total ^{39}Ar released, form the plateau at 63.8 ± 0.8 Ma. However, no relation is reflected in the K/Ca ratio diagram. Thus, the stair case pattern observed in the initial temperature steps could be due to some experimental errors/recoil effect of ^{39}Ar during irradiation which may result either in loss of ^{39}Ar or increase of ^{39}Ar in slightly higher activation sites.

The isochron (Fig. 4.25) and total age of this sample are 62.8 ± 2.9 Ma and 63.3 ± 1.0 Ma, respectively. The conformity of plateau, isochron and total age of this sample suggest that there has not been any loss of argon after its formation and the age obtained from this sample infact indicates the time of its formation. Thus, the potassic rhyolite (VA/168) was formed 63.8 Ma ago.

In addition to the differentiated rocks, two hawaiites (VA/119 and K/69A) have also been dated. These samples have yielded good plateaus (Fig. 4.26 and 4.27) at 63.8 ± 0.8 Ma and 64.9 ± 0.8 Ma, comprising 84.7% and 67.7% of total ^{39}Ar released, respectively. The isochron ages (Fig. 4.28 and 4.29) for these samples are 64.2 ± 1.7 Ma and 65.3 ± 2.9 Ma, while the total ages are 64.5 ± 1.7 Ma and 61.7 ± 1.7 Ma, respectively. The total age of K/69A is slightly discordant from the total, plateau and isochron ages of VA/119 as well as plateau and isochron ages of K/69A itself. This discordance in the total age of K/69A is due to loss of argon in the initial as well as in the last three temperature steps, as is evident from the Fig. 4.27, resulting in lowering the total age of this sample. However, mutual similarity of plateau and isochron ages of these hawaiites indicate their emplacement about 64 Ma ago.

The plateau ages of Tavidar mildly alkaline rocks (see Table 4.20 for summary)

Table 4.16. Step heating argon isotopic compositions and apparent ages of sample VA/183 (TAVIDAR RHYOLITE)
J=0.00227 ± 0.00002

Temp. (°C)	$^{36}Ar/^{39}Ar$	$^{37}Ar/^{39}Ar$	$^{40}Ar/^{39}Ar$	Age (Ma)	^{39}Ar (%)	$^{40}Ar^{*}$ (%)
450	0.0366 ±0.0006	0.0581 ±0.0008	27.44 ±0.17	66.9 ±2.0	2.50	60.60
500	0.0114 0.0001	0.0476 0.0007	19.41 0.11	64.5 1.0	7.29	82.50
550	0.0104 0.0001	0.0591 0.0023	19.21 0.11	64.8 1.0	6.55	83.86
600	0.0123 0.0001	0.0293 0.0007	19.57 0.12	64.1 1.0	8.37	81.31
650	0.0059 0.0001	0.0154 0.0003	17.65 0.11	64.0 0.9	7.02	90.07
700	0.0059 0.0001	0.2162 0.0004	17.92 0.11	65.0 1.0	4.15	90.19
750	0.0076 0.0001	0.0321 0.0003	18.45 0.11	65.1 0.9	5.64	87.72
800	0.0092 0.0001	0.0211 0.0001	18.99 0.11	65.4 0.9	11.61	85.53
900	0.0123 0.0001	0.0246 0.0008	19.89 0.12	65.4 1.0	9.60	81.72
1000	0.0151 0.0001	0.0213 0.0007	20.78 0.12	65.6 1.0	10.69	78.43
1050	0.0204 0.0001	0.0301 0.0001	22.27 0.14	65.4 1.2	8.13	72.93
1150	0.0251 0.0001	0.2287 0.0016	23.74 0.14	65.6 1.1	12.13	68.68
1250	0.0370 0.0004	0.0404 0.0008	27.32 0.22	65.9 1.9	2.47	59.92

contd.

Table 4.16. (contd.)

Temp. (°C)	$^{36}Ar/^{39}Ar$	$^{37}Ar/^{39}Ar$	$^{40}Ar/^{39}Ar$	Age (Ma)	^{39}Ar (%)	$^{40}Ar^{*}$ (%)
1300	0.0372 ±0.0007	0.0878 ±0.0078	27.36 ±0.32	65.8 ±3.0	1.40	59.97
1350	0.0436 0.0008	0.0970 0.0047	28.75 0.35	63.8 3.4	1.20	55.10
1500	0.0359 0.0017	0.1044 0.0051	26.95 0.49	65.7 5.6	1.20	60.60
TOTAL	0.0155 0.0000	0.0651 0.0003	20.78 0.04	65.1 0.6	100.00	77.86

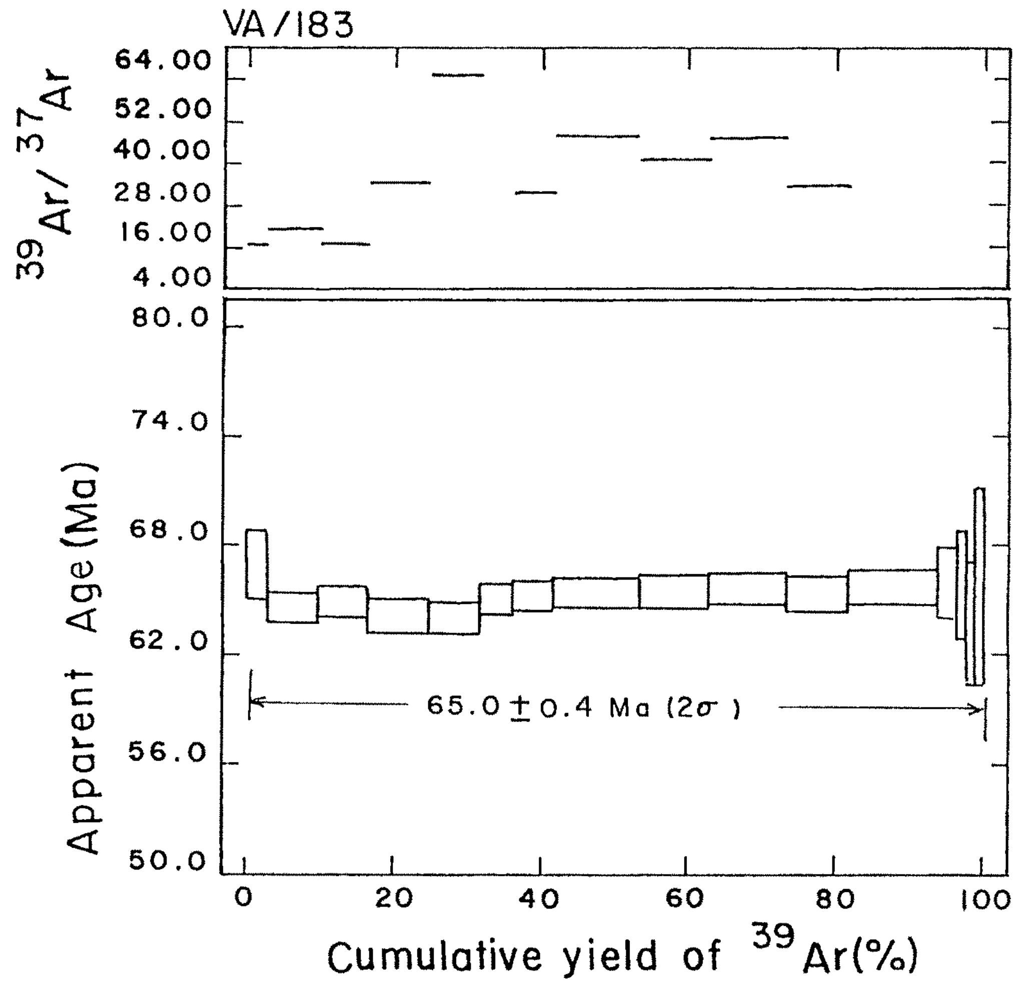

Fig. 4.22. ^{40}Ar-^{39}Ar Age Spectrum for Tavidar Rhyolite (VA/183).

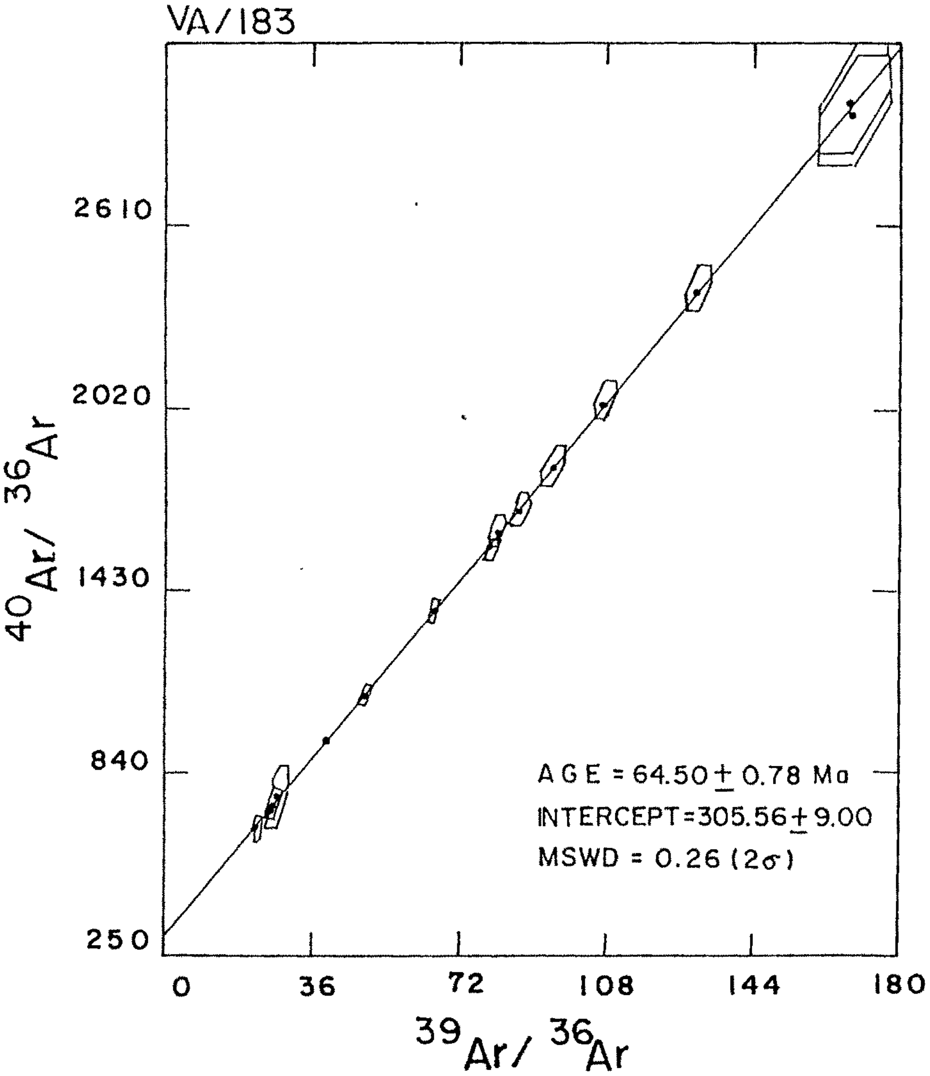

Fig. 4.23. $^{40}Ar/^{36}Ar$ vs. $^{39}Ar/^{36}Ar$ Isochron Plot for Tavidar Rhyolite (VA/183).

Table 4.17. Step heating argon isotopic compositions and apparent ages of sample VA/168 (TAVIDAR POTASSIC RHYOLITE) J=0.00233 ± 0.00003

Temp. (°C)	$^{36}Ar/^{39}Ar$	$^{37}Ar/^{39}Ar$	$^{40}Ar/^{39}Ar$	Age (Ma)	^{39}Ar (%)	$^{40}Ar^*$ (%)
450	1.0385 ±0.0036	0.0326 ±0.0047	314.10 1.80	30.0 14.0	1.60	2.30
500	0.2599 0.0009	0.0132 0.0013	93.08 0.54	67.0 4.2	4.20	17.50
550	0.1235 0.0004	0.0078 0.0006	51.74 0.30	62.8 2.4	7.10	29.40
600	0.1101 0.0004	0.0079 0.0006	47.02 0.27	59.8 2.2	6.80	30.80
650	0.0602 0.0002	0.0154 0.0008	31.58 0.18	57.0 1.5	5.73	43.65
700	0.0469 0.0002	0.0158 0.0001	30.66 0.18	69.2 1.6	4.72	54.78
750	0.0417 0.0002	0.0121 0.0004	28.88 0.17	68.1 1.5	5.29	57.24
800	0.0417 0.0002	0.0121 0.0004	28.73 0.17	67.6 1.5	5.06	57.09
900	0.0504 0.0002	0.0000 0.0000	30.47 0.18	64.2 1.6	6.95	51.07
1000	0.0683 0.0002	0.0068 0.0003	34.99 0.20	61.1 1.7	9.38	42.30
1050	0.0924 0.0003	0.0038 0.0001	42.63 0.25	63.2 1.9	14.63	35.92
1150	0.1085 0.0003	0.0074 0.0001	48.10 0.28	66.1 2.2	9.80	33.30
1250	0.1207 0.0004	0.0054 0.0007	50.84 0.29	62.5 2.2	15.10	29.80
1350	0.0802 0.0008	0.0366 0.0002	39.90 0.24	66.8 2.8	2.40	40.60

contd.

Table 4.17 (contd.)

Temp. (°C)	$^{36}Ar/^{39}Ar$	$^{37}Ar/^{39}Ar$	$^{40}Ar/^{39}Ar$	Age (Ma)	^{39}Ar (%)	$^{40}Ar^{*}$ (%)
1400	0.0825 ±0.0012	0.1354 ±0.0002	41.04 0.50	68.7 5.0	0.60	40.60
1500	0.0818 0.0023	0.1236 0.0002	41.59 0.66	71.7 7.6	0.60	41.90
TOTAL	0.1086 0.0001	0.0102 0.0001	47.43 0.08	63.2 1.0	100.00	32.30

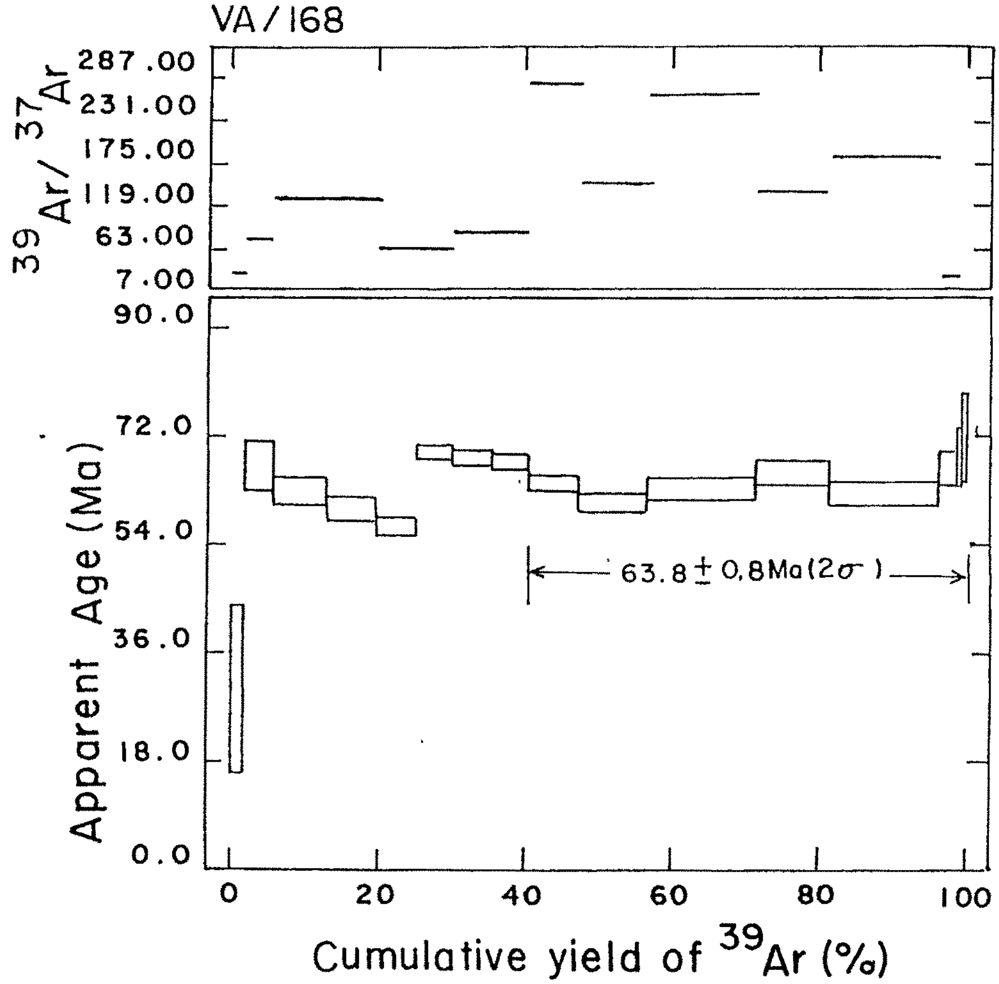

Fig. 4.24. ^{40}Ar-^{39}Ar Age Spectrum for Tavidar Potassic Rhyolite (VA/168).

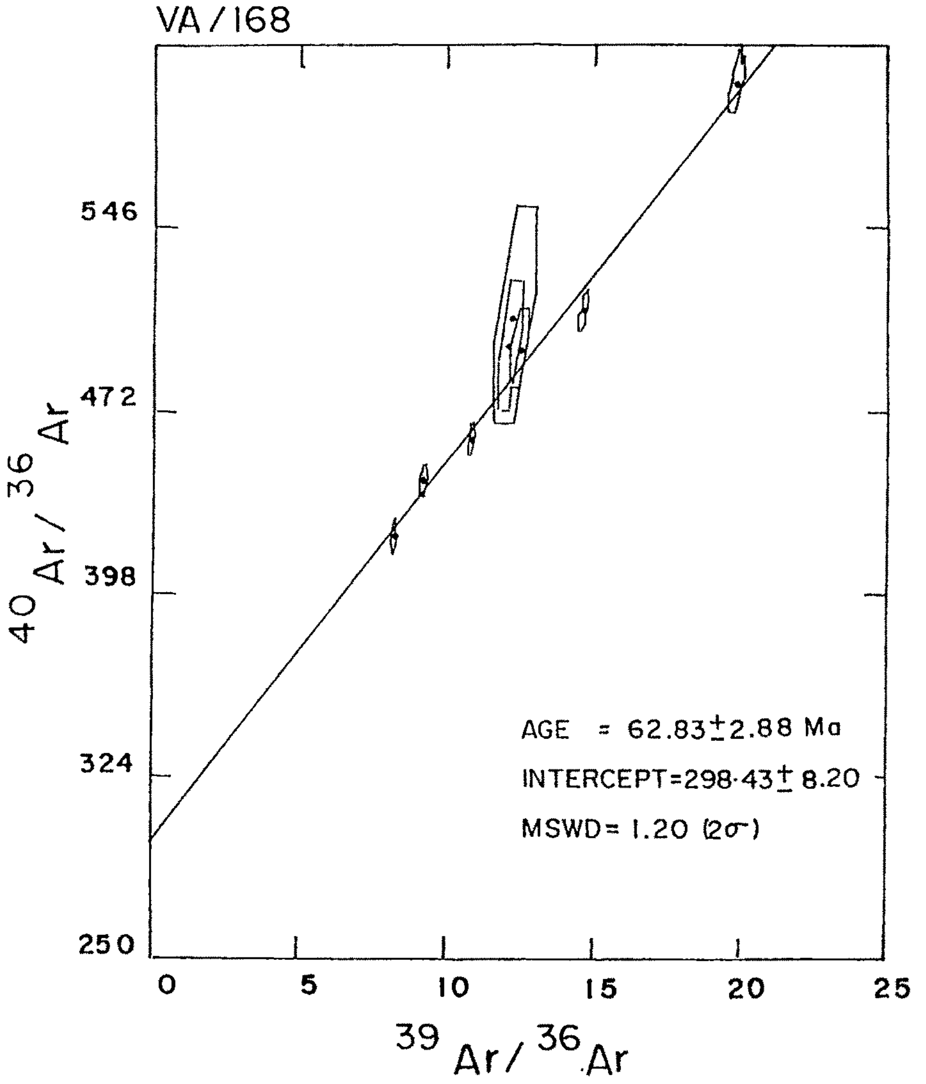

Fig. 4.25. $^{40}Ar/^{36}Ar$ vs. $^{39}Ar/^{36}Ar$ Isochron Plot for Tavidar Potassic Rhyolite (VA/168).

Table 4.18. Step heating argon isotopic compositions and apparent ages of sample VA/119 (TAVIDAR HAWAIITE)
J=0.00234 ± 0.00005

Temp. (°C)	$^{36}Ar/^{39}Ar$	$^{37}Ar/^{39}Ar$	$^{40}Ar/^{39}Ar$	Age (Ma)	^{39}Ar (%)	$^{40}Ar^{*}$ (%)
500	0.0741 ±0.0004	1.1012 ±0.0022	36.67 ±0.25	61.3 ±2.6	2.90	40.30
550	0.0411 0.0004	1.3066 0.0026	27.23 0.19	62.4 2.4	3.60	55.30
600	0.0461 0.0003	1.3351 0.0027	30.38 0.20	69.3 2.4	4.20	55.10
650	0.0452 0.0003	1.8148 0.0036	31.07 0.20	73.1 2.4	4.60	56.90
700	0.0678 0.0006	3.1631 0.0063	35.48 0.23	64.0 2.8	3.80	43.50
750	0.0531 0.0007	5.0971 0.0011	31.19 0.19	64.1 2.8	5.40	49.60
800	0.0077 0.0002	1.5023 0.0031	17.85 0.11	64.4 1.9	7.81	87.16
850	0.0064 0.0001	0.8309 0.0027	17.53 0.11	64.7 1.9	9.29	89.14
900	0.0073 0.0001	0.6767 0.0014	17.83 0.10	64.9 1.8	21.79	87.90
950	0.0097 0.0001	0.8911 0.0018	18.28 0.11	63.7 1.8	22.96	84.16
1000	0.0143 0.0003	3.6797 0.0074	19.25 0.13	62.2 2.0	5.64	77.98
1050	0.0218 0.0004	4.0811 0.0011	21.27 0.14	61.4 2.2	5.80	69.60
1100	0.0261 0.0008	4.0936 0.0082	23.24 0.28	64.3 5.4	2.20	66.80
TOTAL	0.0207 0.0001	1.6958 0.0012	21.72 0.04	64.5 1.7	100.00	71.70

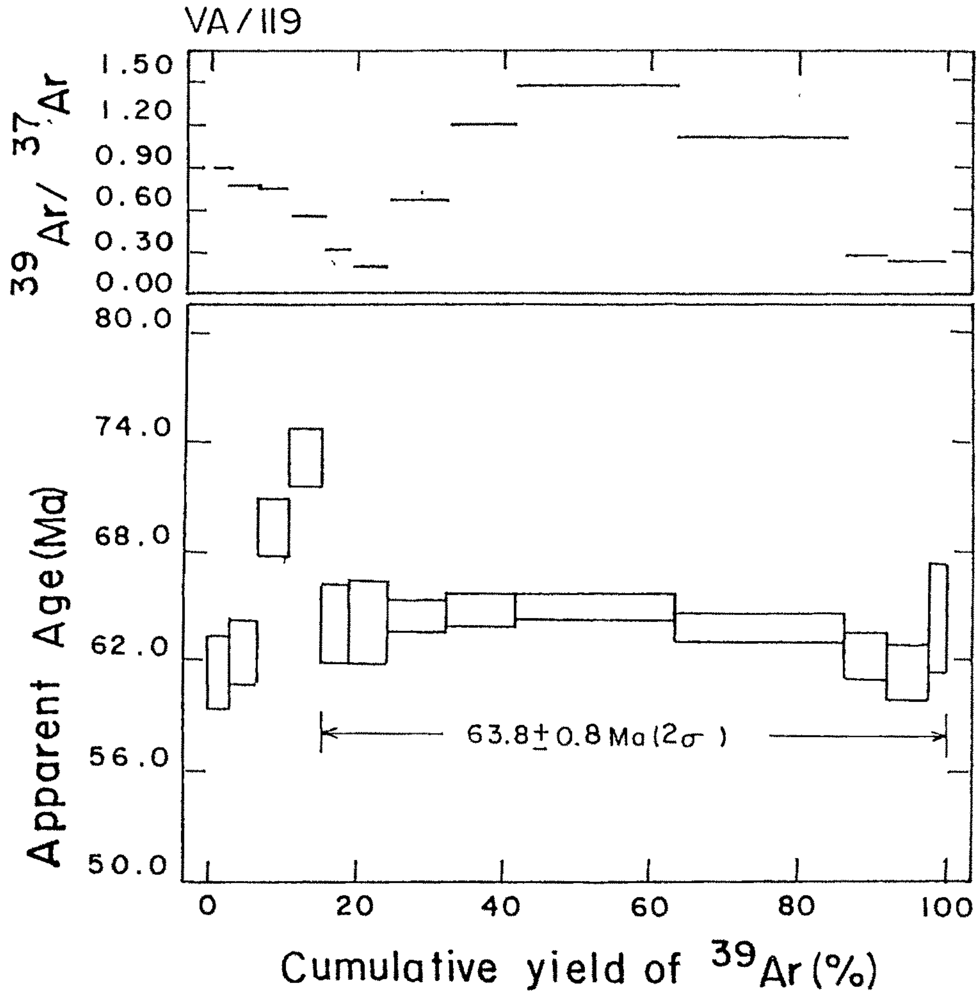

Fig. 4.26. ^{40}Ar-^{39}Ar Age Spectrum for Tavidar Hawaiite (VA/119).

Table 4.19. Step heating argon isotopic compositions and apparent ages of sample K/69A (TAVIDAR HAWAIITE)
J=0.00229 ± 0.00005

Temp. (°C)	$^{36}Ar/^{39}Ar$	$^{37}Ar/^{39}Ar$	$^{40}Ar/^{39}Ar$	Age (Ma)	^{39}Ar (%)	$^{40}Ar^{*}$ (%)
500	0.2179 ±0.0008	1.7071 ±0.0241	76.80 ±0.45	50.5 ±3.6	5.80	16.10
550	0.0261 0.0003	1.4125 0.0034	23.59 0.14	64.5 2.2	12.10	67.30
600	0.0132 0.0006	0.9035 0.0257	20.09 0.13	65.7 2.6	10.20	80.60
650	0.0171 0.0002	1.0231 0.0026	20.92 0.13	64.4 1.9	9.74	75.88
700	0.0167 0.0003	1.2161 0.0024	20.95 0.15	64.9 2.2	6.40	76.30
750	0.0143 0.0003	1.0053 0.0053	19.84 0.16	63.4 2.2	6.10	78.70
800	0.0142 0.0002	0.7575 0.0015	20.29 0.13	65.3 2.0	10.10	79.30
850	0.0164 0.0002	0.8767 0.0021	21.08 0.13	65.8 2.0	13.06	76.92
900	0.0248 0.0002	1.4801 0.0029	22.31 0.14	60.9 1.9	13.89	67.13
950	0.0581 0.0004	6.9947 0.0141	31.03 0.21	56.4 2.4	8.10	44.70
1050	0.2630 0.0015	39.4270 0.0788	86.85 0.54	37.3 5.0	4.50	10.50
TOTAL	0.0443 0.0001	3.3299 0.0048	28.28 0.06	61.7 1.7	100.00	53.66

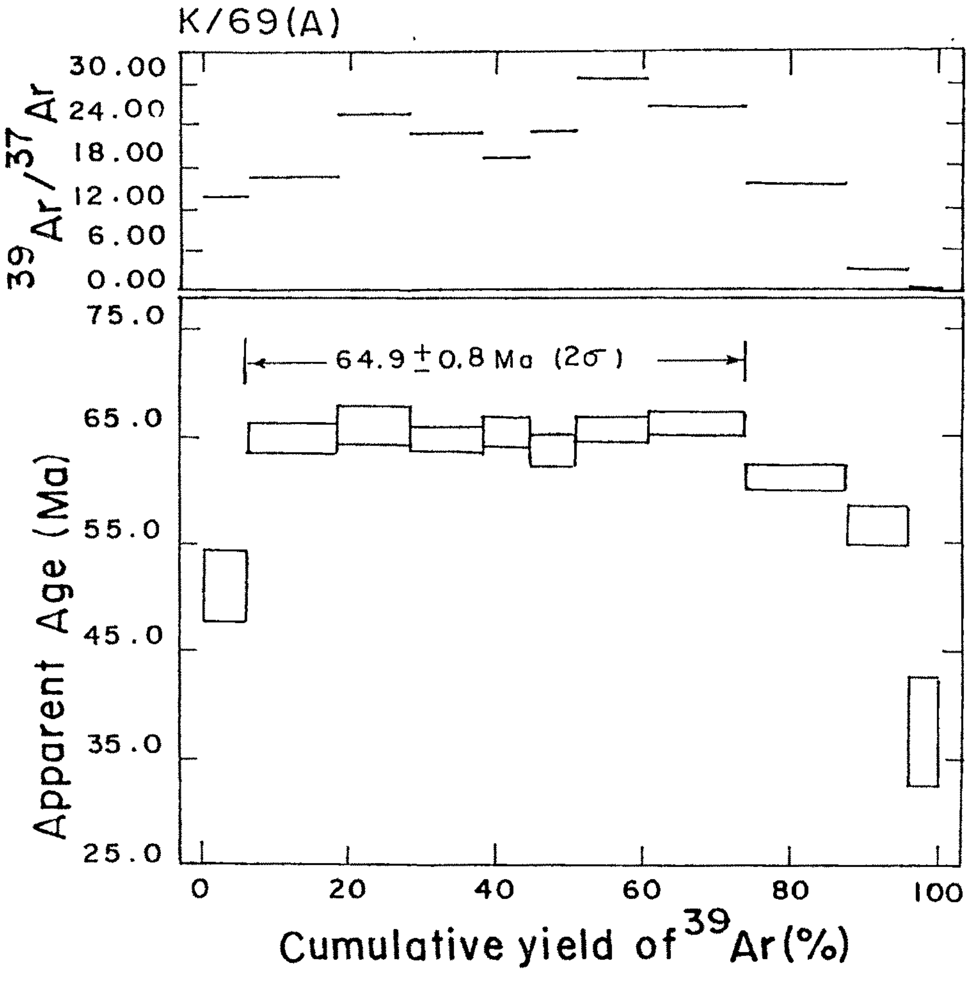

Fig. 4.27. ^{40}Ar-^{39}Ar Age Spectrum for Tavidar Hawaiite (K/69A).

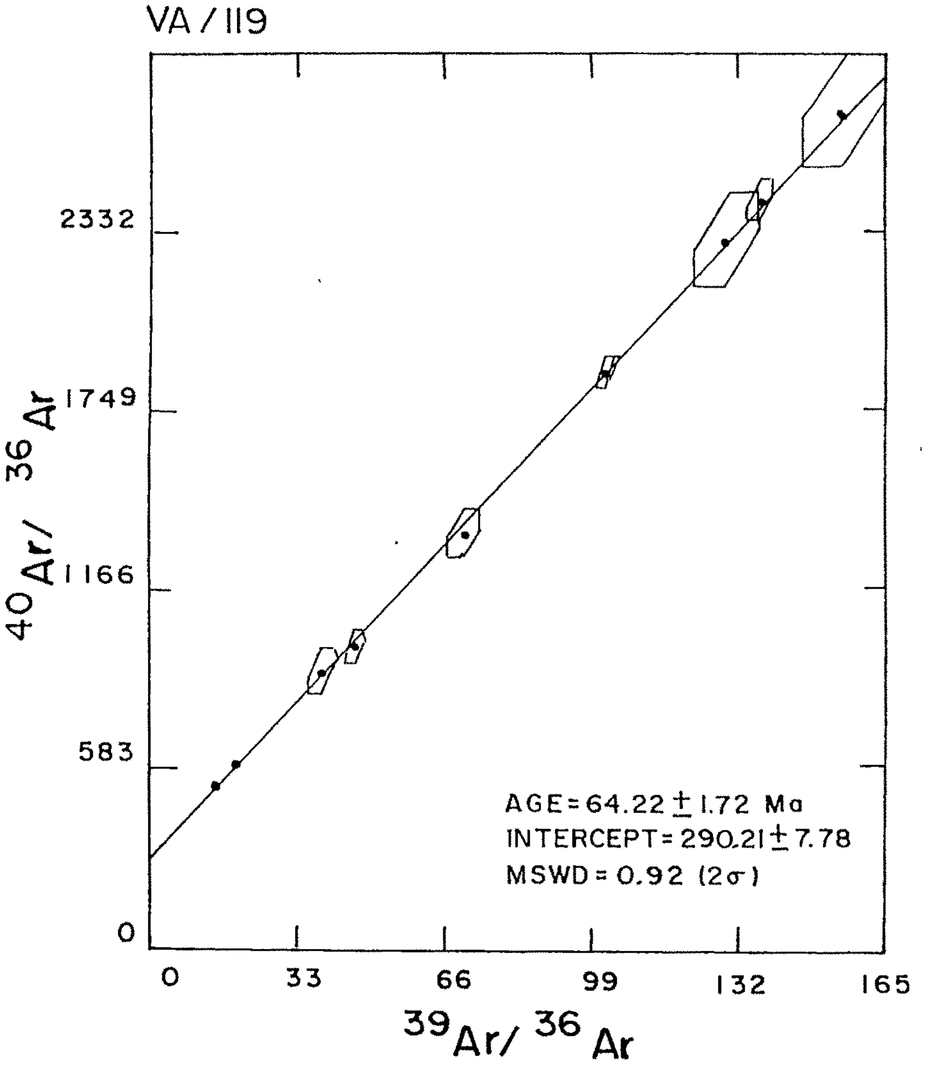

Fig. 4.28. $^{40}Ar/^{36}Ar$ vs. $^{39}Ar/^{36}Ar$ **Isochron Plot for Tavidar Hawaiite (VA/119).**

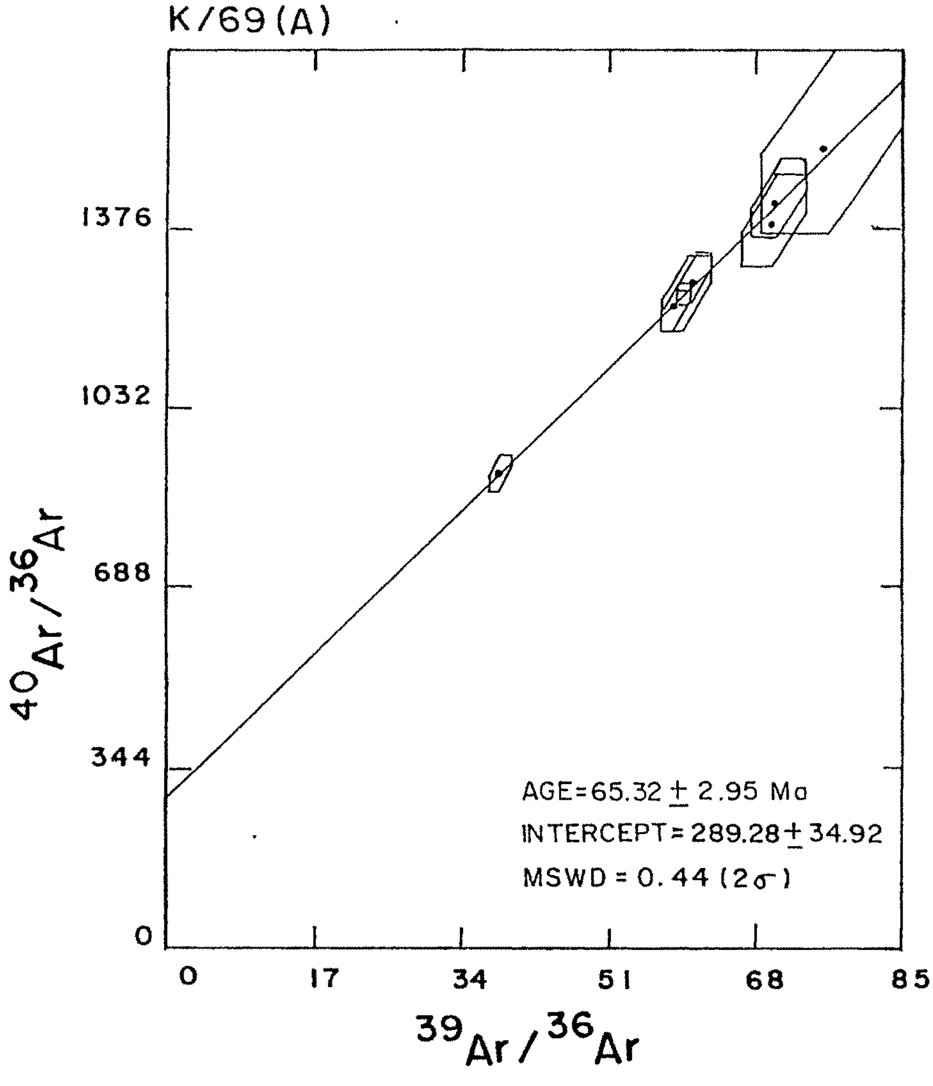

Fig. 4.29. $^{40}Ar/^{36}Ar$ vs. $^{39}Ar/^{36}Ar$ Isochron Plot for Tavidar Hawaiite (K/69A).

Table 4.20. Summary of $^{40}Ar/^{39}Ar$ results from Tavidar volcanics, Jalore district, Rajasthan.

Sample No.	Rock type	Plateau age (Ma)			Total Age, Ma (±2σ)	Correlation diagram $^{40}Ar/^{36}Ar$ vs. $^{39}Ar/^{36}Ar$		
		Temp. steps (°C)	% ^{39}Ar included	Weighted mean age, Ma (±2σ)		Age, Ma (±2σ)	Intercept (±2σ)	MSWD (2σ)
VA/181	K-Andesite	750-Fusion	94.0	65.9±0.4	66.6±0.7	65.5±0.9	311±28	0.43
K/67	K-Andesite	800-Fusion	65.9	64.6±0.8	65.7±1.7	63.5±1.8	308±13	0.92
VA/58	Trachyte	700-Fusion	80.4	67.2±0.4	65.6±0.7	67.6±1.1	288±14	0.92
K/30	Trachyte	500-Fusion	100.0	65.5±0.6	65.6±1.7	65.5±1.7	296±04	0.50
VA/183	Rhyolite	450-Fusion	100.0	65.0±0.4	65.1±0.6	64.5±0.8	306±09	0.26
VA/168	K-Rhyolite	900-Fusion	59.5	63.8±0.8	63.2±1.0	62.8±2.9	298±08	1.20
VA/119	Hawaiite	700-Fusion	84.7	63.8±0.8	64.5±1.7	64.2±1.7	290±08	0.92
K/69A	Hawaiite	550-850	67.7	64.9±0.8	61.7±1.7	65.3±2.9	289±35	0.44

are consistant with the progress of fractional crystallization model resulting in the formation of different rock types. The earliest differentiated rock i.e. andesite was formed about 66 Ma ago, while the end member of the differentiated sequence i.e. K-rhyolite was last formed about 64 Ma ago. These results, thus, demonstrate that at Tavidar the igneous activity (i.e. differentiation) continued for about 2 Ma starting from 66 to 64 Ma ago, resulting in the formation of a cogenetic suite of mildly alkaline rocks of andesite-trachyte-rhyolite-K-rhyolite. Further the hawaiites, which occur in very small proportion, were emplaced about 64 Ma ago, suggesting their contemporaneity with the mildly alkaline rocks of Tavidar.

4.4.3. Sr ISOTOPIC DATA

To understand the petrogenesis of Tavidar volcanics Sr isotopic studies were carried out at KDMIPE, ONGC, Dehradun. The initial Sr ratios have been calculated assuming an average age of 65 Ma for the Tavidar volcanics (Table 4.21). Though the initial ratios of the differentiated rocks and the hawaiites cannot be distinguished mainly because of the high errors associated with the initial ratios, due to very low abundances of Sr, of K-rhyolites (Table 4.21).

However, the mean initial $^{87}Sr/^{86}Sr$ ratio for the differentiated rocks (0.70525) is different from that of the hawaiites (0.70441), suggesting a different source for the hawaiites. It is worth mentioning here that Upadhyaya et al. (1988) have also postulated, based on correlation coefficient studies (Chayes, 1960; Le Maitre, 1982) and pincipal components analysis (PCA) (Le Maitre, 1968; Till and Colley, 1973), that the basalts are not cogenetic with the rest of the rocks.

When the initial $^{87}Sr/^{86}Sr$ ratios are plotted against Sr content (Fig. 4.30) they fall in a field of continental volcanics (felsic as well as basaltic) rocks as defined by Faure and Powell (1972). The mean of initial $^{87}Sr/^{86}Sr$ ratios of Tavidar volcanics lie just below the ***'source region of basalt'*** boundary on the Sr evolution diagram (Faure and Hurley, 1963), suggesting generation of magma from top of upper mantle (Fig. 4.31). Further, as Faure and Powell (1972) suggested that there is a decrease in the initial

Table 4.21. Rb-Sr content and Sr isotopic ratios of samples from Tavidar volcanics, Jalore district.

Sample No.	Rock Type	Rb (ppm)	Sr (ppm)	K/Rb	Rb/Sr	$^{87}Sr/^{86}Sr$ (normalized)	$^{87}Sr/^{86}Sr$ (initial)
VA/181	K-Andesite	68	428	494.12	0.159	0.70634	0.70592±0.00013
K/67	K-Andesite	58	317	639.66	0.183	0.70635	0.70586±0.00013
VA/58	Trachyte	74	195	464.89	0.379	0.70620	0.70519±0.00019
K/30	Trachyte	76	106	700.00	0.717	0.70674	0.70482±0.00031
VA/168	K-Rhyolite	359	22	238.10	16.318	0.74866	0.70488±0.0063
VA/183	K-Rhyolite	168	14	347.02	12.0	0.73699	0.70483±0.00466
VA/119	Hawaiite	75	290	269.33	0.259	0.70528	0.70459±0.00015
K/69A	Hawaiite	56	460	183.93	0.122	0.70456	0.70423±0.00012

Notes to Table:(a) Initial $^{87}Sr/^{86}Sr$ ratios have been calculated assuming an average age of 65±1.0 Ma as indicated by ^{40}Ar-^{39}Ar studies. (b) Rb ad Sr concentrations are determined by XRF with an accuracy of ±5%. (c) $^{87}Sr/^{86}Sr$ ratios are normalized with $^{86}Sr/^{88}Sr = 0.1194$. (d) Errors on mass spectrometric $^{87}Sr/^{86}Sr$ measurements are taken maximum as 0.008%. (e) Errors on $(^{87}Sr/^{86}Sr)_i$ are calculated using eqn. (11) given in Chapter 3. (f) Errors are quoted at 2σ level.

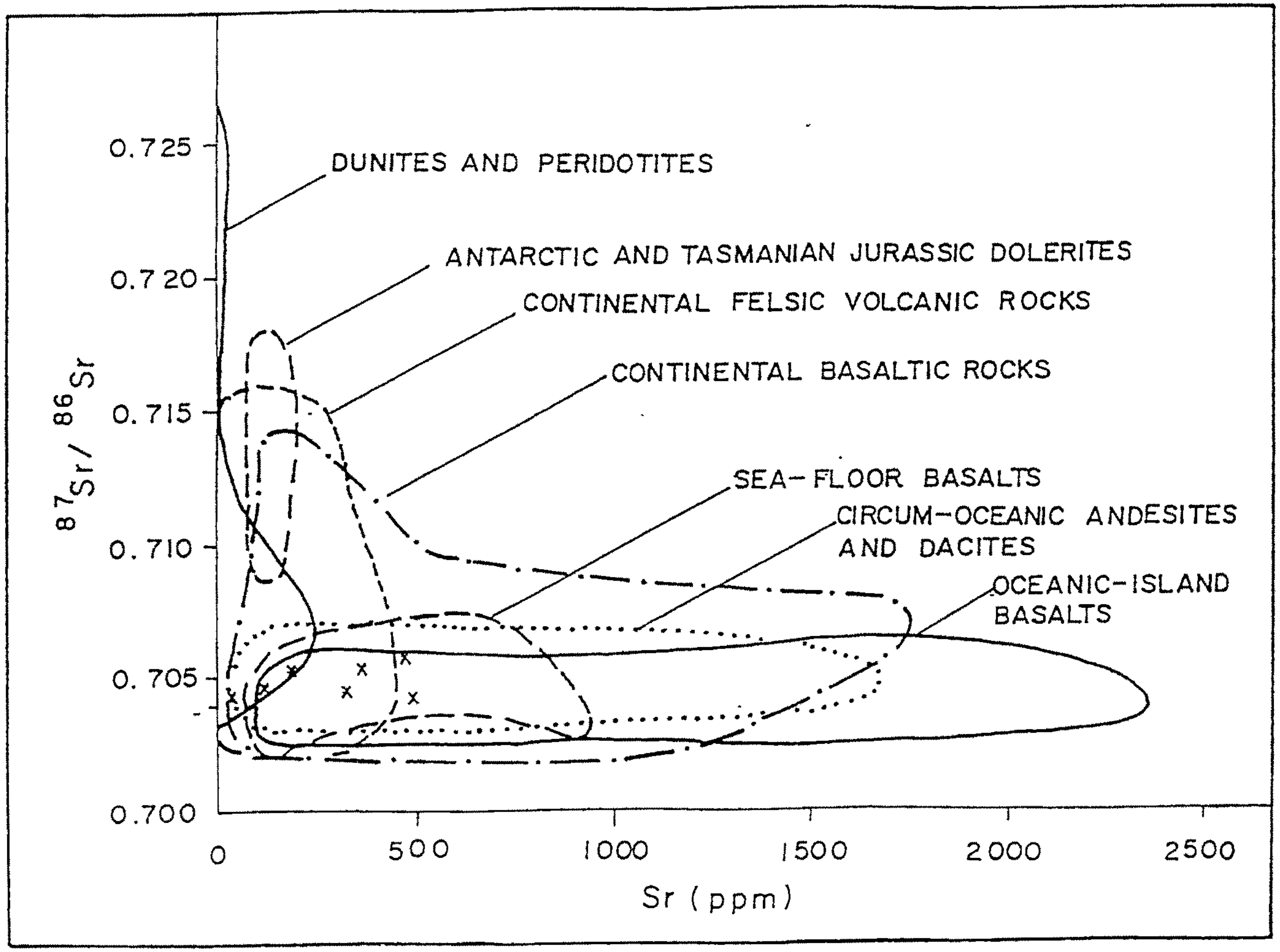

Fig. 4.30. Plot of Initial Sr Ratios Against Sr Content of Tavidar Volcanics (after Faure and Powell, 1972).

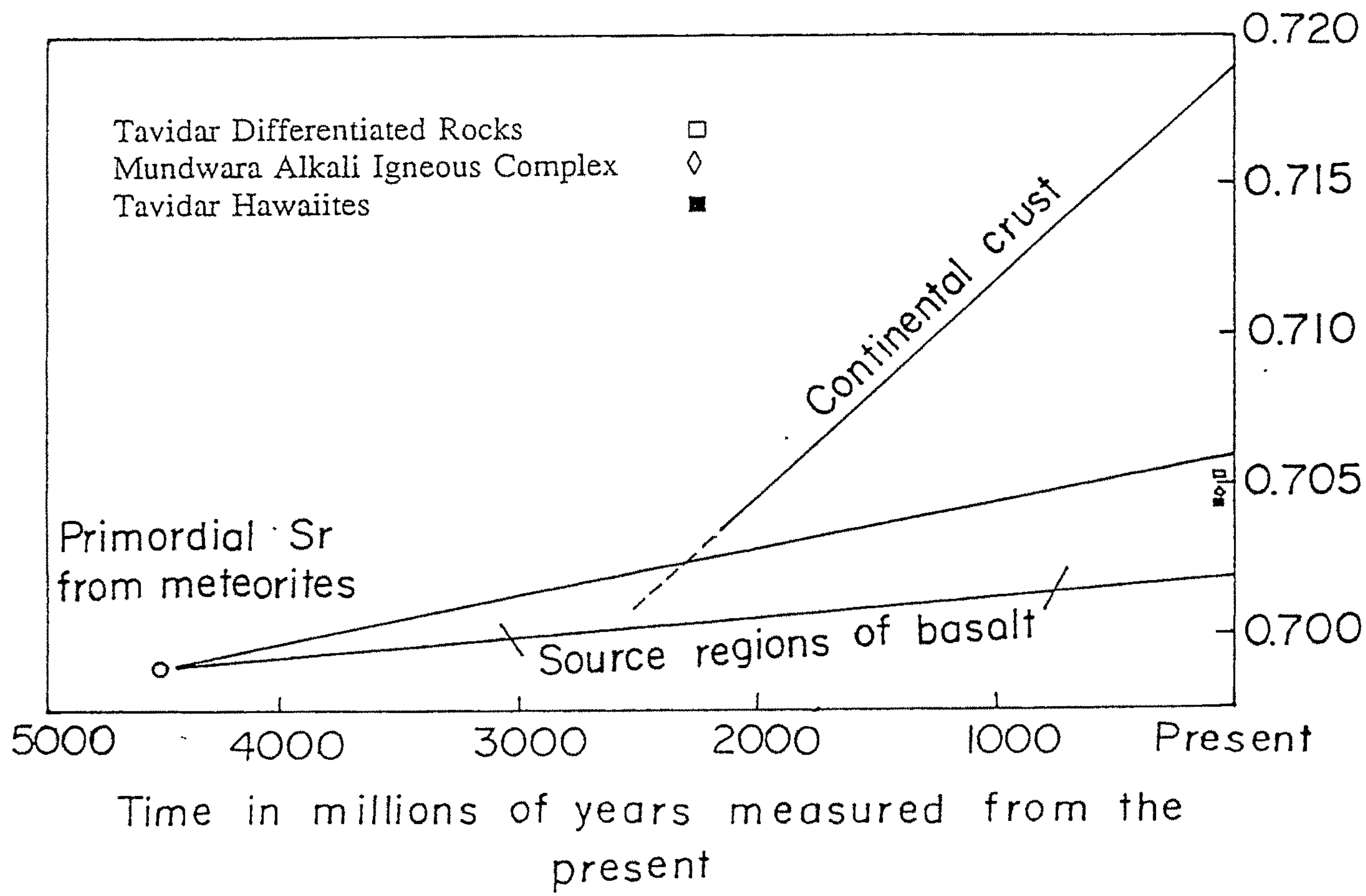

Fig. 4.31. Plot of Mean initial Sr Ratio of Tavidar Volcanics and Mundwara Alkali Igneous Complex on Sr Evolution Diagram (After Faure and Hurley, 1963).

$^{87}Sr/^{86}Sr$ ratio with an increase in the depth, therefore the hawaiites, having a mean initial ratio of 0.70441, have probably been derived from the magma generated still at deeper level in the upper mantle.

4.5. ASSOCIATION IV (*MUNDWARA ALKALI IGNEOUS COMPLEX*)

4.5.1. ^{40}Ar-^{39}Ar STUDIES

Six whole rock samples were dated by ^{40}Ar-^{39}Ar method to assign the emplacement time to the Mundwara alkali igneous complex, Rajasthan, India (Fig. 2.10). The dated samples include four from Musala (MR 86/1, MR 86/2, MR 86/4 and MR 86/5) hill and one each from Mer (MR 86/7) and Toa (MR 86/9) hills of the complex.

The samples were irradiated in two batches. The J factor varied from 0.00220 ± 0.00002 to 0.00237 ± 0.00005. The minimum and maximum values of J were those obtained for samples MR 86/1 and MR 86/7, respectively.

The argon isotopic composition and abundances of these samples are given in Tables 4.22 to 4.27. Their age spectra and correlation diagrams are shown in Fig. (4.32 to 4.41).

4.5.1.A. MUSALA HILL

The dated rocks consist of an essexite, a basalt and two syenites. The samples were collected during a field trip to Rajasthan in 1986.

Sample MR 86/1: This is an essexite collected from the base of Musala hill, and forms the dominant rock type of the hillock. The sample shows a saddle shaped spectrum (Fig. 4.32) with intermediate five steps forming a pseudo plateau between 600-850°C temperature. The pseudo plateau steps constitute 48.6% of the total ^{39}Ar evolved and corresponds to an age of 74.8 ± 1.0 Ma. Such saddle shaped spectra have been considered diagnostic of excess argon (Lanphere and Dalrymple, 1976) with its minima marking the upper limit to the time of formation. The last two high temperature

Table 4.22. Step heating argon isotopic compositions and apparent ages of sample MR 86/1 (MUNDWARA ESSEXITE)
J=0.00220 ± 0.00002

Temp. (°C)	$^{36}Ar/^{39}Ar$	$^{37}Ar/^{39}Ar$	$^{40}Ar/^{39}Ar$	Age (Ma)	^{39}Ar (%)	$^{40}Ar^*$ (%)
400	0.0482 ±0.0006	0.9826 ±0.0211	25.98 ±0.26	46.1 ±2.4	1.00	45.20
450	0.0093 0.0001	0.8179 0.0028	21.01 0.14	71.1 1.2	3.20	86.91
500	0.0031 0.0001	0.5065 0.0048	22.09 0.14	82.3 1.2	6.73	95.94
550	0.0017 0.0001	0.3605 0.0007	20.65 0.12	78.3 1.1	7.79	97.55
600	0.0019 0.0001	0.3303 0.0014	19.92 0.12	75.3 1.1	7.63	97.12
650	0.0046 0.0001	0.3854 0.0011	20.45 0.13	74.3 1.1	4.71	93.31
700	0.0071 0.0001	0.5235 0.0011	21.01 0.13	73.5 1.2	3.83	89.91
750	0.0045 0.0002	0.5736 0.0012	21.08 0.13	76.8 1.3	11.27	93.67
850	0.0041 0.0001	1.2051 0.0024	20.31 0.12	74.4 1.0	21.11	94.13
900	0.0051 0.0002	2.4258 0.0048	23.56 0.14	85.5 1.3	16.20	93.61
1000	0.0231 0.0001	8.2266 0.0164	33.42 0.20	103 2	15.34	79.63
1100	0.09082 0.0025	0.5341 0.0473	77.79 0.72	192 7	1.00	65.50
1200	0.1151 0.0101	19.4451 0.0909	69.60 2.40	136 28	1.00	51.00
TOTAL	0.0086 0.0001	2.3875 0.0027	23.83 0.05	82.6 0.8	100.00	89.31

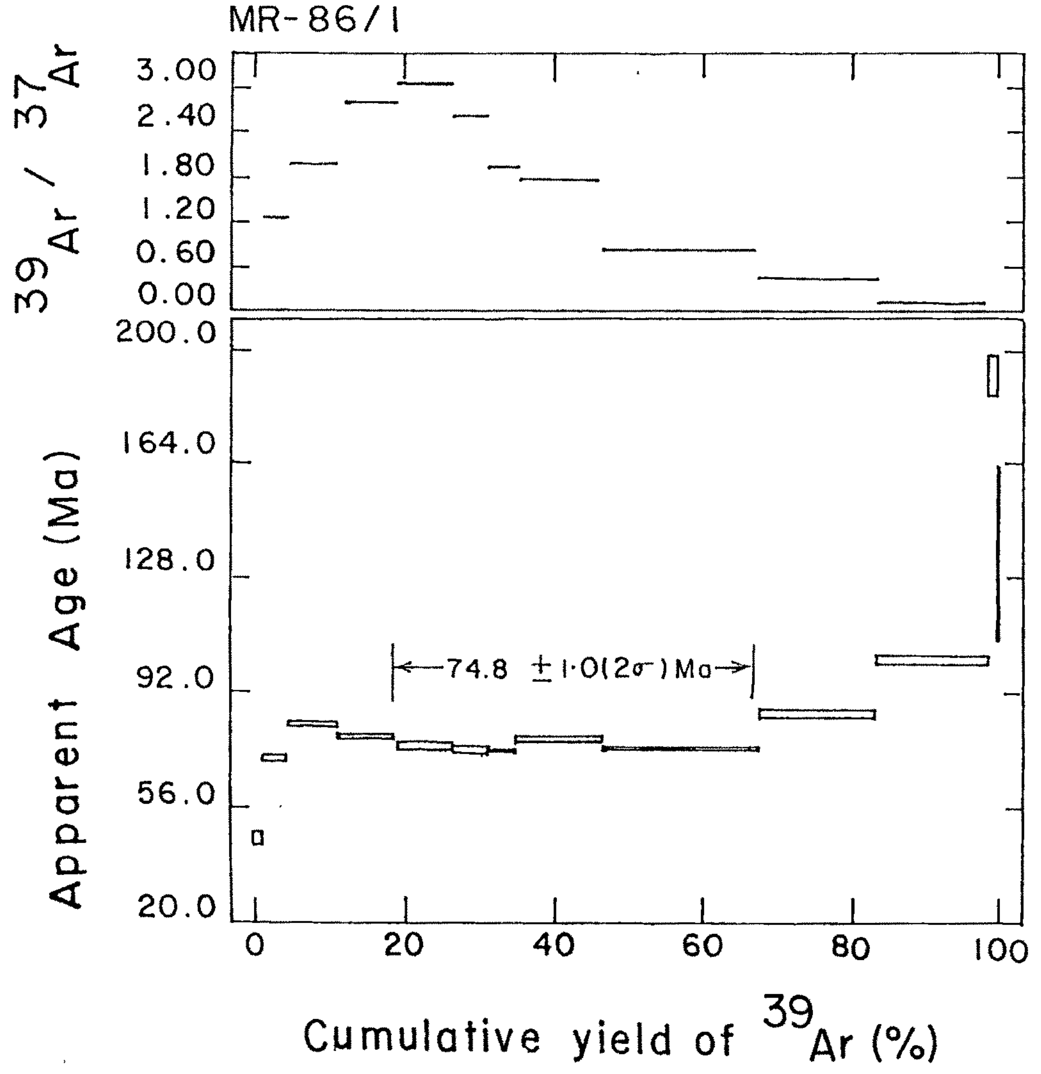

Fig. 4.32. ^{40}Ar-^{39}Ar Age Spectrum for Musala Essexite (MR 86/1).

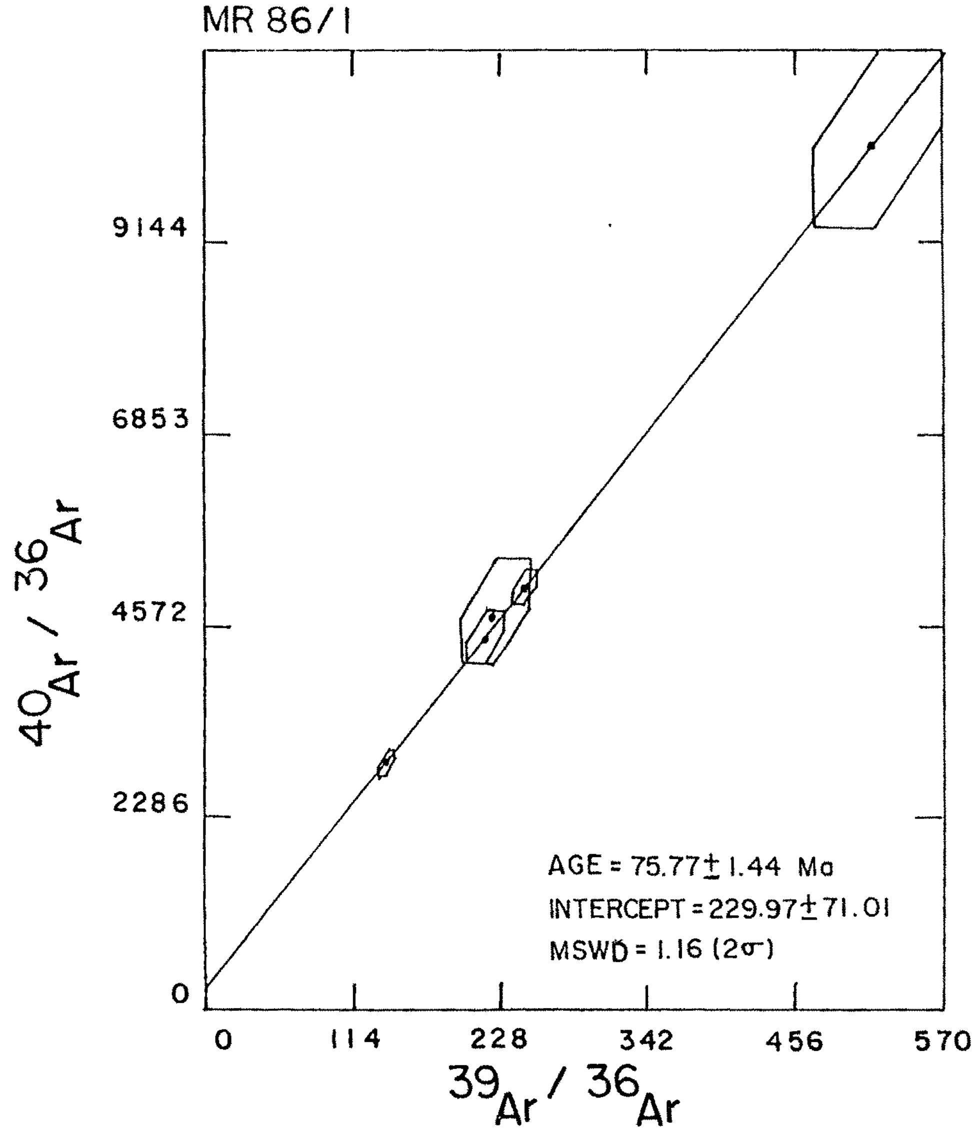

Fig. 4.33. $^{40}Ar/^{36}Ar$ vs. $^{39}Ar/^{36}Ar$ **Isochron Plot for Musala Essexite (MR 86/1).**

increments (1100 and 1200°C) record anomalously old apparent ages but together comprise 1% of the total ^{39}Ar evolved from the sample.

The apparent K/Ca ratio varies systematically over the experiment. The increase in $^{39}Ar/^{37}Ar$ ratio during the initial five temperature steps (i.e. up to 600°C) indicates that the argon is released from K-dominant phase, while in the remaining steps it is released from Ca-rich phase, resulting in continuous lowering of $^{39}Ar/^{37}Ar$ ratio. The isochron (Fig. 4.33) age is 75.8 ± 1.4 Ma.

Sample MR 86/2: This is a basalt occurring above the essexite body. This sample also shows a saddle shaped spectrum (Fig. 4.34) typical of sample containing excess argon. The pseudo plateau consisting of intermediate five temperature steps (i.e. 630 to 820°C) contain 45.9% of the released ^{39}Ar and yields an age of 73.9 ± 0.4 Ma. One temperature step (i.e. 770°C) gives a slightly discordant age but as it occurs in between, it has been included in the pseudo plateau.

The apparent K/Ca ratio remains almost uniform up to 770°C, followed by increase in the ratio in the next three steps, but beyond this temperature more and more argon is released from the Ca-dominant phase resulting in the continuous lowering of $^{39}Ar/^{37}Ar$ ratio. The isochron age is 71.8 ± 1.5 Ma (Fig. 4.35). However, when all the data points (steps) are used in $^{40}Ar/^{36}Ar$ vs. $^{39}Ar/^{36}Ar$ regression analysis, the slope of regression line corresponds to an age of 69.7 ± 0.8 Ma which can be considered as the formation age of the basalt.

Sample MR 86/4: This is a syenite occurring above the basalt and represents the chilled margin of the syenite body. The sample shows a perfect plateau (Fig. 4.36) consisting of all the thirteen temperature steps (100% ^{39}Ar release). The plateau age is 64.1 ± 0.6 Ma while its isochron (Fig. 4.37) and total ages are 64.5 ± 1.7 Ma and 63.8 ± 1.7 Ma, respectively.

There is good agreement between the plateau, isochron and total ages of this sample, within the experimental error, indicating that this syenite sample has not lost any radiogenic argon during its history. The concordance of plateau, isochron and total ages of this sample suggest that the syenite was emplaced about 64 Ma ago.

Sample MR 86/5: This is again a syenite collected from centre of the syenite body on

Table 4.23. Step heating argon isotopic compositions and apparent ages of sample MR 86/2 (MUSALA BASALT)
$J=0.00223 \pm 0.00002$

Temp. (°C)	$^{36}Ar/^{39}Ar$	$^{37}Ar/^{39}Ar$	$^{40}Ar/^{39}Ar$	Age (Ma)	^{39}Ar (%)	$^{40}Ar^{*}$ (%)
500	0.0209 ±0.0002	0.2363 ±0.0007	36.04 ±0.21	116 ±2	2.37	82.84
550	0.0084 0.0001	0.2901 0.0012	23.86 0.14	84.0 1.2	6.60	89.56
600	0.0035 0.0000	0.3015 0.0006	20.92 0.12	78.2 1.1	7.72	94.98
630	0.0027 0.0001	0.2864 0.0005	19.78 0.11	74.7 1.0	11.21	95.83
670	0.0021 0.0001	0.3324 0.0006	19.44 0.11	74.1 1.0	11.47	96.74
750	0.0025 0.0001	0.2978 0.0005	19.50 0.11	73.9 1.0	9.38	96.14
770	0.0026 0.0003	0.2381 0.0006	18.89 0.11	71.4 1.3	5.97	95.82
820	0.0043 0.0001	0.1891 0.0004	20.14 0.12	74.3 1.0	7.87	93.55
880	0.0036 0.0001	0.1745 0.0003	20.53 0.12	76.7 1.1	6.95	94.77
950	0.0035 0.0001	0.2481 0.0005	22.59 0.13	84.7 1.2	7.83	95.34
1000	0.0058 0.0001	0.8636 0.0017	23.17 0.13	84.2 1.2	9.18	92.48
1080	0.0081 0.0001	6.4496 0.0128	24.47 0.14	86.6 1.2	11.31	90.12
1120	0.0184 0.0004	22.8721 0.0773	27.28 0.20	85.8 1.9	1.72	80.00
1210	0.01681 0.0023	8.1831 0.0363	26.11 0.70	83.2 7.4	0.40	81.00
TOTAL	0.0051 0.0003	1.4991 0.002	21.70 0.04	79.6 0.7	100.00	93.17

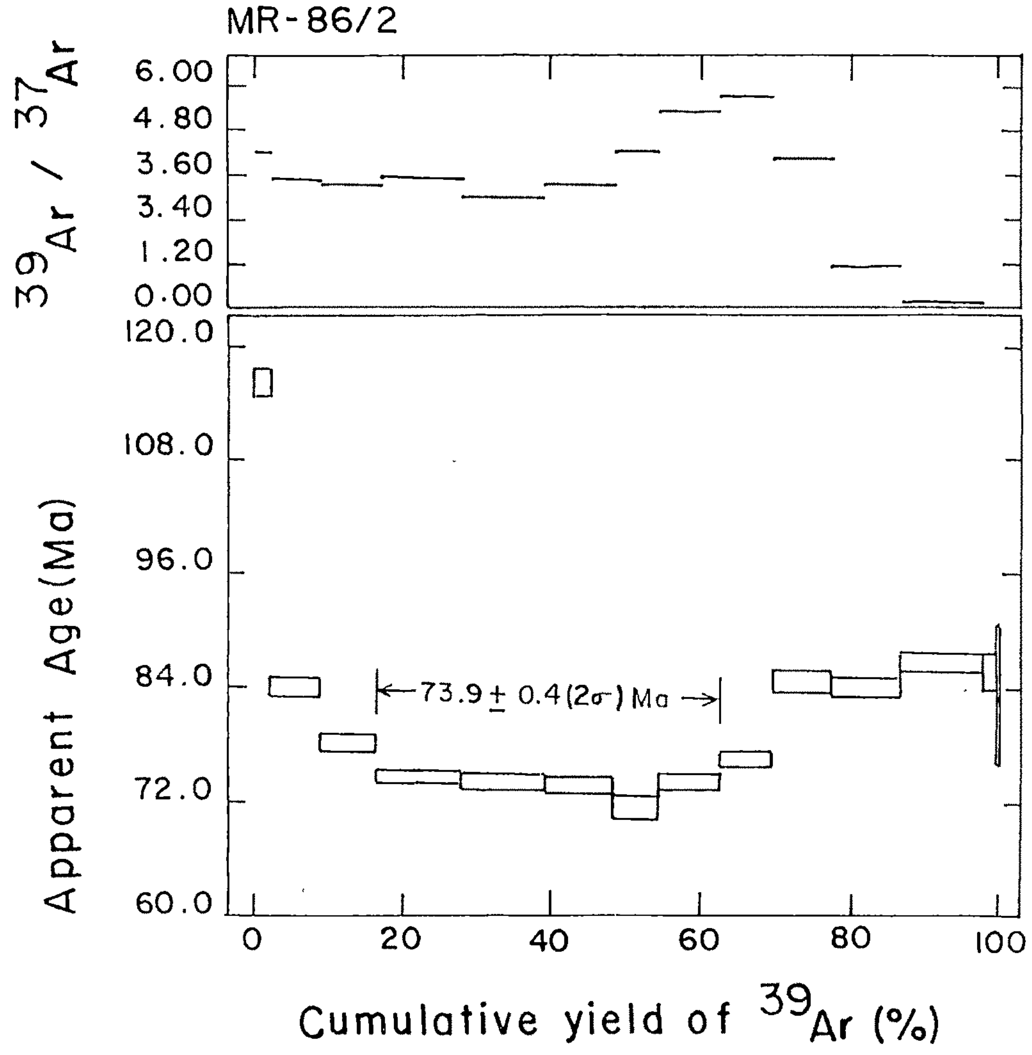

Fig. 4.34. ^{40}Ar-^{39}Ar Age Spectrum for Musala Basalt (MR 86/2).

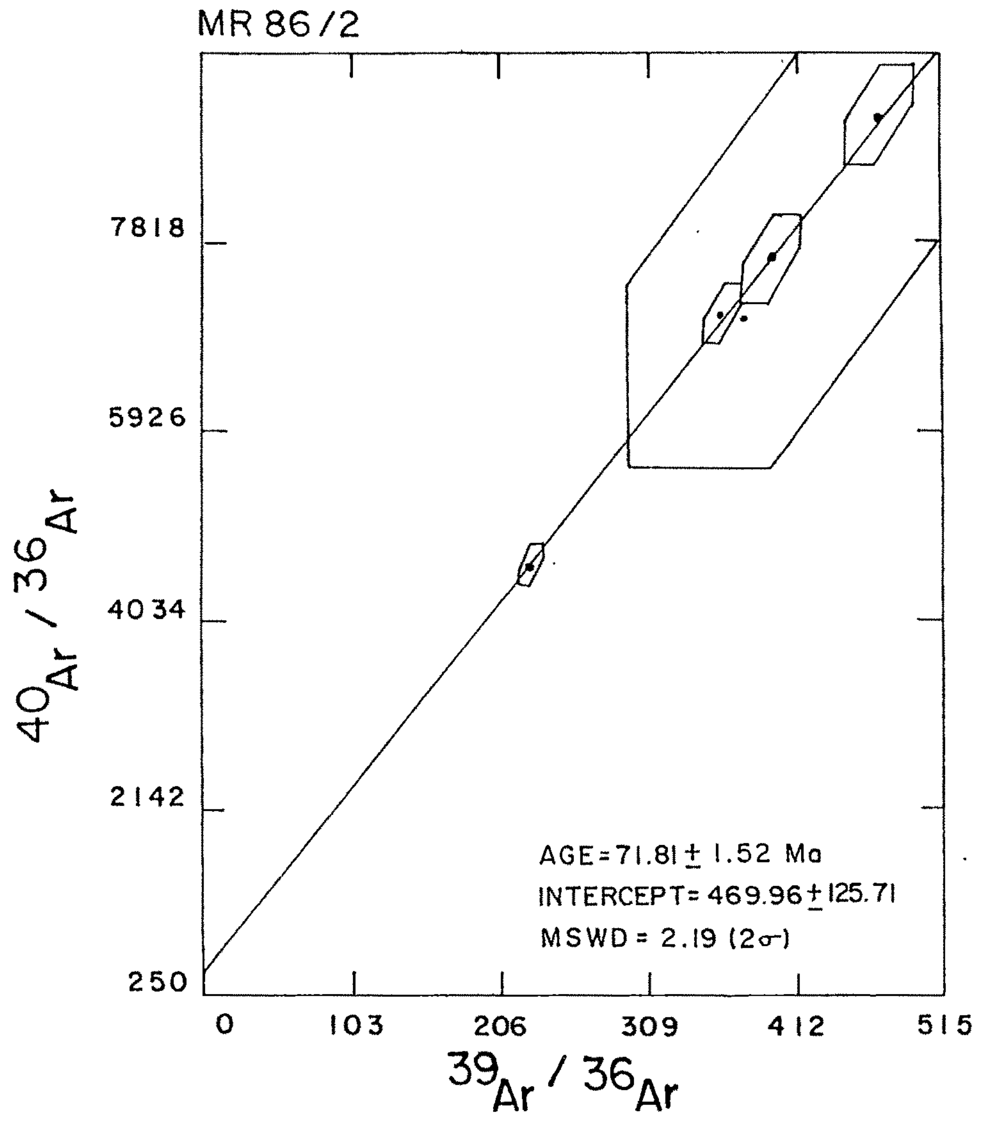

Fig. 4.35. $^{40}Ar/^{36}Ar$ vs. $^{39}Ar/^{36}Ar$ **Isochron Plot for Musala Basalt (MR 86/2).**

Table 4.24. Step heating argon isotopic compositions and apparent ages of sample MR 86/4 (MUSALA SYENITE) J=0.00233 ± 0.00005

Temp. (°C)	$^{36}Ar/^{39}Ar$	$^{37}Ar/^{39}Ar$	$^{40}Ar/^{39}Ar$	Age (Ma)	^{39}Ar (%)	$^{40}Ar^*$ (%)
500	0.1453 ±0.0018	-	57.44 ±0.33	60.0 ±5.2	6.40	25.30
550	0.0265 0.0011	-	22.83 0.14	61.9 3.2	4.50	65.60
600	0.0157 0.0001	0.0521 ±0.0027	19.89 0.12	62.9 1.9	6.16	76.60
650	0.0128 0.0001	0.0396 0.0003	19.42 0.11	64.5 1.9	8.20	80.43
700	0.0084 0.0003	-	18.20 0.11	64.8 1.9	9.51	86.30
750	0.0096 0.0003	-	18.39 0.11	64.2 2.0	9.30	84.50
800	0.0144 0.0002	-	19.65 0.15	63.6 1.9	6.31	78.32
850	0.0149 0.0002	0.0452 0.0007	19.89 0.17	63.9 1.9	7.45	77.86
900	0.0127 0.0002	0.1364 0.0039	19.36 0.11	64.4 1.9	9.86	80.54
950	0.0127 0.0002	0.3088 0.0013	19.02 0.11	62.9 1.8	14.29	80.14
1000	0.0127 0.0002	0.7446 0.0019	19.39 0.11	64.5 1.9	10.05	80.56
1050	0.0108 0.0004	1.7833 0.0036	19.28 0.14	66.4 2.2	4.30	83.40
1200	0.0154 0.0015	4.9281 0.0098	21.30 0.43	69.0 5.2	1.60	78.60
TOTAL	0.0215 0.0001	0.3134 0.0005	21.83 0.04	63.8 1.7	100.00	70.81

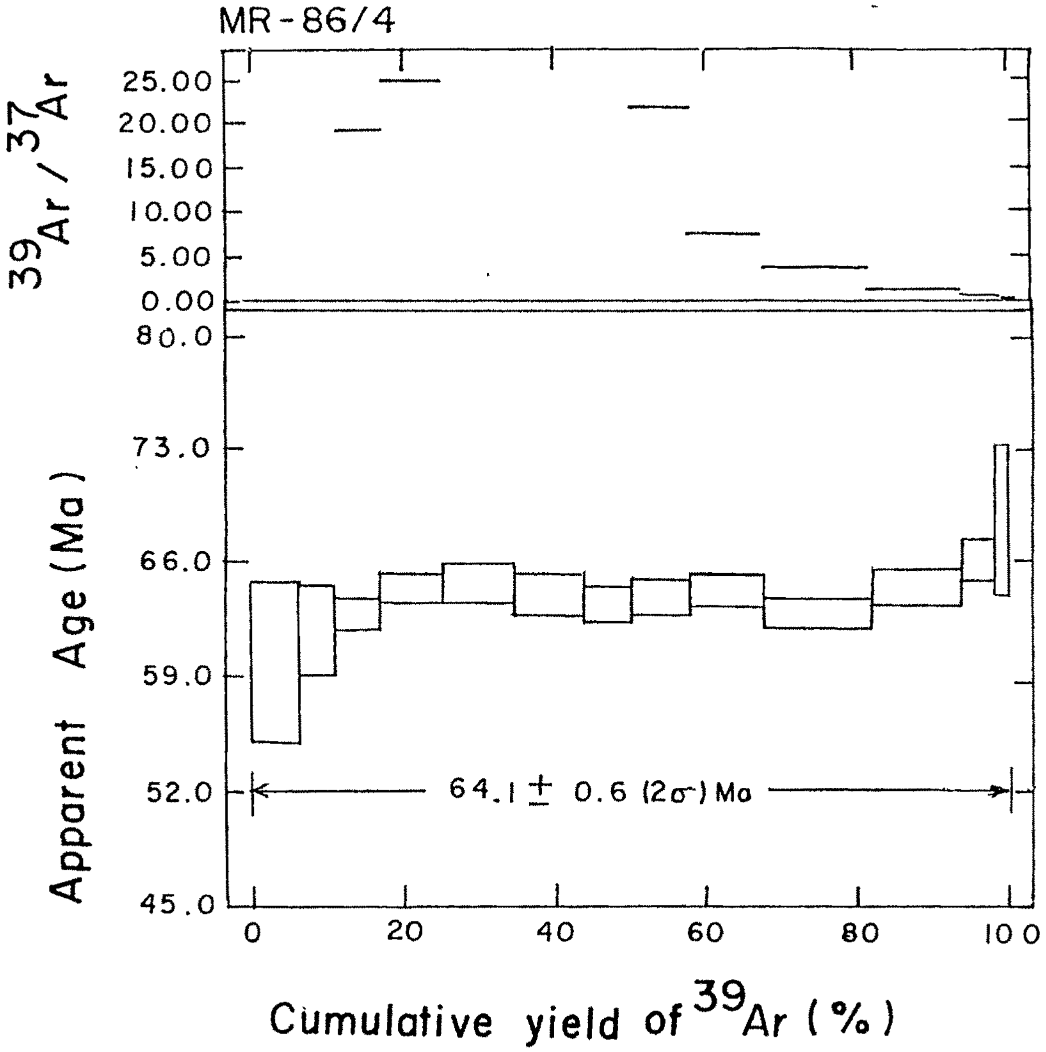

Fig. 4.36. ^{40}Ar-^{39}Ar Age Spectrum for Musala Syenite (MR 86/4).

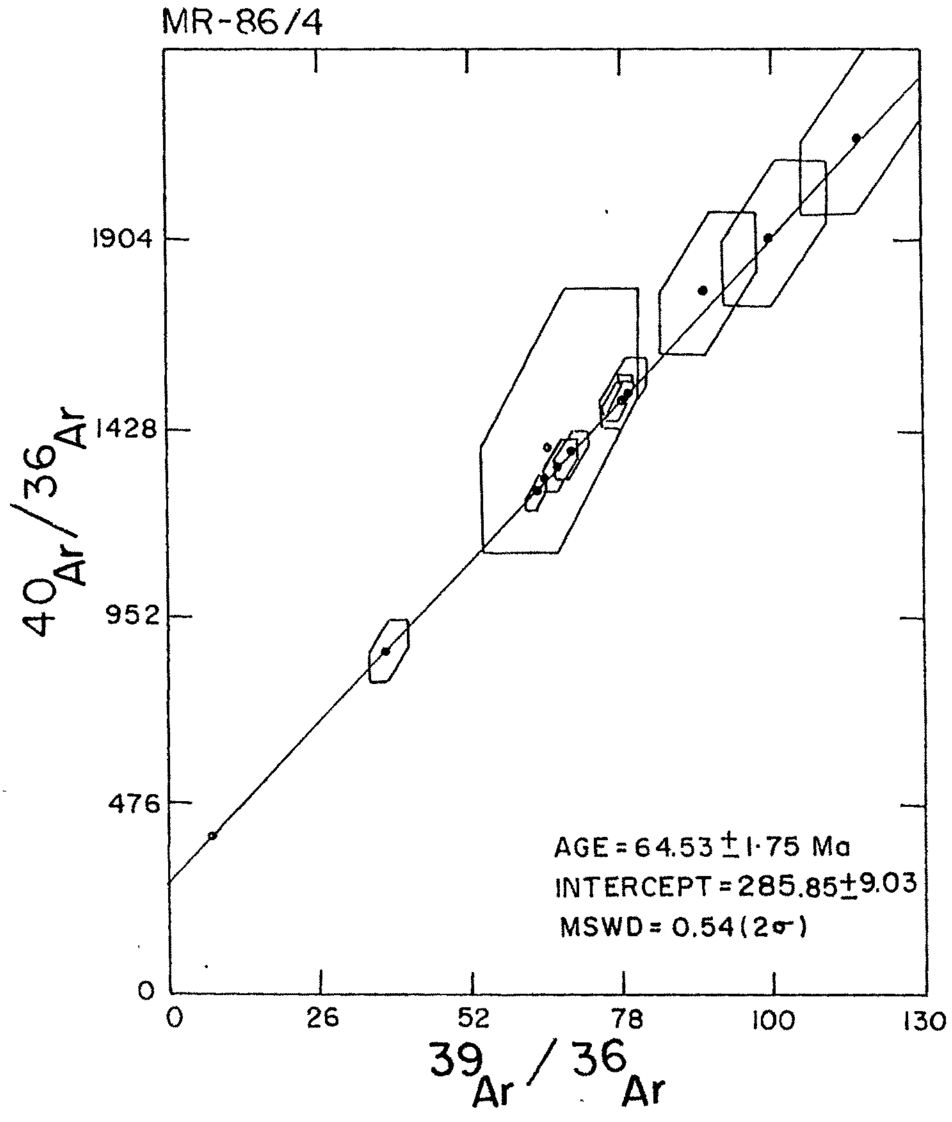

Fig. 4.37. $^{40}Ar/^{36}Ar$ vs. $^{39}Ar/^{36}Ar$ Isochron Plot for Musala Syenite (MR 86/4).

top of the Musala hill. The sample shows a saddle shaped spectrum (Fig. 4.38) indicating excess argon. The minimum age (three steps, 20.9% of total ^{39}Ar evolved) is 69.5 ± 0.9 Ma. Even though this age marks the upper boundary to the time of formation, the formation/emplacement age of this sample should be equal to that of the other syenite (MR 86/4) collected from the same hill, which is 64.1 ± 0.6 Ma.

The apparent K/Ca ratio does not vary systematically over the experiment and instead shows a double stage release pattern. The step-wise decrease in $^{39}Ar/^{37}Ar$ ratio indicates that argon is preferentially released from the Ca-dominant phase during the first four(i.e. upto 650°C) and the last five temperature steps(i.e. from 900-1200°C). The intermediate four temperature steps (700-850°C) do not produce any ^{37}Ar indicating that in these steps the argon is released solely from K-bearing phases.

4.5.1.B. MER HILL

Sample MR 86/7: This is a syenite collected from Mer hill. The sample shows a nine step plateau (Fig. 4.39) from 500 to 900°C constituting 54% of total ^{39}Ar released. The plateau age is 64.4 ± 0.8 Ma, while its isochron (Fig. 4.40) and total ages are 64.8 ± 1.7 Ma and 66.5 ± 1.7 Ma, respectively. The plateau and isochron ages of this sample are in good agreement, though the total age is slightly higher. The discordance in the total age is due to relatively higher ages obtained from the higher temperature steps. However, the concordance of plateau, isochron and total ages of this sample indicate that the syenite of Mer hill was also emplaced at about 64 Ma ago.

The behavior of argon release in this sample is different from that of MR 86/4 and MR 86/5. In the first ten steps i.e. up to 950°C, argon appears to be released from K-rich fraction while in the remaining steps, it is released from Ca-dominant phase.

4.5.1.C. TOA HILL

Sample MR 86/9: This is a gabbro which forms the most important rock type of Toa hill. This sample also shows a U-shaped spectrum (Fig. 4.41) like MR 86/1, MR 86/2

Table 4.25. Step heating argon isotopic compositions and apparent ages of sample MR 86/5 (MUSALA SYENITE) J=0.00236 ± 0.00005

Temp. (°C)	$^{36}Ar/^{39}Ar$	$^{37}Ar/^{39}Ar$	$^{40}Ar/^{39}Ar$	Age (Ma)	^{39}Ar (%)	$^{40}Ar^*$ (%)
500	0.1323 ±0.0004	0.0547 ±0.0001	61.48 ±0.35	92.8 ±3.4	5.7	36.4
550	0.0451 0.0002	0.1719 0.0008	32.16 0.19	78.4 2.4	5.5	58.6
600	0.0383 0.0002	0.6522 0.0041	30.07 0.17	78.0 2.4	5.1	62.3
650	0.0371 0.0003	0.9511 0.0026	28.45 0.17	73.0 2.2	5.4	61.5
700	0.0268 0.0001	-	24.42 0.14	68.8 2.0	7.4	67.5
750	0.0376 0.0002	-	27.87 0.16	69.8 2.2	5.1	60.0
800	0.0585 0.0002	-	34.17 0.20	70.3 2.2	8.4	49.3
850	0.0521 0.0002	-	33.24 0.19	74.5 2.4	9.5	53.8
900	0.0387 0.0001	0.0568 0.0008	31.20 0.18	82.1 2.4	12.3	63.3
950	0.0356 0.0001	0.1265 0.0015	31.75 0.18	88.0 2.6	14.1	66.8
1000	0.0331 0.0001	0.3621 0.0031	32.70 0.19	94.9 2.8	10.9	70.0
1050	0.0273 0.0002	0.4345 0.0008	30.44 0.18	92.7 2.6	6.9	73.5
1200	0.0312 0.0016	0.9331 0.0168	32.70 1.40	97.1 3.4	3.8	71.8
TOTAL	0.0442 0.0001	0.2261 0.0008	32.80 0.08	82.0 2.0	100.0	60.1

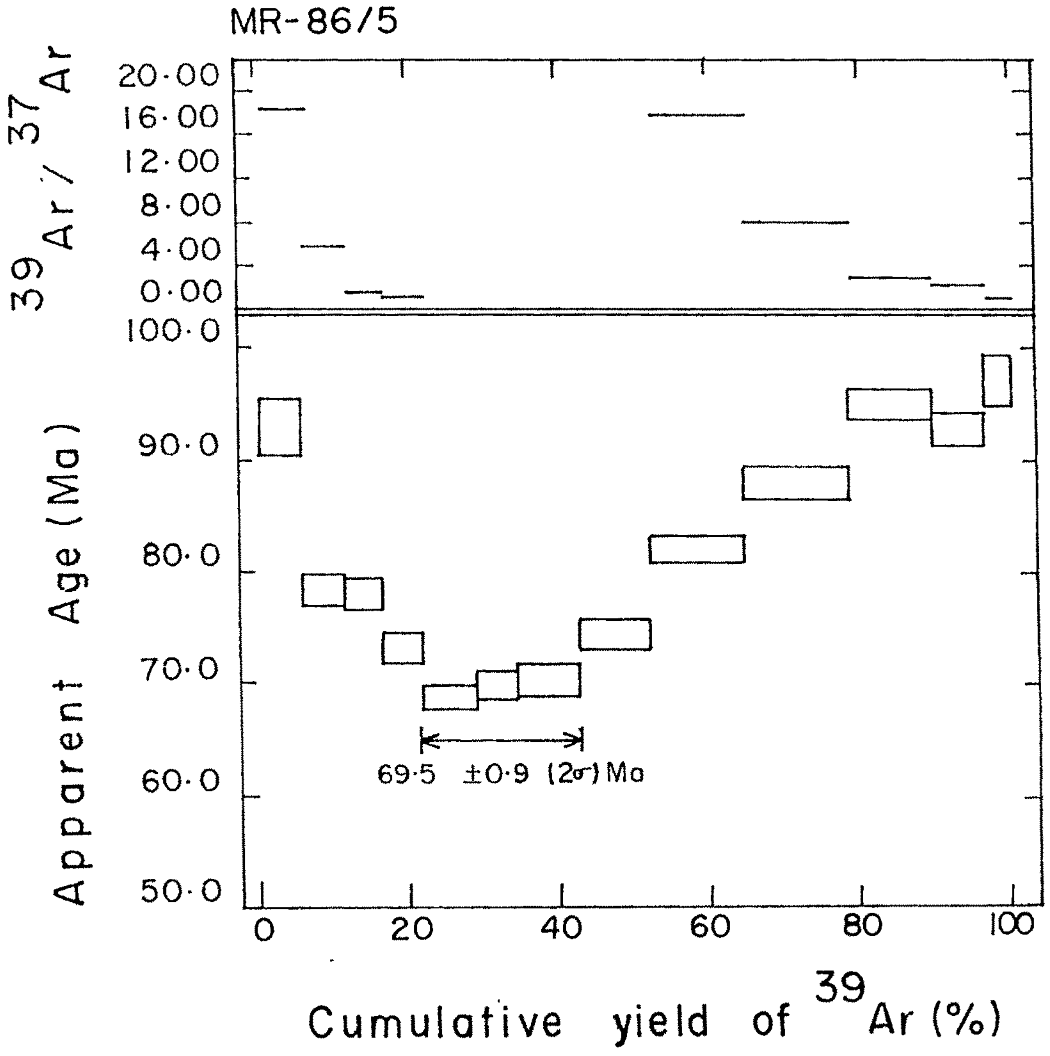

Fig. 4.38. ^{40}Ar-^{39}Ar Age Spectrum for Musala Syenite (MR 86/5).

Table 4.26. Step heating argon isotopic compositions and apparent ages of sample MR 86/7 (MUNDWARA SYENITE)
J=0.00237 ± 0.00005

Temp. (°C)	$^{36}Ar/^{39}Ar$	$^{37}Ar/^{39}Ar$	$^{40}Ar/^{39}Ar$	Age (Ma)	^{39}Ar (%)	$^{40}Ar^{*}$ (%)
500	0.2711 ±0.0014	0.4509 ±0.0022	94.69 ±0.56	61.3 ±5.2	1.30	15.40
550	0.0474 0.0008	0.3417 0.0022	29.04 0.20	63.0 3.0	1.80	51.70
600	0.0297 0.0004	0.3421 0.0006	24.06 0.15	64.0 2.2	2.90	63.40
650	0.0235 0.0002	0.3251 0.0012	22.16 0.13	63.7 1.9	5.87	68.62
700	0.0104 0.0001	0.3147 0.0031	18.33 0.11	63.9 1.8	10.26	83.12
750	0.0107 0.0001	0.2417 0.0032	18.76 0.11	65.4 1.9	7.78	83.15
800	0.0168 0.0002	0.1931 0.0022	20.42 0.12	64.7 1.9	6.31	75.63
850	0.0218 0.0002	0.2271 0.0016	22.20 0.16	66.0 1.9	7.30	70.98
900	0.0199 0.0001	0.3153 0.0065	21.24 0.12	64.4 1.8	10.50	72.26
950	0.0181 0.0001	0.2478 0.0004	21.44 0.13	67.4 1.9	23.42	75.06
1000	0.0233 0.0001	0.6311 0.0012	23.61 0.15	69.9 2.0	14.40	70.80
1050	0.0364 0.0002	1.7526 0.0035	27.68 0.17	70.7 2.2	6.40	61.00
1100	0.0491 0.0013	4.0349 0.0101	32.49 0.28	75.2 4.2	1.80	55.40
TOTAL	0.0241 0.0001	0.4887 0.0009	22.98 0.05	66.5 1.7	100.00	69.11

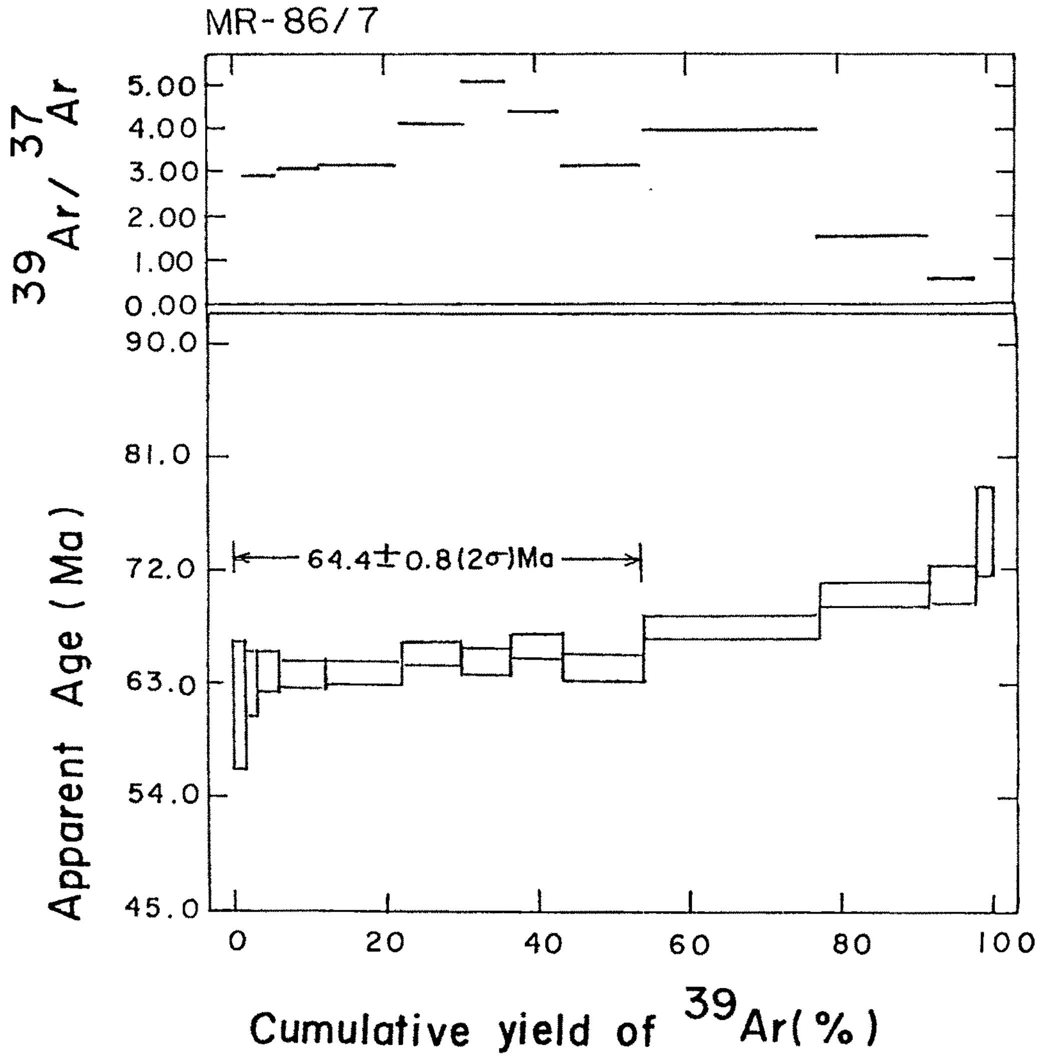

Fig. 4.39. ^{40}Ar-^{39}Ar Age Spectrum for Mer Syenite (MR 86/7).

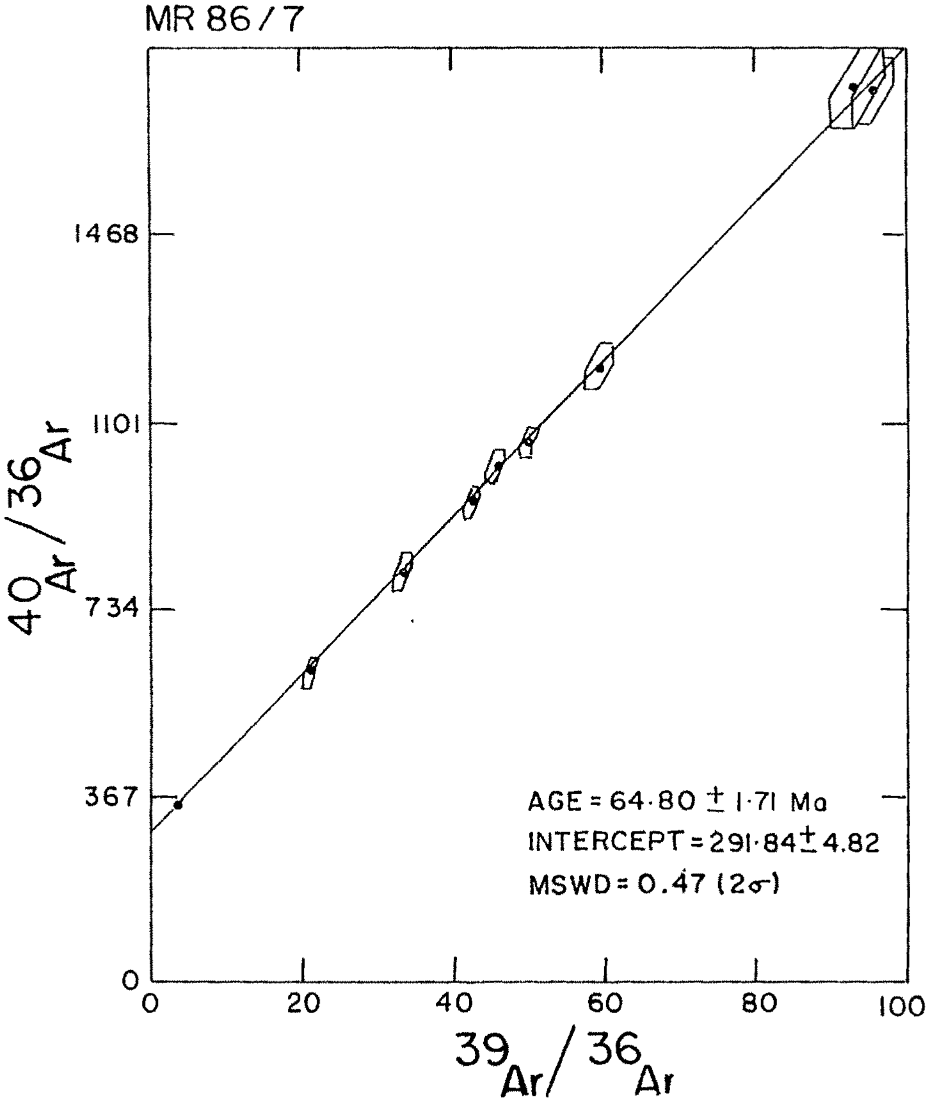

Fig. 4.40. $^{40}Ar/^{36}Ar$ vs. $^{39}Ar/^{36}Ar$ Isochron Plot for Mer Syenite (MR 86/7).

Table 4.27. Step heating argon isotopic compositions and apparent ages of sample MR 86/9 (MUNDWARA GABBRO)
J=0.00232 ± 0.00005

Temp. (°C)	$^{36}Ar/^{39}Ar$	$^{37}Ar/^{39}Ar$	$^{40}Ar/^{39}Ar$	Age (Ma)	^{39}Ar (%)	$^{40}Ar^{*}$ (%)
550	1.0236 ±0.0063	15.9721 ±0.3865	422.50 ±2.70	444.0 ±22.0	1.0	28.0
600	0.4762 0.0055	19.3091 1.9066	254.10 3.20	422.0 22.0	1.0	45.0
650	0.3196 0.0022	15.7261 0.0488	173.00 1.10	302,.2 11.0	2.7	45.4
700	0.1653 0.0015	8.0193 0.0243	74.08 0.52	102.7 5.6	4.8	34.0
750	0.0476 0.0007	4.2403 0.0084	37.09 0.28	93.9 3.6	8.2	62.0
800	0.0234 0.0005	2.6636 0.0053	28.94 0.21	90.0 3.0	12.9	76.1
850	0.0177 0.0005	2.7055 0.0054	24.45 0.20	78.8 2.8	13.7	78.6
900	0.0104 0.0006	2.6470 0.1937	20.44 0.16	71.2 2.6	12.8	84.8
950	0.0120 0.0006	3.5217 0.0071	21.68 0.19	74.4 2.8	17.4	83.6
1000	0.0241 0.0007	12.5711 0.0251	32.52 0.27	103.3 3.8	14.2	78.1
1050	0.0824 0.0028	83.3201 0.1666	61.77 0.72	150.3 9.2	4.6	60.6
1200	0.0855 0.0035	115.051 0.2301	73.16 0.93	190.3 11.2	6.2	65.5
TOTAL	0.0591 0.0003	16.7711 0.0391	44.62 0.12	110.3 3.0	100.0	60.8

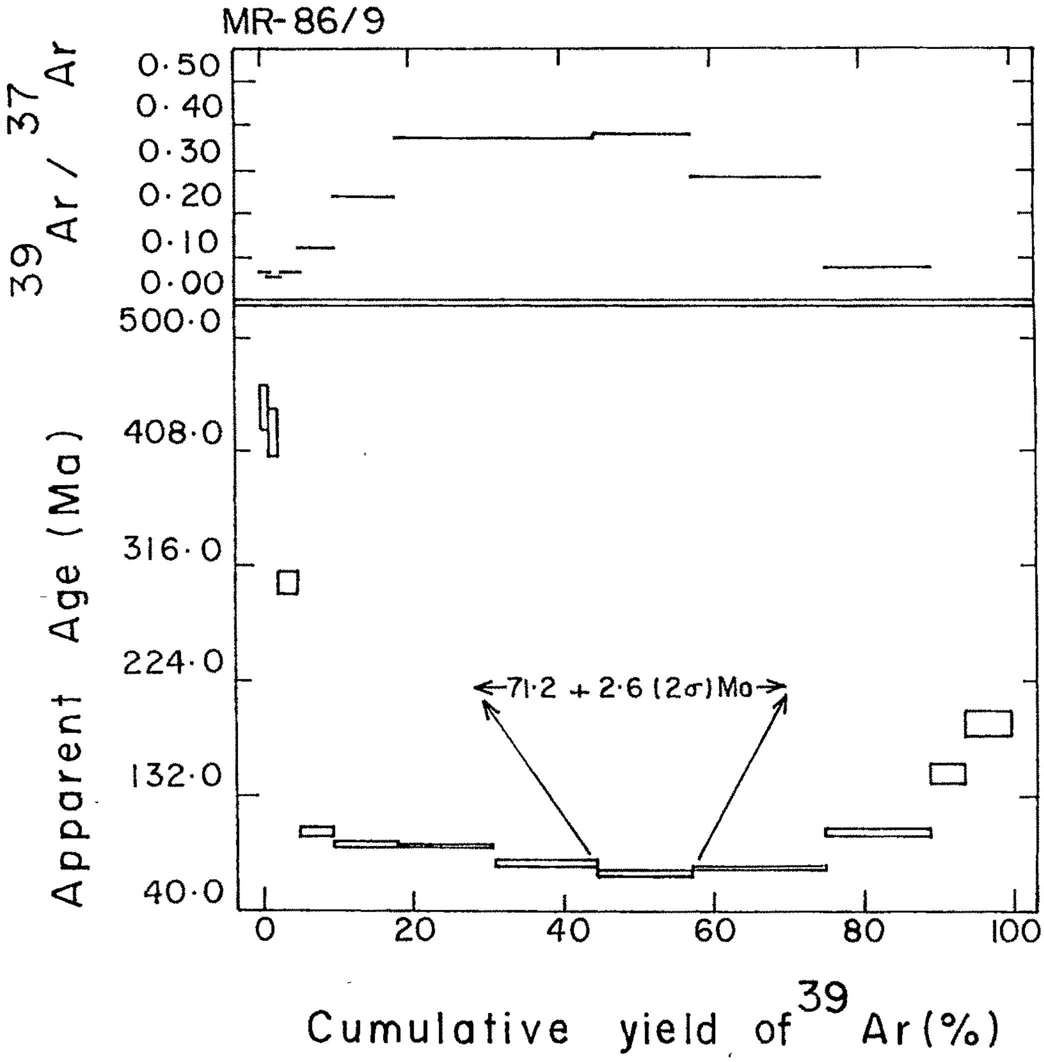

Fig. 4.41. ^{40}Ar-^{39}Ar Age Spectrum for Toa Gabbro (MR 86/9).

and MR 86/5. The minima of the age spectrum is at 71.2 ± 2.6 Ma (12.8% of total ^{39}Ar release), which again marks the upper limit to the time of formation. However, a $^{40}Ar/^{36}Ar$ vs. $^{39}Ar/^{36}Ar$ regression analysis of all the data points provide an age of 69.8 ± 2.1 Ma, which could be considered as its formation age.

From the results presented above it is clear that, out of six samples analyzed from the Mundwara complex, only two syenite samples viz. MR 86/4 and MR 86/7 have shown good plateaus, which are concordant at 64 Ma. This suggests that the syenites of Musala as well as Mer hills are contemporary and were emplaced about 64 Ma ago. The remaining samples viz. MR 86/1 (essexite), MR 86/2 (basalt), MR 86/5 (syenite) and MR 86/9 (gabbro) have, however, exhibited saddle shaped spectra with their minima at 74.8 ± 1.0 Ma, 73.9 ± 0.4 Ma, 69.5 ± 0.9 Ma and 71.2 ± 2.6 Ma, respectively.

Subsequent to reporting our results (Rathore and Venkatesan, 1991 and 1993: Venkatesan et al., 1990), Basu et al. (1993) have reported recently a ^{40}Ar-^{39}Ar weighted mean age of 68.53 ± 0.16 Ma (2σ) for the biotites separated from alkali olivine gabbro of Toa hill of the complex. This confirmed the age obtained by regression analysis of sample MR 86/9. Further, these authors have also reported saddle shaped spectra for two hornblendes separated from melagabbro with their minima at 71 Ma, exactly similar to the minima of 71.2 ± 2.6 Ma obtained for the sample MR 86/9 (gabbro) of our study.

It is to mention here that the regression analysis of total data points of essexite (MR 86/1) has given an age similar to its minima of 74 Ma only. However, based on the above results of gabbro (MR 86/2) as well as that of Basu et al. (1993) it is presumed that the essexite, which is essentially a type of gabbro, is also formed about 70 Ma ago.

As the Mundwara complex exhibits a complete suite of differentiated rocks with the syenites representing the end member of differentiation (Bose and Das Gupta, 1973), therefore, in the light of recent publication of Basu et al. (1993) and the present study it is proposed that the igneous activity at Mundwara commenced about 70 Ma ago. The differentiation continued and the activity seems to have culminated about 64 Ma ago as indicated by the perfect plateaus of syenites from the Musala and Mer hills, suggesting a total span of about 6 Ma for the igneous activity.

4.5.2. Sr ISOTOPIC DATA

Strontium isotopic compositions together with Rb and Sr contents of six whole rock samples are given in Table 4.28. The Rb/Sr ratios in the Mundwara alkali igneous complex show variation from 0.021 to 0.230. The initial $^{87}Sr/^{86}Sr$ ratios calculated assuming an age of 64 Ma for the syenites and 69 Ma for the other rock types vary from 0.70384 to 0.70551 (Table 4.28). Similar variations in cogenetic rocks have also been observed from the Tertiary volcanics of South Arabia (Dickinson et al., 1969; Cox et al., 1970). According to these authors, if a fractionated magma freezes with different Rb/Sr ratios at different levels within its chamber and these different levels were later remelted and brought to the surface without mixing, isotopic variations would be observed in a suite of apparently cogenetic rocks, as has been observed at Mundwara.

The Mundwara complex displays initial $^{87}Sr/^{86}Sr$ ratios similar to those of the least contaminated Deccan tholeiitic lavas, such as those of the Ambenali, Mahabaleshwar and Panhala Formations of upper sequence (Mahoney, 1988). The average $^{87}Sr/^{86}Sr$ value of the complex is 0.70457 which is similar to 0.70484 obtained by Subrahmanyam and Leelanandan (1989) and is slightly less than the average value of 0.7063 for the Girnar complex (Paul et al., 1977).

When the initial $^{87}Sr/^{86}Sr$ ratios are plotted against Sr content (Fig. 4.42) they fall in a field of ***oceanic island basalts*** as defined by Faure and Powell (1972). The mean of initial $^{87}Sr/^{86}Sr$ ratio (0.70457) of Mundwara igneous complex lie in the ***'source region of basalt'*** on the Sr evolution diagram (Fig. 4.31), suggesting upper mantle origin of the magma (Faure and Hurley, 1963).

The mantle source has also been charaterized by high $^{3}He/^{4}He$ ratio of 13.9 and 10.5 times the air ratio (R_A) for the pyroxene separates from two different rocks of the Mundwara complex (Basu et al., 1993). Further, the least differentiated carbonatites of Mundwara have given $\delta^{13}C$ and $\delta^{18}O$ values of -6.4 per mil (PDB) and +6.1 per mil (SMOW), respectively, which are also indicative of their mantle source (Sarkar and Bhattacharya, 1992).

Bose (1972, 1980) has suggested plume generated fracture zones responsible for

Table 4.28. Rb-Sr content and Sr isotopic ratios of Mundwara Alkali Igneous Complex.

Sample No.	Rock Type	Rb (ppm)	Sr (ppm)	K/Rb	Rb/Sr	$^{87}Sr/^{86}Sr$ (normalized)	$^{87}Sr/^{86}Sr$ (initial)
MR 86/1	Essexite	56	751	425.43	0.075	0.70518	0.70497±0.00012
MR 86/2	Basalt	75	417	244.60	0.179	0.70436	0.70384±0.00014
MR 86/4	Syenite	118	960	434.75	0.132	0.70504	0.70471±0.00012
MR 86/5	Syenite	163	709	232.73	0.230	0.70486	0.70426±0.00014
MR 86/7	Syenite	149	857	403.35	0.174	0.70597	0.70551±0.00013
MR 86/9	Gabbro	16	777	798.97	0.021	0.70415	0.70409±0.00011

Note: Initial $^{87}Sr/^{86}Sr$ ratios have been calculated assuming an age of 64±1 Ma for syenites and 70±1.5 Ma for other rock types as indicated by $^{40}Ar/^{39}Ar$ studies.

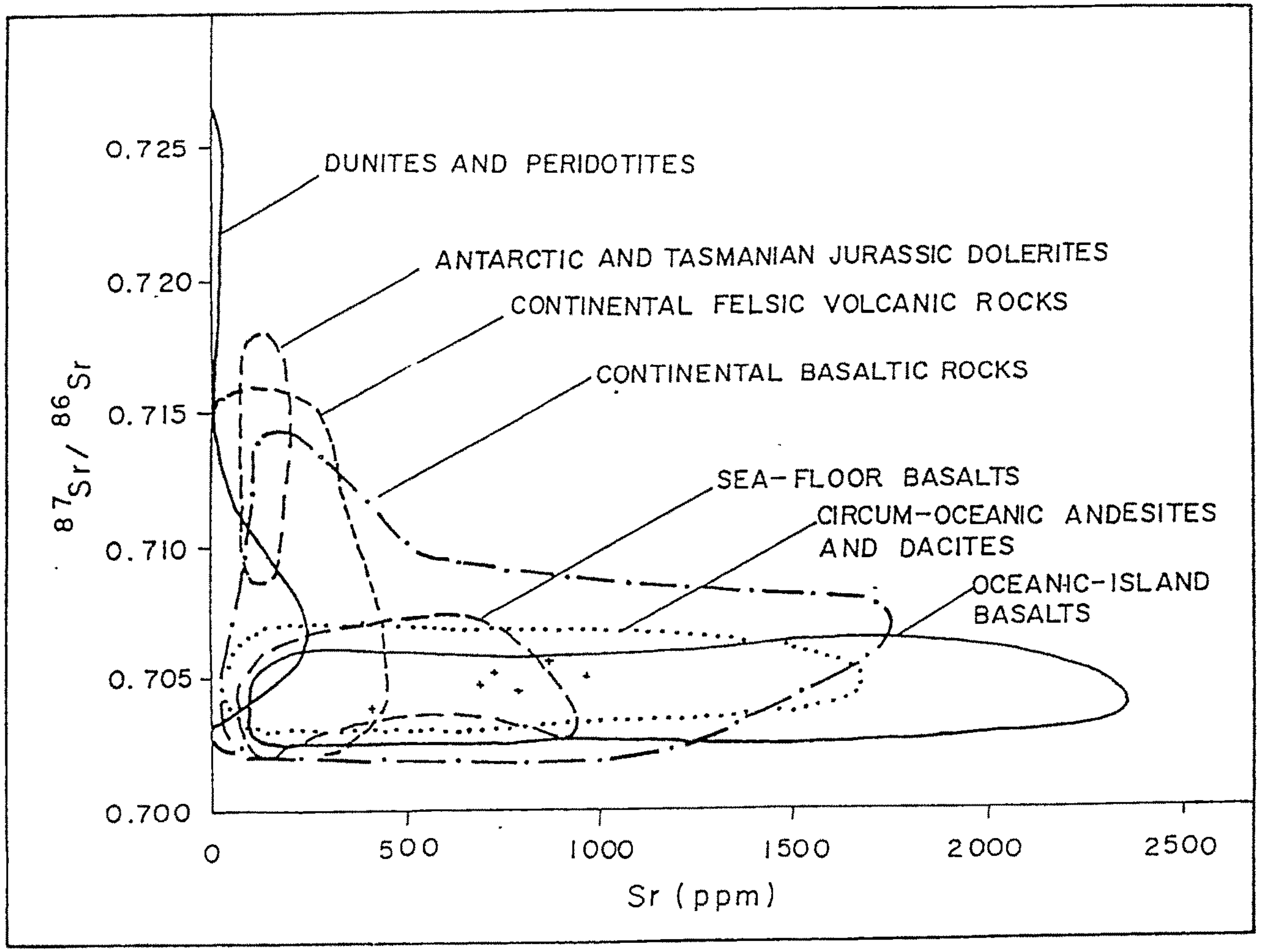

Fig. 4.42. Plot of Initial Sr Ratios Against Sr Content Of Mundwara Alkali Igneous Complex (after Faure and Powell, 1972).

the alkaline magmatism. Srivastava (1983, 1988) has suggested that the alkaline rocks associated with the Deccan volcanic province and those of the southwest Rajasthan belong to a Palaeocene igneous cycle. The reason of this Palaeocene activity was the northward drift of Indian plate which resulted in the reactivation of the ancient lineaments or faults.

Recently Basu et al. (1993) have also postulated a mantle plume origin for the Deccan volcanism and that of Mundwara complex. These authors have envisaged that the alkali magmatism began 3.5 Ma before the main pulse of Deccan volcanism at 65 Ma. They, further, suggested that the spatial-temporal relation between the Mundwara complex and the Deccan flood basalt, centered 600 km to the south, is consistent with northward motion of the Indian plate at 10-15 cm/yr over a nascent Reunion hotspot. Their observation indicates that the Cambay Graben was active 3.5 Ma before the rapid eruption of the bulk of the Deccan traps.

However, the present study indicates that at Mundwara the magmatic activity was not short spanned and instead continued for about 6 Ma from 70 to 64 Ma, which is not in keeping with the model postulated by Basu et al. (1993). Keeping in view the mantle plume theory of Basu et al. (1993) and the present studies, it is proposed that the igneous activity at Mundwara might have been triggered by the mantle plume, which might be responsible for the Deccan volcanism at 67 Ma (Venkatesan et al. 1993), at about 70 Ma ago and then the magma was residing at some depth to give pulsatic magmatic activity, supported by Subrahmanyam and Leelanandam (1989), and the activity seems to have culminated about 64 Ma ago with the emplacement of syenites.